UNIVERSITY OF PADOVA

DEPARTMENT OF BIOLOGY

DOTTORATO IN BIOSCIENZE

GENETICA E BIOLOGIA MOLECOLARE DELLO SVILUPPO

CICLO XXI

CELL THERAPY FOR MUSCULAR DYSTROPHIES:
IN VIVO DELIVERY OF MYOGENIC PRECURSOR CELLS VIA BIOCOMPATIBLE SCAFFOLDS

School Director: Dr. Tullio Pozzan

Supervisor: Dr. Libero Vitiello

Candidate : Silvia Carnio

Table of contents

Chapter 3

Hyaluronic-based hydrogel for cell delivery in normal and dystrophic muscle **55**

SUMMARY

Duchenne muscular dystrophy (DMD) is characterized by mutations in the dystrophin gene, which lead to the absence of a functional protein and consequent muscle fibers degeneration and necrosis. In dystrophic muscles, the regenerative potential of endogenous satellite cells (the muscle resident stem cell population) is exhausted due to repeated degeneration-regeneration cycles and affected muscle tissue is progressively replaced by fibrotic connective tissue and fat.

No effective therapy is available for DMD patients yet, despite years of ongoing research on gene- and cell-based therapies. Cell therapy is aimed at delivering dystrophin-expressing cells into dystrophic muscle, in order to generate new, non-defective fibers and, most importantly, to replenish the endogenous stem cell pool. This way, during the ongoing regeneration processes non-diseased delivered satellite cells would generate healthy muscle fibers that would eventually replace the defective ones. Last but not least, once developed an effective cell-therapy protocol for DMD could be immediately applied to the many others monogenic forms of inherited muscular dystrophies.

At present, cell therapy is still suffering from several problems, which can be summarized in two main points: the identification of the best-suited type of myogenic

cell and its efficient delivery into the diseased muscles. Several studies have clearly demonstrated that the use of biomaterials can improve cell delivery *in vivo*; in particular our group has first demonstrated its potential in specifically delivering myogenic cells into regenerating skeletal muscle. The design of biomaterials for cell-delivery purposes involves several challenging aspects, as the biomaterial should appropriately mimic the recipient tissue *in vivo* and, in the case of stem cells, behave as an artificial niche capable of preserving the proliferative and differentiative potential of the implanted cells.

In this work two different types of biomaterials were explored as potential vehicles to perform cell delivery in the muscles of the murine model for DMD (*mdx* strain). This work has been carried out in close collaboration with the Biological Engineering Research and Application laboratory at Chemical Engineering Department of University of Padova.

Initially, a three-dimensional collagen sponge was investigated as a cell reservoir to accomplish long-term cell delivery in dystrophic muscles. Collagen sponge is a three-dimensional scaffold, natural and highly elastic, whose architecture is suitable to host high numbers of mononucleated cells inside. In this series of experiments, collagen scaffolds were used to deliver high numbers of *in vitro* expanded myogenic precursor cells. Scaffold features were first evaluated *in vitro* and then its performance as a cell carrier was analyzed *in vivo*, both *wt* and *mdx* mice. Our data showed that cellularized collagen scaffolds did behave as a cell reservoir, releasing cells in the muscle while it was degraded *in vivo*. However, the general efficiency of this approach, measured as number of dystrophin-positive fibers formed in the transplanted muscles, was too low to be of clinical interest.

For this reason, we decided to work with a different cell/biomaterial combination. In particular, we moved from *in vitro* expanded myogenic precursors to freshly isolated satellite cells and from collagen sponges to a hyaluronic-based hydrogel. This latter is a novel, natural injectable polymer, polymerizable *in situ*, which can moreover be produced through fermentative process and therefore easily prepared in clinical grade immediately. Hydrogel mechanical and elastic properties were characterized and conditions to encapsulate cells into the polymer were set up for both *in vitro* cultures and *in vivo* transplantation. Therefore, freshly isolated satellite cells were encapsulated into hydrogel and delivered into *tibialis anterior* muscles of both *wt* and *mdx* mice in

order to analyze hydrogel efficiency as a cell carrier *in vivo*. Hydrogel-encapsulated cells yielded very good regeneration in *wt* mice, with many new fibers derived from donor cells. However, so far these promising results did not translate into such an efficient dystrophin delivery into the *mdx* model. These experimental observations are fundamental to develop a suitable combination of hydrogel and stem cells in order to face the different physiological conditions existing between the *wt* and the dystrophic muscle (e.g., its chronic state of inflammation).

The first chapter will give an overview of the main issues concerning myogenic cell transplantation. It will introduce muscle-resident satellite cells and the pathologic state of Duchenne Muscular Dystrophy (DMD). Then therapeutical approaches for DMD are discussed, with particular attention to cell therapy and cell-delivery aspect; to this end the use of biomaterials is discussed as an alternative to face cell delivery issue, in order to finally introduce the aim of this work.

The second chapter will describe the use of three-dimensional collagen sponge as a vehicle to perform cell delivery into dystrophic muscles.

Chapter 3 will present the injectable hyaluronic-based hydrogel and its potentialities as a cell carrier *in vivo*. Finally, general conclusions of the work are given.

VIII

SOMMARIO

La distrofia muscolare di Duchenne (DMD) è caratterizzata da mutazioni nel gene della distrofina, che portano all'assenza di una proteina funzionale, con conseguente degenerazione e necrosi delle fibre muscolari. Nei muscoli distrofici, il potenziale rigenerativo delle cellule satelliti endogene, (la popolazione staminale del muscolo) è esaurito a causa dei continui cicli di degenerazione-rigenerazione che il muscolo distrofico subisce, per cui il tessuto muscolare viene con il tempo rimpiazzato da grasso e da tessuto fibrotico. Al momento, nonostante l' assidua ricerca di una terapia di tipo genico o cellulare, non esiste una terapia efficace per i pazienti DMD.

Lo scopo di una terapia cellulare è quello di rilasciare cellule che esprimono distrofina all'interno di un muscolo distrofico, al fine di rigenerare nuove fibre muscolari, non difettive per 'espressione della proteina, e, più importante, al fine di reintegrare il pool di cellule satelliti endogene. In questo modo, durante la rigenerazione, le cellule rilasciate che esprimono distrofina, andrebbero a formare nuove fibre muscolari non difettive per l'espressione della proteina che con il tempo, andrebbero idealmente a sostituire, almeno in parte, quelle difettive. Infine, un'importante caratteristica di una terapia di tipo cellulare è che, una volta messo a

punto un protocollo per una terapia efficace in pazienti DMD, questa potrebbe essere subito applicata ad altre distrofie di tipo monogenico.

Al momento una terapia di tipo cellulare presenta diversi problemi che possono essere raggruppati in due punti principali: l'identificazione del miglior precursore miogenico da rilasciare e il modo con cui esso è rilasciato all'interno del muscolo malato al fine di un efficiente risultato. Diversi lavori hanno già dimostrato che l'utilizzo di biomateriali in questo campo può migliorare l'efficienza di rilascio *in vivo*. In particolare il mio gruppo ha già dimostrato queste potenzialità, utilizzando cellule miogeniche rilasciate nel muscolo rigenerante attraverso diversi tipi di biomateriali.

La realizzazione di biomateriali per il rilascio di cellule implica diverse difficoltà, perché un biomateriale dovrebbe idealmente mimare il tessuto nel quale dovrà effettuare rilascio di cellule, e ricreare una nicchia per le cellule rilasciate, in grado cioè di preservarne le potenzialità proliferative e differenziative.

In questo lavoro si sono trattati due diversi tipi di biomateriali, con modalità differenti, ma con lo scopo comune di effettuare un efficiente rilascio di cellule (e quindi di distrofina) nel topo *mdx* (modello murino per i pazienti DMD). Questo lavoro è stato condotto in stretta collaborazione con il laboratorio BioERA. (Biological Engineering Research and Application) presso il Dipartimento di Ingegneria Chimica dell'università degli studi di Padova.

Inizialmente si è utilizzata una spugna tri-dimensionale in collagene, altamente elastica e la cui struttura è adatta a contenere un elevato numero di cellule mononucleate al suo interno, da essere rilasciate nel lungo termine all'interno del muscolo distrofico. In questa serie di esperimenti, scaffolds di collagene sono stati utilizzati per rilasciare *in vivo* un elevato numero di precursori miogenici precedentemente espansi in coltura.

Le proprietà e le caratteristiche dello scaffold sono state analizzate prima *in vitro* e successivamente *in vivo,* sia in modelli sani *wt* che distrofici *mdx,* per valutarne le potenzialità come mediatore di rilascio cellulare. I nostri dati mostrano che lo scaffold di collagene ha effettivamente agito come un serbatoio cellulare, rilasciando le cellule che conteneva, mentre veniva degradato *in vivo*. Tuttavia però, il grado di efficienza generale di questa combinazione di cellule e biomateriale, quantificata come numero di fibre distrofina positive formatosi nei muscolo impiantati, era troppo bassa per avere una rilevanza clinica. Per questo motivo è stata proposta una alternativa che utilizza cellule satelliti isolate a fresco al posto di mioblasti espansi *in vitro,* e come

biomateriale un hydrogel derivato dell'acido ialuronico al posto delle spugne in collagene.

Quest'ultimo in particolare è un biomateriale iniettabile, di nuova realizzazione che viene reticolato *in situ;*l'acido ialuronico inoltre può essere prodotto per mezzo di processi fermentativi, caratteristica per la quale questo hydrogel può essere facilmente preparato per applicazioni di tipo clinico.

Le proprietà meccaniche ed elastiche dell'hydrogel, così come le condizioni migliori per l'incapsulamento di cellule all'interno sono state caratterizzate sia in colture *in vitro* che per le applicazioni *in vivo.* Quindi, cellule satelliti isolate a fresco sono state incapsulate dentro l'hydrogel e rilasciate *in vivo* in muscoli tibiali anteriori di topi sia *wt* che distrofici *mdx*, al fine di valutare l'efficienza di rilascio di cellule da parte dell'hydrogel *in vivo.* Le cellule sospese in hydrogel hanno indotto una ampia rigenerazione in topi *wt* dove si sono osservate molte fibre derivanti dalle cellule donatrici rilasciate. L'efficienza di questi risultati tuttavia, non si è ripetuta quando lo stesso approccio è stato usato per ottenere rilascio di distrofina nel modello *mdx*.

Questi dati pongono i presupposti per sviluppare una combinazione di hydrogel e staminali *ad hoc* per le diverse condizioni fisiologiche tra ambiente *wt* e distrofico (caratterizzato da infiammazione cronica).

Il primo capitolo presenterà una panoramica dei principali problemi riguardanti il rilascio di cellule miogeniche *in vivo.* Introdurrà quindi le cellule satellite e lo stato patologico della distrofia muscolare di Duchenne; in seguito vengono descritti gli approcci terapeutici per questo tipo di distrofina, con particolare attenzione a una terapia di tipo cellulare e al modo in cui le cellule vengono rilasciate *in vivo.* A questo proposito l'utilizzo di biomateriali si pone come possibile alternativa per la risoluzione del problema del rilascio *in vivo.* Successivamente viene descritto lo scopo della tesi.

Il secondo capitolo descriverà l'utilizzo di uno scaffold tri-dimensionale di collagene come mediatore per rilascio di cellule *in vivo.*

Il capitolo 3 invece descriverà l'utilizzo di un hydrogel derivato dall'acido ialuronico per lo stesso fine. Nella parte finale infine, sono riportate le conclusioni di tutto il lavoro.

CHAPTER 1

Myogenic cell delivery for muscular dystrophies: state of the art

1.1   MYOGENIC PRECURSORS IN MUSCLE GROWTH/REPAIR

Skeletal muscle display limited nuclear turnover in normal conditions, but on injury or physiological need, it displays remarkable capacity of regeneration, thanks to an heterogeneous population of muscle-specific progenitors, called satellite cells (SC). These cells are also responsible for muscle post-natal growth and maintenance. At birth, satellite cells comprise approximately 32% of muscle nuclei, whereas in adults their number decrease to account for 2-5% of sub-laminar nuclei associated with myofibers (*1*).

Satellite cells are mononucleated precursors defined morphologically by their sub-laminar position, directly attached to the myofibers (*2*), and functionally by their unique capacity to both self-renew and generate large numbers of muscle precursor cells that can then differentiate to form muscle fibers.

Under normal conditions, SC are mitotically quiescent, but, unlikely myonuclei, they can undergo mitosis (*3*) when activated by regenerative cues. On injury, they respond to proliferative signals by starting to proliferate very quickly, giving rise to many muscle precursor cells (also defined as 'myoblasts') that express a fairly well-defined array of myogenic regulatory factors (MRFs) and migrate to the site of injury. Here they either fuse to pre-existing myofibers or together, thus repairing damaged muscle fibers (*2, 4, 5*) (*6*).

When muscle formation and repair occurs, proliferating myoblasts initially express MyoD and/or Myf-5; as the process continues, they withdraw from cell cycle, thus becoming differentiated myocytes, expressing late MRFs such as myogenin or MRF4. These mononucleated cells then fuse together to form multinucleated syncytia called myotubes, which express muscle structural genes (e.g., myosin heavy chain, MHC, and muscle creatine kinase, MCK). Finally, after innervation and vascularization myotubes develop into mature muscle fibers.

Satellite cells are characterized by the expression of specific surface markers including M-cadherin, c-Met (*7*), CD34 (*8*), syndecan-4 (*9*), and the paired box homeodomain-containing transcription factor PAX7. This latter characterizes both quiescent and activated satellite cells (*10*).

During muscle regeneration quiescent satellite cells can either symmetrically give rise to two self-renewal daughter cells or asymmetrically generate a self-renewal and a committed cell. Upon activation, PAX7 positive satellite cells are activated and start to

co-express MyoD within 24 hours; after forty eight hours, most of the cells down-regulate PAX7 while maintaining MyoD expression and progressing towards myogenic differentiation; others, however, down-regulate MyoD, maintain PAX7 expression and go back to a quiescent state, thereby replenishing the satellite cell pool (*11*). Recent experiments from Rudnicki's group revealed an heterogeneity within the satellite cell compartment, that is dependent on Myf-5 expression and seems to determine which cells will proceed along the differentiation path and which will instead self-renew and go back to quiescence (*12*).
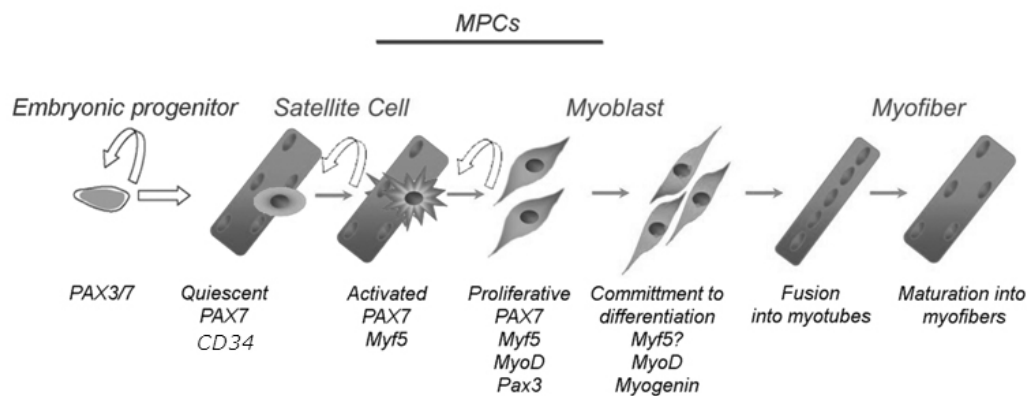
Figure 1.1   **Schematic representation of satellite cell myogenesis with typical markers of each stage, adapted from (13). Satellite cells embryonic progenitors display PAX3 and PAX7 expression; in the adult muscle quiescent satellite cells express PAX7 and CD34, on injury or proliferative cues satellite cells are activated and start to proliferate giving rise to a population of myoblasts (characterized by PAX7 expression at first, that is gradually lost while Myf5 and Myod are up-regulated). After a first wave of proliferation, myoblasts start to differentiate and fuse into myotubes that will generate new myofibers in vivo, or, in part, will go back to quiescence.**

It is now widely recognized that the even though the satellite niche is univocally characterized under the morphological point of view, it actually comprise several different cell sub-populations (*14*). Besides, it has also been proven that cells from other sources, such as side populations and hematopoietic stem cells (*15, 16*), can also contribute to the satellite cell niche.

Still, satellite cells constitute the main source for muscle regeneration (*17, 18*); the engraftment of a single intact myofiber in injured muscles has been shown to suffice to obtain regeneration and expansion of satellite cell pool (*19*), as well as the transplantation of myofiber associated $Cd45^-$ $Sca-1^-$ $Mac-1^-$ $CXCR4^+$ $\beta1\text{-integrin}^+$ (*17*);

satellite cells dissociated from their parental myofibers (*19*) and FACS-purified PAX3-GFP+ cells from diaphragm(*20*) yielded very good engraftment as well.

1.2   DUCHENNE MUSCULAR DYSTROPHY (DMD)

Duchenne Muscular Dystrophy (DMD) is a severe muscle-wasting disease that affects 1 out of 3500 male newborns, and causes progressive muscle degeneration. DMD arises from mutations in the dystrophin gene (*21*), that is located in the short arm of the X chromosome (Xp2.11) and codes for a very large (~400kDa) cytoskeletal protein that provides a physical link between the sarcolemmal cytoskeleton and the basal lamina (*22-24*). Mutations that disrupt the reading frame of the main transcript of the DMD gene cause the absence of a functional protein, which translates into progressive muscle weakness and degeneration (*25, 26*).

Dystrophin N-terminal is linked to cytoplasmic actin filaments (*27, 28*), whereas its C-terminal is bound to the sarcolemmal dystrophin-associated protein complex (DAPC), formed by dystroglycans, sarcoglycans, integrins and caveolin. On the outside of the sarcolemma, the complex is linked to the extracellular marix. Dystrophin is therefore part of the structure linking the extracellular matrix to the cytoskeleton of the fiber, which plays an important structural role during muscle contraction and muscle stretch. Lack of dystrophin destabilizes the DAPC, leading to diminished levels of DAPC proteins (*29, 30*); this in turn leads to membrane damage and fiber necrosis (*31*).

For this reason, even during normal muscle activity the absence of dystrophin triggers continuous cycles of muscle degeneration-regeneration. In fact, resident satellite cells obviously carry the same mutation and the newly formed fibers undergo the same destiny as their predecessors. This ongoing process eventually depletes the satellite cells reservoir and in the long run the regenerative potential of the muscle is exhausted. Once this happens, muscle tissue is gradually replaced by connective tissue and fat. Clinically, DMD is characterized by progressive muscle weakness and atrophy, with patients being confined to a wheelchair before the age of 12 and eventually dieing due to cardio/respiratory failure around the second decade of life.

1.3 *THE MURINE MODEL FOR DMD*

The *mdx* strain derived from a naturally occurring mutant that arose within a C57BL /10 colony, initially identified by its abnormally high plasma levels of creatine kinase (*32*). With the identification of the *DMD* gene and the protein product, the *mdx* mouse was confirmed as having a dystrophin deficiency which was subsequently shown to be due to a nonsense point mutation in exon 23 (base 3185), which forms a premature stop codon.

The *mdx* mouse is the most widely used model of DMD due to its small size and ease husbandry, which makes it a cost effective model. Moreover, the vast array of molecular and breeding technologies available for the mouse allowed the design and performance of countless different experiments aimed at elucidating the different aspects of the pathology. Still, despite the genetic similarities, the human and murine diseases are quite different at the phenotypic level. Generally speaking, *mdx* mice are not as severely affected as DMD patients; in fact, in mice there is no obvious weakness (*33*) and most of the limb musculature does not undergo major fibrosis and loss of function. The lifespan is shortened, although not nearly as much as in humans, and a marked deterioration of general mobility becomes obvious only in older animals (*34*). Muscle histopathology is pronounced mostly between 2 and 8 weeks of age, a period characterized by the presence of numerous necrotic foci, newly regenerated centrally nucleated myofibres and high plasma concentrations of creatine kinase. Mild myopathy with its associated fibrosis and hypertrophy persists for the remainder of the animal's life, but does not become acute until senility (*35*). As opposed to what happens in humans, muscle degeneration and regeneration continue for the whole lifespan and satellite cells continue to express markers of activation.

There are many theories as to why the *mdx* mouse is less severely affected by the dystrophin deficiency compared to DMD youth. These hypotheses involve differences in the murine muscle regeneration capacity as well as the effects of reduced body size and quadrupedal stance. It is also possible that the relative mildness of the *mdx* phenotype is, in part, an artifact of the animal house environment which does not require or encourage much active movement and may therefore spare muscle. Indeed, it has been shown that moderate exercise can accelerate the course of the disease (*35*) and

the diaphragm is the most severely affected muscle in *mdx* animals, both in terms of fibrosis and loss of muscle fibers (*36*).

Altogether, years of research have clearly shown that, provided that the physiological differences are properly acknowledged, *mdx* mice are invaluable tools in DMD research (*35*).

1.4   THERAPEUTIC APPROACHES FOR DMD

There is currently no effective therapy for DMD, although the increasing understanding of the molecular processes involved in the progression of the muscular wasting has driven the design of several prospective treatments (*37*). At any rate, given the structural nature of the protein involved any definitive solution for DMD would have to lead to the restoration of dystrophin production, either via gene- or cell-based approaches.

The main current therapeutic approaches for DMD are:

- ✓ Gene therapy by i) introducing (through viral or non-viral vectors), or ii) repairing the genetic message (exon-skipping approach)
- ✓ Pharmacological approach
- ✓ Cell-therapy by transplantation of dystrophin-expressing cells

Gene therapy

Gene therapy for DMD patients is based on two different approaches: gene addition and gene repair. The former is based on the idea to deliver a functional copy of the dystrophin gene, through viral or non-viral vectors, in the muscle fibers of the patients. The latter is based on the delivery of synthetic oligonucleotides, that could either modify the DNA at genomic level, e.g., correcting a point mutation via DNA repair mechanisms, or induce patient-specific exon skipping aimed at restoring an open reading frame in the mutated dystrophin mRNA. Exon skipping can also been obtained by delivering specifically engineered snRNA (see (*38*) for a recent review).

Recently, Hoshiya et al., (*39*) have developed a Human Artficial Chromosome (HAC) vector containing the entire human dystrophin gene with all its regulatory elements, (DYS-HAC), that showed to produce multiple tissue-specific isoforms of

human dystrophin in mice, while being stably maintained in both mice and human immortalized cell lines, thus holding great promise for DMD treatment.

At present, the gene addition approach still suffers from several hurdles, both under the biological and technical point of view, especially for what concerns the use of viral vectors (*40*).

Exon skipping, when based on antisense oligo delivery, presents less issues and promising results have already been reported also in patients (*41*). On the downside, though, although this approach could be applied to the majority of DMD mutations it would still leave out approximately 25% of them.

Last but not least, it should be pointed out that all types of gene-based approaches would be of little benefit for elderly patients, in which there would be little muscle fibers and satellite cells left to treat.

Pharmacological approaches

Many steroid/supplemental treatments have been proposed for DMD, although not many are currently in clinical use. At present the drug most widely used is prednisone, a catabolic steroid that slows down muscle degeneration. Its beneficial effect is due to its anti-inflammatory and immunosuppressant effects, although the exact molecular mechanisms are still not know.

Gentamycin is an antibiotic that interferes with bacterial ribosomes and in doing so can also allow read-through of stop codon. Researches on mdx mice suggested that when gentamycin was administered, the premature stop codon could be ignored and dystrophin could be produced (*42*). However, a preliminary trial on suitable DMD patients showed no increase of dystrophin expression; furthermore, other researchers later reported that they could not replicate the results of gentamycin treatment in the *mdx* mouse (*43*). More recently, another molecule (PTC-124) has been proposed as a read-through agent. Its preliminary results in animal studies and initial clinical trials are quite encouraging (*44*).

Other drug-based approaches have also been proposed, starting from the observation that molecules capable of interfering with the inflammatory and catabolic pathways of the muscles could improve the dystrophic phenotype in mdx mice (see (*45*) for a comprehensive review). However, given the structural nature of the genetic defect

underlying DMD it is unlikely that these approaches could ever play other than a support role to gene- or cell-therapies.

1.5   CELL THERAPY

Cell therapy is an appealing approach for Muscular Dystrophy because should a solid protocol be developed, it could be potentially used for all forms of dystrophy. The first demonstration that C2C12 mouse myoblasts could induce synthesis of dystrophin in dystrophin-deficient mdx mice came at the end of the 80's (*46*). Results were further confirmed using primary myoblasts (*47*), which were easy to obtain and expand *in vitro* to obtain sufficient quantities for subsequent delivery via intramuscular injection. The exciting results obtained in *mdx* mice (*46, 47*), and in *dy/dy* mice (*48*), led to immediate clinical trials in DMD patients in the early 1990s with repeated injections of large amount of cells ($>10^6$) distributed over multiple sites (*49-56*).

Unfortunately, myoblast transfer to treat DMD patients failed to produce significant physiological correction of the dystrophic phenotype, mostly because the majority of transplanted cells quickly died (at least 75%) after intramuscular injection (*5, 57-60*). High cell loss was due partly to inflammatory/immune response (*61*) elicited by donor myoblasts in the early stages after transplantation, that was partially limited by using immunosuppressive agents (*48, 62, 63*). Other causes were linked to cell handling before transplantation (*64*). Last but not least, transplanted myoblasts show limited migration in the host tissue (*52*). Despite these limitations, researches on myoblast transplantation are still ongoing and Tremblay's group has developed a so called "high-density" implant protocol that has already been transferred into clinical trials (*65, 66*).

These findings led to research on better cell types that could survive the early post-transplantation phases (*5*) while preserving a high myogenic potential (*20*). Recent data showed that satellite cells are capable of extensive muscle regeneration throughout the muscle into which they are injected, only when injected as soon as they are isolated; with *in vitro* culture expansion they lose this property generating more specialized myoblasts (*20*). Collins and colleagues showed the regenerating power of freshly dissociated satellite cells, associated or not with their parental fiber (*19*), obtaining great improvement in cell integration and proliferation in host *mdx* mice. Importantly, these Authors unequivocally showed that satellite cells have sufficient regenerative and

myogenic potential to constitute an exclusive source in regenerating muscles, a finding also confirmed recently by studies performed by Sacco and colleagues (*67*).

As already mentioned above, satellite cells are not a homogeneous population. In this regard, Cerletti and colleagues showed that transplantation into injured muscles of *mdx* mice of a subset of skeletal muscle progenitor cells enriched for a particular combination of cell-surface markers (CD45$^-$Sca-1$^-$Mac-1$^-$CXCR4$^+$ß1-integrin$^+$) led to widespread dystrophin restoration and force recovery (*67, 68*).

In the past, different groups had already reported that small subsets of mononucleated cells derived from whole-muscle preparations (as opposed to single-fiber preparations) had the features of myogenic stem cells. In particular, cells obtained by enzymatic digestion of mouse muscles have been separated according to their adhesion capability using serial platings. With this procedure Huard's group has been able to separate three different cells populations. The first one (*Early Preplate*) adheres early, had poor proliferative but excellent differentiation potential. The second one adhered later (*Late Preplate*), proliferated poorly and did not fuse *in vitro*. A third one, very rare, was obtained by clonal seeding of late preplates and comprised what the Authors called *Muscle-Derived Stem Cells*, MDSC, (*69*). MDSC are highly proliferating cells with many stem-like features, such as the capability of trans-differentiate into several tissues (*70*), including the myeloid line (*71*). Furthermore, once injected in damaged muscle MDSC fuse very easily with pre-existing myofibers (*72, 73*).

Considering the large mass of tissue that would have to be treated with cell therapy of DMD, it is easy to understand why a systemic delivery would be preferable to intramuscular injection. Unfortunately, satellite cells cannot cross the endothelial barrier and therefore other types of myogenic cells have being sought. In the past years it has been shown that after intravenous injection of whole bone marrow in myelo-ablated hosts, hematopoietic cells have been observed to contribute to muscle regeneration (*74*). More recently it has been demonstrated that the bone marrow contribution to adult mouse muscle regeneration occurs by means of an intermediate with satellite-like features. These marrow-derived cells expressed *in vivo* and *in vitro* muscle specific markers, were able of self-renewal *in vitro* and originated myoblasts that fused *in vitro* with myotubes and *in vivo* with myofibers (*16*). However, other findings suggested that the differentiation process from bone marrow to muscle cells could represent a non-

physiological process. In particular, Camargo and colleagues have proposed that BM-derived cells contributing to liver and muscle regeneration are myeloid differentiated cells, as macrophages or granulocytes, that fuse directly with recipient cells (*75*). At any rate, even though bone-marrow derived stem cells might not physiologically contribute to the regeneration of other tissues, they might still be able to promote repair by providing growth and survival factors (*76*).

A subpopulation of circulating cells expressing AC133, a well-characterized marker of hematopoietic stem cells has been shown to undergo myogenic differentiation under specific *in vitro* conditions and *in vivo*, when delivered intramuscularly or through the arterial circulation of transgenic scid/mdx mice (*77*) , also expresses early myogenic markers. These cells have recently been used in a clinical trial with DMD boys (*78, 79*).

Another cell type that has received a lot of attention in the field of cell therapy for muscular dystrophies is the mesoangioblasts. These are vessel-associated multi-potent progenitor cells that can be extracted from mesodermal tissues and can differentiate in myoblasts (*80, 81*). They show an endothelial-like appearance in culture, express endothelial markers (for example Flk-1) and, importantly, can home in the musculature upon systemic delivery. Once injected in the femoral artery of α -sarcoglycan knock-out mice, meso-angioblasts isolated from mouse fetal dorsal aorta were able to restore the α-sarcoglycan and dystrophin-glycoprotein complex, leading to the reversion of the dystrophic phenotype (*82*); these results were then confirmed in a set of experiments with dystrophic dogs (GRMD animals, the canine model of DMD) (*83*). Moreover, these cells migrate in vitro and in vivo in response to HMGB1, a nuclear protein that is released by macrophages and necrotic cells and acts as a potent inflammatory cytokine (*84*). A clinical trial with DMD patients is in advanced stages of preparations; it should be noted, however, that the actual efficacy of mesoangioblasts as a therapeutic tool in DMD has been questioned by some researchers (*85*).

In conclusion, even though "atypical" (i.e., non muscle-derived) myogenic cell progenitors have the potential to participate to muscle regeneration under conditions of severe trauma and are capable of migration into muscles through the circulation, it remains clear that the growth and regeneration of skeletal muscle is mediated largely by muscle satellite cells (*17, 18, 86, 87*) and the other cell populations can only play a secondary role.

1.6 *OPEN ISSUES IN MYOGENIC CELL TRANSPLANTATION*

At present, all cell based approaches for muscular dystrophy are still far from being close to clinical effectiveness, as there are still several hurdles to overcome in order to reach such goal. These can be summarized as follows:

a. Cell source and availability (scale-up to clinical development)
b. Survival rate and proliferative capacity of transplanted cells
c. Functional re-engraftment of the satellite cell niche
d. Delivery method

a. Cell source and availability

Skeletal muscle is a convenient source of cells, given the ease in obtaining muscle biopsies with safe and minimally invasive procedures. Still, beside the open debate about what constitutes the most efficient cell type, a main hurdle to face is the availability of sufficient amounts of cells for human patients. That's why in the initial studies, researchers used large amount of previously *in vitro* expanded myoblasts. Unfortunately, as detailed above, when using this cell type only a small percentage of the whole population survives after transplantation.

Rather than myoblasts, more profound myogenic stem cells (i.e., cells that are endowed both with self-renewal and differential potential) would thus be preferable for therapeutic applications (*88*). Researchers have then focused on the isolation of cell populations able to both survive the initial transplantation stages and efficiently contribute to muscle regeneration although not previously expanded *in vitro* (*89, 90*), obtaining indeed, efficient engraftment (*67, 68, 90*). A common problem is that almost all emerging cell-therapy-based candidates start as "open" laboratory scale cultures (multiwell plates, flasks), in which the evaluation the impact of key parameters on target cell output and productivity is difficult (*91*). Effective cell availability and the methods to achieve it are increasingly urgent issues that involve a challenging transition from biological observations to clinical developmental platforms.

b. Survival rate and proliferative capacity of transplanted cells

At present, cell death (75%-80%) after myoblast transplantation is one of the most problematic and not yet fully elucidated issues in field of cell therapy for DMD.

One factor that likely accounts for the loss of transplanted cells is the acute inflammatory response that occurs immediately after injection (*5, 57-59*). Of course, when thinking in clinical terms for humans, one should also take into account the immune response elicited by transplanted myoblasts. These aspects would made necessary the use of immuno- (*48, 62*), and non-specific-inflammatory response-suppressive (*63*) drugs.

As for the other cell types (freshly isolated satellite cells, FACS-isolated myogenic stem cells and so on), data available so far seem to indicate that cell death after transplant does not represent a major hurdle for any of them.

    c. <u>Functional re-engraftment of the satellite cell niche inside the muscle</u>

Most injected myoblasts fuse to pre-existing myofibers thus contributing transiently to dystrophin expression, and being therefore excluded by following rounds of regeneration. The same situation has been reported to be true for mesoangioblasts. Considering the intrinsic characteristic of skeletal muscle biology, even if one could envisage providing every body muscle with a sufficient number of dystrophin-expressing myonuclei, any use of the musculature would eventually lead to some levels of regeneration. This in turn would require continuous cell re-administrations, something that would be at least problematic. A possible solution would obviously be the injection of myogenic stem cells capable of amplification and self-renewal in the host muscle, capable of engrafting the satellite cell pool and thus restore muscle functionality in future rounds of regeneration.

    d. <u>Delivery methods</u>

There are two possible routes of cell delivery for skeletal muscle: localized injection and systemic injection. Systemic delivery would be advantageous in terms of safety, simplicity and effectiveness; in the case of DMD it would be the best solution, considering that virtually all body muscles are affected. Unfortunately, "true" myogenic stem cells (that is, freshly- and FACS isolated satellite cells) and MPC/myoblasts cannot be delivered in this way, as they are incapable of passing the endothelia to reach their final destination. On the other hand, localized cell delivery requires more invasive procedures, especially when considering hard-to-reach muscles such as the diaphragm. In fact, the large majority of cell-based clinical trials carried out so far in DMD patients

used multiple localized injections. In this regard, the migration of transplanted cells acquires a particular relevance. Myoblasts possess little ability to actively diffuse inside the muscle upon injection. Some improvements have been obtained with the use of metalloproteinases both induced in, or co-injected with, transplanted myoblasts (*92-94*), but of course this would pose several problems in a clinical setting. This problem seems to be much less relevant when using either freshly isolated or FACS-sorted satellite cells (*19, 67*), although one should keep in mind that data reported so far were obtained in murine leg muscles, which of course have a very small volume.

1.7   CELL DELIVERY THROUGH TISSUE ENGINEERING APPROACH: BIOMATERIALS

Tissue engineering applies to clinical scenarios where tissue is lost through trauma or disease; it was first defined as an interdisciplinary field "*that applies the principles of engineering and life sciences to develop biological substitutes that restore, maintain or improve tissue function or a whole organ*" (*95*). In order to develop biological substitutes for functional tissue regeneration, tissue engineering combines viable cells, biomimetic matrices, spatio-temporal presentation of morphogenic factors and external biophysical cues (*96*). Those "matrices" are also generically called biomaterials and are any material intended to interact with a biological system, used (or adapted) for medical applications. A biomaterial could be porous or densly packed, made of either natural or synthetic polymers. In general it needs to be designed depending on the therapeutic target and on what it will deliver *in vivo*. There are two different tissue engineering approaches (*97*): when biomaterials are used to generate artificial tissues *in vitro* that are afterwards delivered *in vivo* (*in vitro* tissue engineering), or when scaffolds are not used for structural applications but rather as vehicles to mediate stem cells or drug delivery *in vivo* to the diseased region to heal or replace (*in vivo* tissue engineering).

In theory, tissue engineering strategy could co-adiuvate the treatment of different types of pathologies. In recent years, the use of biocompatible scaffolds for cell delivery has holded great promise (*98*). Since the mid-1990s the combination of novel biomaterials with living cells has yielded clinical success in the reconstruction of a wide range of functional tissues, some of which are listed below: replacement of damaged

livers (*98*), thumb (*99*), reconstruction of artificial ligaments, tendons, to replace damaged articular cartilage and joints (*98, 100, 101*) and for the treatment of skin damage, either by coupling cells with biomaterials or using a-cellular dermal analogs.

Moreover, several biomaterials have been used as vehicles to release <u>angiogenic</u> factors (*102, 103*) as well as a-celluarized scaffolds to induce angiogenesis *in vivo* (*104*).

Tissue Engineering applied to muscle tissue is one of the most studied; entire tissue-engineered arteries were reconstructed *in vitro* with vascular smooth cells that expressed telomerase (*105*). Tissue-engineered grafts have also been broadly investigated for heart valve reconstruction (*106*) as well as for myocardial repair (*107*).

Other approaches involved the realization of cardiac muscle constructs *in vitro* using layered sheets of micropatterned cells that were grown orderly in order to generate sufficient force for contraction (*108-110*). Rather than seeding on a pre-formed scaffold, Zimmermann et al., were able to induced formation of new myocardium *in vivo* (*111, 112*), by coupling cells with naturally derived protein (collagen, fibronectin) matrigel and culture medium. Eventually, less invasive and more appealing injectable biomaterials, reviewed in (*113*), are being explored like fibrin glue (*114*), collagen or self-assembling peptides scaffolds (*115*).

For what it concerns skeletal muscle, similarly to what happens for cardiac muscle regeneration, both muscle construct as well as not previously *in vitro* differentiated myoblasts are being delivered. Micro structured bi-dimensional scaffolds, with oriented micro-patterned myoblasts, have been used (*116-118*), and showed to induce muscle regeneration in injured mice *in vivo* (*119*). Some groups have been working on the realization of three-dimensional artificial muscles of differentiated aligned muscle fibers (*120-123*), aimed *in vivo* transplantation as well (*124, 125*); other had focus on delivery of myoblasts coupled with growth factors through three-dimensional gels, obtaining improvement in cells outward migration.(*126*).

The past decade has witnessed a wide array of novel injectable hydrogels. The possibility to inject scaffolds in the body, is appealing in such that minimal surgical wounds is required for their insertion, whereas on the contrary polymers like for example PLA, PLGA require surgical insertion. Hydrogels are biocompatible, with tunable visco-elastic properties, as well as physical properties (*127*) and can be polymerized *in situ*.

From a structural point of view, hydrogel is formed by a polymeric network of hydrophilic chain, that are connected together by cross-links at defined chain length; for this peculiar properties they can absorb up to 95% of water. They have been used in drug delivery as well as scaffolds for tissue-engineering in a wide variety of tissues and cell types (*114, 128-130*). Hydrogels show great potentiality to be efficient vehicles for both stem cell delivery (instead of a whole tissue construct) and drug release.

Fig. 1.2, A schematically represents the main issues concerning the transplantation of a biomaterial inside muscle. The situation is complicated since different events will take place at the same time, and so for example host and transplanted cells will interact together in a way that is dependent on the characteristics and degradation rate of the biomaterial; moreover transplanted cell can migrate outward in a way that is dependent on the surrounding tissue. Part B summarizes the requirements needed for a biomaterial to be suitable for an *in vivo* application.

A

B

Biological source

In vitro tissue engineering

Generation of muscle construct *in vitro*

In vivo tissue engineering

Drug/ cell delivery
Stem cell like properties

Biomaterials

Clinical perspective
Biocompatibility
Biodegradability
(Stem) cell niche within the biomaterial
Biomimetic characteristics
Physical support
Possibility of functionalization with biological factors
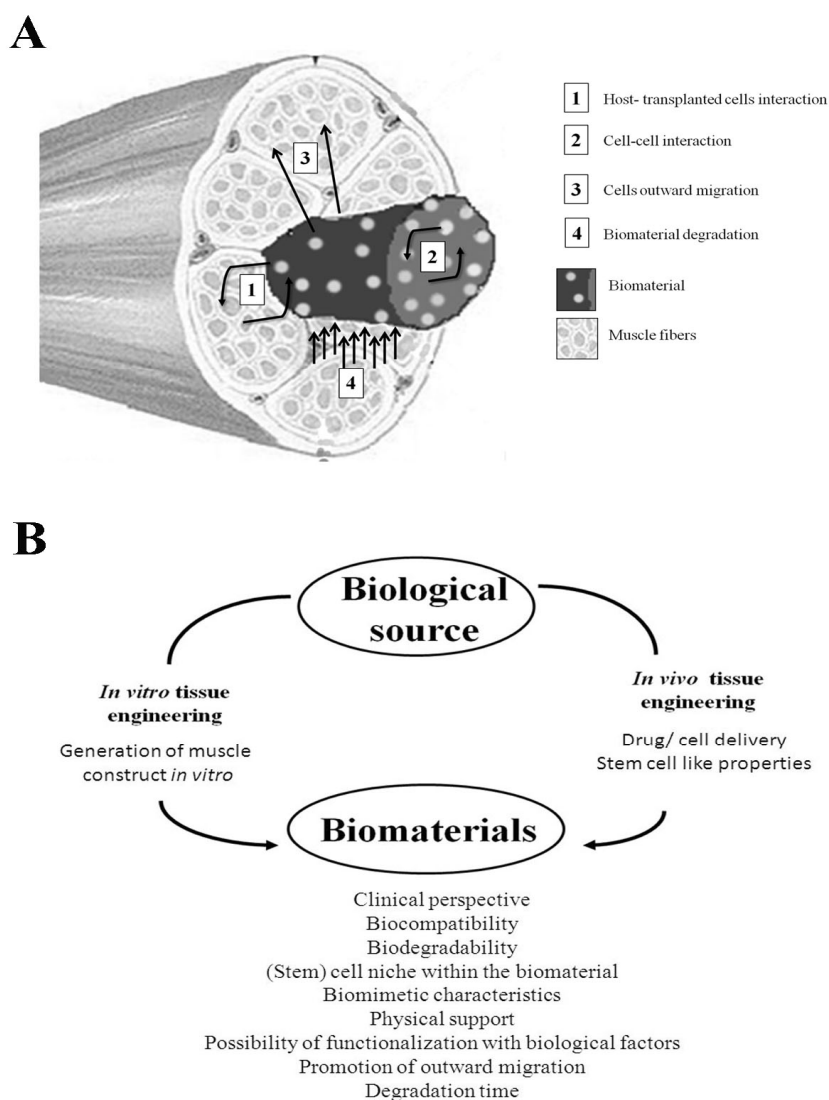Promotion of outward migration
Degradation time

Figure 1.2   A. Schematic representation of the main issues concerning the transplantation of a cell carrier inside muscle. Interactions between donor cells (2) as well as donor cells-host environment (1) are going to occur in a way that inevitably affects the graft; moreover biomaterial degradation (4), and consequently cell release and/or migration (3) occur in vivo as well, at different degrees. B. Requirements needed for a biomaterial to be suitable for an in vivo application. The starting point is the biological source that is meant to be reproduced by the coupling of cells with biomaterials. One possible approach is the delivery of cells previously differentiated in vitro (In vitro tissue engineering) that would replace damaged tissue once implanted in vivo; another way would involve the delivery of cells with stem like properties (In vivo tissue engineering), that would differentiate and replace the damaged tissue in vivo. Regardless the approach used, a suitable biomaterial should display features listed here and deepened in Table 1.1 (see text for details).

When designing a tissue engineering system, or improving upon current technologies, one must consider the choice of cell, biomaterials and biological signals or cues that must be provided. In the case of cells, both stem cells or differentiated organ constructs can be delivered, depending on the target.

In the last decades, new advances in the field of biomaterials properties, biomimetic environments as well as stem cells, have progressed in parallel with the real need for tissue engineered constructs.

A suitable biomaterial to be used in a tissue engineering approach should combine the characteristics described in Table 1:

Table 3.1   **Requirements for a suitable biomaterial for cell-delivery.**

REQUIREMENTS	GOAL
Clinical perspective	✓ Minimal invasive delivery procedure (injection)
Biocompatibility	✓ Minimal inflammatory reaction/immune response to the foreign body (biomaterial+cells)
Biodegradability	✓ Traceability of the possible products
(Stem) cell niche within the biomaterial	✓ Microenvironment for cell growth, proliferation, differentiation, and ideally self-renewal
Biomimetic characteristics	✓ Mimicking of the host tissue architecture ✓ Cell-cell cross talking ✓ Cell-host tissue interaction
Physical support	✓ Substrate for cells to grow ✓ Diffusion of soluble molecules ✓ Physical barrier for host cells (e.g. macrophages)
Possibility of functionalization with biological factors	✓ Microenvironment more similar to *in vivo* ✓ To affect/control/ direct cell response
Promotion of outward migration	✓ Colonization of the surrounding tissue without limitation to the delivery site
Degradation time	✓ Long/short term depending on the goal

The basic feature for any cell-therapy product is the clinical perspective, being its utility ultimately based on its function in the human patient (*91*). Therefore, in general an injectable scaffold is preferable to another that requires open-surgery for ease

of application into the body; that is particularly true when degenerative diseases like muscular dystrophy are treated, because of the severe deterioration of muscles.

The design of biomaterials is aimed at creating scaffolds that are meant to behave dynamically *in* vivo, thus delivering cells while fully integrating in the host muscle; to this end the scaffold needs to be biocompatible and biodegradable. Biocompatibility relates to material's ability to exist within the body without damaging adjacent cells, or lead to a significant scarring, or otherwise elicit a response that could affect its function (*127*); biodegradability is intimately correlated to biocompatibility, as long as the biological system needs to be able to break down the biomaterial.

In order to accomplish an efficient cell delivery, the biomaterial is supposed to provide an artificial niche for cells to be transplanted; that means to provide biological signals in order to create a suitable environment inspired to the *in vivo* environmental cues, that therefore allows the cells to proliferate and differentiate once they have been implanted *in vivo*. The niche is not meant to be static, but instead it evolve in time by supporting stem cell fate during regeneration.

The biomaterial should display biomimetic properties that would mimic the *in vivo* native-like structural properties of the host tissue (*131*), and so acting as an artificial engineered extracellular matrix *ad hoc* for cells that will be delivered. A suitable scaffold for muscle should ideally re-create a 3D environment, being the architecture of muscle three-dimensional (*97, 132*). In the case of muscle constructs the 3D environment would force cells to differentiate in aligned muscle fibers; in the case of cell delivery, the scaffold would be first of all a physical support for muscle cells, being myoblasts cells that grow adhered, and not in suspension as they are during intramuscular injection.

The combination cells + biomaterial, provides a "microcosm", were cells either cross-talk together and, once implanted *in* vivo, interact with the host environment; being this microenvironment a contingent reality that depends on both cells and biomaterial, it needs to be investigated deeply. Inside the scaffold, cells need to maintain their phenotype, their ability to proliferate, differentiate and, when stem cells are delivered, to self-renew, as it would happen *in vivo*. To this end the scaffold should provide for an efficient transport/diffusion of metabolites and soluble molecules towards and from donor cells (fundamental for cell viability), but on the other hand it should ideally protect carried cells from the aggressive acute inflammatory response

that is responsible for the majority of cell loss in the early stages post transplantation (See Table 2 for characteristic time in a wound-healing response).

Table 3.2   Characteristic times of the wound-healing response

WOUND-HEALING RESPONSE	TIME
Hemostasis	Seconds to minutes
Inflammation	Minutes to day
Proliferation	Days to weeks
Remodeling	Weeks to year

It is getting more and more evident that beside the need of physical support to deliver cells, the biomaterial is equally important to provide biological cues to improve cell survival and ability to regenerate damaged tissues (*133*). To this end a biomaterial that allow an unsophisticated encapsulation of growth factors or drugs, beside cells, encompasses several advantages in the potential combination of cells with different molecules that, beside promoting cell growth, could induce cells to exert specific functions.

A biomaterial should finally promote outward migration of cells inside the recipient tissue*,* and so, beside hosting them at first, it is supposed to release donor cells that would colonize the surrounding tissue, afterwards. Migration aspect is correlated to biomaterial degradation as well, because as biomaterial is degraded, cells are inevitably released. For what it concerns degradation, there is no universally accepted guidelines, being the scaffold meant to behave dynamically *in vivo*; in any case, this issue is intimately correlated with the system under investigation, and so biomaterial degradation and how it is related to delivery efficiency in the host tissue, necessarily needs to verified *in vivo.* In general the scaffold should persist in the host tissue for some time in order to provide for long term delivery, thus avoiding continuous material refill; on the other hand though, a slow degradation could entrap cells inside the biomaterial, thus hampering their outward migration and therefore leading to a not efficient delivery in the host tissue.

The biomaterial that incorporates all the features listed above doesn't exist yet. Nevertheless the increasing intercommunication with different scientific disciplines, together with the urgency in having more functional devices will constitute a strong input to face the challenge of the realization of functional tissues substitutes or delivery devices.

So far conventional surgical treatments for the reconstruction of lost skeletal muscle tissue function, caused by congenital defects, tumor ablation, traumatic injury or different myopathies (*131, 134*), yielded a limited degree of success. In the case of muscular dystrophy, generation of artificial muscles *in vitro* to be later on transplanted *in vivo* cannot be pursued; in fact supplying the dystrophic muscle with new muscular mass that it is no longer able to provide for, is important, but it doesn't accomplish the ultimate goal, that is the correction of the genetic defect, achievable by recreating a pool of healthy satellite cells in the diseased host muscle. Therefore, instead of an already differentiated muscle construct, a more functional approach would be the delivery of stem cells (satellite cells or myoblasts) that would proliferate, differentiate, and hopefully self-renew, *in vivo*.

1.8   AIM OF THE THESIS

The aim of this work was to investigate the design of a cell delivery protocol in dystrophic muscle, based on the coupling of myogenic cells and biomaterials.

For this purpose, biomaterials with different characteristics were combined with different types of myogenic cells and their efficacy was tested in the murine mdx dystrophic model.Our   ultimate goal is the development of a cell-based therapeutic protocol for muscular dystrophies in humans.

1.1 BIBLIOGRAPHY

1. R. Bischoff, in *Myology*. (In A. G. Engel, C. Franzini-Armstrong (Eds.) McGraw-Hill, New York, 1994), pp. 97-118.
2. A. Mauro, *J. Biohys. Biochem. Cytol.* **9**, 493 (1961).
3. F. P. Moss, C. P. Leblond, *J. Cell Biol.* **44**, 459 (February 1, 1970, 1970).
4. H. L. Beauchamp Jonathan R., Yu David S. W., Tajbakhsh Shahragim, Kelly Robert G., Wernig Anton, Buckingham Margaret E., Partridge Terence A., Zammit Peter S., *J. Cell Biol.* **151**, 1221 (December 11, 2000, 2000).
5. M. J. E. Beauchamp Jonathan R., Pagel Charles N., Partridge Terence A., *J. Cell Biol.* **144**, 1113 (March 22, 1999, 1999).
6. P. S. Zammit *et al.*, *Experimental Cell Research* **281**, 39 (2002).
7. D. D. W. Cornelison, B. J. Wold, *Developmental Biology* **191**, 270 (1997).
8. R. I. Sherwood, J. L. Christensen, I. L. Weissman, A. J. Wagers, *Stem Cells* **22**, 1292 (December 1, 2004, 2004).
9. D. D. W. Cornelison, M. S. Filla, H. M. Stanley, A. C. Rapraeger, B. B. Olwin, *Developmental Biology* **239**, 79 (2001).
10. P. Seale *et al.*, **102**, 777 (2000).
11. P. S. Zammit *et al.*, *J. Cell Biol.* **166**, 347 (August 2, 2004, 2004).
12. S. Kuang, K. Kuroda, F. Le Grand, M. A. Rudnicki, **129**, 999 (2007).
13. T. A. P. a. Z. Y.-R. Peter S. Zammit, *Journal of Histochemistry and Cytochemistry* **54**, 1177 (2006 Aug).
14. S. Kuang, M. A. Gillespie, M. A. Rudnicki, *Cell Stem Cell* **2**, 22 (Jan, 2008).
15. S. P. Asakura Atsushi, Girgis-Gabardo Adele, Rudnicki Michael A., *J. Cell Biol.* **159**, 123 (October 14, 2002, 2002).
16. M. A. LaBarge, H. M. Blau, **111**, 589 (2002).
17. R. I. Sherwood *et al.*, **119**, 543 (2004).
18. T. Partridge, **119**, 447 (2004).
19. C. A. Collins *et al.*, **122**, 289 (2005).
20. D. Montarras *et al.*, *Science* **309**, 2064 (September 23, 2005, 2005).
21. R. H. B. Eric P. Hoffman, Jr. d and Louis M. Kunkel, *Cell* **51**, 919 (1987).
22. J. M. Ervasti, K. P. Campbell, *Cell* **66**, 1121 (1991).
23. K. Matsumura, J. M. Ervasti, K. Ohlendieck, S. D. Kahl, K. P. Campbell, *Nature* **360**, 588 (1992).
24. E. Ozawa *et al.*, *Hum. Mol. Genet.* **4**, 1711 (September 1, 1995, 1995).
25. E. Bonilla *et al.*, *Cell* **54**, 447 (1988).

26. S. C. Watkins, E. P. Hoffman, H. S. Slayter, L. M. Kunkel, *Nature* **333**, 863 (1988).

27. L. Hemmings, P. A. Kuhlman, D. R. Critchley, *J. Cell Biol.* **116**, 1369 (March 1, 1992, 1992).

28. I. N. Rybakova, K. J. Amann, J. M. Ervasti, *J. Cell Biol.* **135**, 661 (November 1, 1996, 1996).

29. O. K. Ervasti James M., Kahl Steven D., Gaver Mitchell G., Campbell Kevin P., *Nature* **345**, 315 (1990).

30. M. Yoshida, E. Ozawa, *J Biochem* **108**, 748 (November 1, 1990, 1990).

31. J. B. S. B J Petrof, H H Stedman, M Kelly, H L Sweeney, *PNAS* **90** 3710 (1993 Apr).

32. G. Bulfield, W. G. Siller, P. A. Wight, K. J. Moore, *Proceedings of the National Academy of Sciences of the United States of America* **81**, 1189 (February 1984, 1984).

33. C. Pastoret, A. Sebille, *Journal of the neurological sciences* **129**, 97 (1995).

34. J. P. Lefaucheur, C. Pastoret, A. Sebille, *Anatomical Record* **242**, 70 (May, 1995).

35. J. E. M. C.A. Collins, *International Journal of Experimental Pathology* **84**, 165 (2003).

36. H. H. Stedman *et al.*, *Nature* **352**, 536 (1991).

37. D. J. Blake, A. Weir, S. E. Newey, K. E. Davies, *Physiol. Rev.* **82**, 291 (April 1, 2002, 2002).

38. A. Scime, M. A. Rudnicki, *Molecular Diagnosis & Therapy* **12**, 99 (2008).

39. H. Hoshiya *et al.*, *Mol Ther*, (2008).

40. W. D. Muntoni F, *Curr Opin Neurol.* **20**, 590 (2007 Oct).

41. J. C. van Deutekom *et al.*, *N Engl J Med* **357**, 2677 (December 27, 2007, 2007).

42. C. L. Barton-Davis E. R., Shoturma D. I., Leland S. E., Sweeney H. L., *Journal of Clinical Investigation* **104**, 375 (Aug, 1999).

43. P. Dunant, Walter, M. C, Karpati, G, Lochmuller, H., *Muscle & Nerve* **27**, 624 (May, 2003).

44. E. M. Welch *et al.*, *Nature* **447**, 87 (2007).

45. G. Cossu, M. Sampaolesi, *Trends in Molecular Medicine* **13**, 520 (2007).

46. T. A. Partridge, J. E. Morgan, G. R. Coulton, E. P. Hoffman, L. M. Kunkel, *Nature* **337**, 176 (1989).

47. J. E. Morgan, E. P. Hoffman, T. A. Partridge, *J. Cell Biol.* **111**, 2437 (December 1, 1990, 1990).

48. G. T. Law PK, Wang MG., *Muscle Nerve* **11**, 525 (1988 Jun).

49. R. G. Miller *et al.*, *Muscle & Nerve* **20**, 469 (Apr, 1997).

50. J. R. Mendell *et al.*, *N Engl J Med* **333**, 832 (September 28, 1995, 1995).

51. A. D. Karpati G, Arnold D, Gledhill RB, Guttmann R, Holland P, Koch PA, Shoubridge E, Spence D, Vanasse M, et al., *Ann Neurol.* **34(1)**, 8 (1993 jul).

52. P. G. K. Gussoni Emanuela, Lanctot Andrea M.,Sharma Khema R., Miller Robert G., Steinman Lawrence, Blau Helen M., *Nature* **356**, 435 (1992).

53. B. J. Huard J, Roy R, Labrecque C, Dansereau G, Lemieux B, Tremblay JP., *Clin Sci (Lond).* **81(2)**, 287 (1991 Aug).

54. B. J. Huard J, Roy R, Malouin F, Dansereau G, Labrecque C, Albert N, Richards CL, Lemieux B, Tremblay JP., *Muscle Nerve* **15(5)**, 550 (1992 May).

55. B. J. Tremblay JP, Malouin F, Théau D, Cottrell F, Collin H, Rouche A, Gilgenkrantz S, Abbadi N, Tremblay M, et al., *Neuromuscul Disord.* **3(5-6)**, 583 (1993 Sep-Nov).

56. M. F. Tremblay JP, Roy R, Huard J, Bouchard JP, Satoh A, Richards CL., *Cell Transplant.* **2(2)**, 99 (1993 Mar-Apr).

57. R. R. Huard J, Guérette B, Verreault S, Tremblay G, Tremblay JP., *Muscle Nerve.* **17**, 224 (1994 Feb).

58. M. M. Fan Y, Beilharz M, Grounds M., *Muscle Nerve* **19**, 853 (1996 Jul).

59. B. H. Gussoni E, Kunkel LM., *Nat Med.* **3**, 970 (1997 Sep).

60. B. M. Hodgetts SI, Scalzo AA, Grounds MD., *Cell Transplant.* **9**, 489 (2000 Jul-Aug).

61. H. S. Smythe GM, Grounds MD., *J Cell Mol Med.* **5**, 33 (2001 Jan-Mar).

62. V. J. Kinoshita I, Guérette B, Asselin I, Roy R, Tremblay JP., *Muscle Nerve.* **17**, 1407 (1994 Dec).

63. B. Guérette, I. Asselin, D. Skuk, M. Entman, J. P. Tremblay, *Cell Transplantation* **6**, 101 (1997).

64. Thomas A. Rando, *Experimental Cell Research* **220**, 383 (1995 Oct).

65. S. Daniel *et al.*, *Neuromuscular disorders : NMD* **17**, 38 (2007).

66. D. M. G. Skuk, Marlyne; Roy, Brigitte; Chapdelaine, Pierre; Bouchard, Jean-Pierre MD; Roy, Raynald PhD; Dugré, Francine J. PhD; Sylvain, Michel MD; Lachance, Jean-Guy MD; Deschênes, Louise MD; Senay, Hélène MD; Tremblay, Jacques P. PhD, *Journal of Neuropathology and Experimental Neurology* **65**, 371 (April 2006).

67. A. Sacco, R. Doyonnas, P. Kraft, S. Vitorovic, H. M. Blau, *Nature* **456**, 502 (2008).

68. M. Cerletti *et al.*, **134**, 37 (2008).

69. J. Y. Lee *et al.*, *Journal of Cell Biology* **150**, 1085 (Sep, 2000).

70. H. R. Peng, J. Huard, *Transplant Immunology* **12**, 311 (Apr, 2004).

71. B. H. Cao *et al.*, *Nature Cell Biology* **5**, 640 (Jul, 2003).

72. Y. Torrente *et al.*, *J. Cell Biol.* **152**, 335 (January 22, 2001, 2001).

73. Z. Qu-Petersen *et al.*, *J. Cell Biol.* **157**, 851 (May 28, 2002, 2002).

74. C. G. Ferrari Giuliana, Angelis De, Coletta Marcello, Paolucci Egle, Stornaiuolo Anna, Cossu Giulio, Mavilio Fulvio, *Science* **279**, 1528 (March 6, 1998, 1998).

75. F. D. Camargo, R. Green, Y. Capetenaki, K. A. Jackson, M. A. Goodell, *Nat Med* **9**, 1520 (2003).

76. D. Hess *et al.*, *Nature Biotechnology* **21**, 763 (Jul, 2003).

77. Y. Torrente *et al.*, *Journal of Clinical Investigation* **114**, 182 (Jul, 2004).

78. Y. Torrente *et al.*, *Cell Transplantation* **16**, 563 (2007).

79. R. Benchaouir *et al.*, **1**, 646 (2007).

80. M. G. Minasi *et al.*, *Development* **129**, 2773 (Jun, 2002).

81. G. Cossu, P. Bianco, *Current Opinion in Genetics & Development* **13**, 537 (Oct, 2003).

82. M. Sampaolesi *et al.*, *Science* **301**, 487 (Jul, 2003).

83. M. Sampaolesi *et al.*, *Nature* **444**, 574 (2006).

84. R. Palumbo *et al.*, *Journal of Cell Biology* **164**, 441 (Feb, 2004).

85. D. G. Miranda, E. D. Kay, *Neuromuscular disorders : NMD* **17**, 206 (2007).

86. B. Peault *et al.*, *Mol Ther* **15**, 867 (2007).

87. I. W. McKinnell, G. Parise, M. A. Rudnicki, P. S. Gerald, in *Current Topics in Developmental Biology*. (Academic Press, 2005), vol. Volume 71, pp. 113-130.

88. Darabi R, *Stem Cell Reviews* **4**, 217 (2008).

89. W. E. Blanco-Bose, C.-C. Yao, R. H. Kramer, H. M. Blau, *Experimental Cell Research* **265**, 212 (2001).

90. Z. Qu *et al.*, *J. Cell Biol.* **142**, 1257 (September 7, 1998, 1998).

91. D. C. Kirouac, P. W. Zandstra, **3**, 369 (2008).
92. . Hijiri Ito, *Muscle & Nerve* **21**, 291 (1998).
93. E. F. E. Torrente Y, Caron NJ, Bresolin N, Tremblay JP., *Cell Transplant.* **9**, 539 (2000 Jul-Aug).
94. A. I. Caron NJ, Morel G, Tremblay JP., *Cell Transplant.* **8**, 465 (1999 Sep-Oct).
95. V. J. Langer R, *Science* **260**, 920 (1993 May 14).
96. L. E. Freed, G. Vunjak-Novakovic, *Advanced Drug Delivery Reviews* **33**, 15 (1998).
97. B. P. Bach A. D., Stern-Staeter J., Horch R. E. , *Journal of Cellular and Molecular Medicine* **8**, 413 (2004).
98. B. S. N. Palsson B. O, *Tissue Engineering*. (Pearson Education, Inc., San Diego, CA, 2004), pp. 407.
99. C. A. Vacanti, L. J. Bonassar, M. P. Vacanti, J. Shufflebarger, *N Engl J Med* **344**, 1511 (May 17, 2001, 2001).
100. A. T. Mehlhorn *et al.*, *Tissue Engineering Part A* **0**.
101. S. Kitahara *et al.*, *Tissue Engineering Part A* **14**, 1905 (2008).
102. M. K. Smith, M. C. Peters, T. P. Richardson, J. C. Garbern, D. J. Mooney, *Tissue Engineering* **10**, 63 (2004).
103. T. P. Richardson, M. C. Peters, A. B. Ennett, D. J. Mooney, *Nat Biotech* **19**, 1029 (2001).
104. S. B. Andrea Callegari, Laura Iopa, Angela Chiavegato, Gianluca Torregrossa, Michela Pozzobon, Gino Gerosa, Paolo De Coppi, Nicola Elvassore, Saverio Sartore, *Biomaterials* **28**, 5449 (2007 Dec).
105. M. Poh *et al.*, *The Lancet* **365**, 2122.
106. G. Zund *et al.*, *European Journal of Cardio-Thoracic Surgery* **11**, 493 (1997).
107. Zimmermann WH et al, *Biotechnology and Bioengineering* **68**, 106 (2000).
108. S. Sekiya, T. Shimizu, M. Yamato, A. Kikuchi, T. Okano, *Biochemical and Biophysical Research Communications* **341**, 573 (2006).
109. T. Shimizu *et al.*, *Circ Res* **90**, e40 (February 22, 2002, 2002).
110. T. Shimizu, M. Yamato, A. Kikuchi, T. Okano, *Biomaterials* **24**, 2309 (2003).
111. W.-H. Zimmermann *et al.*, *Nat Med* **12**, 452 (2006).
112. W.-H. Zimmermann *et al.*, *Circulation* **106**, I (September 24, 2002, 2002).
113. K. L. Christman, R. J. Lee, *Journal of the American College of Cardiology* **48**, 907 (2006).
114. P. S. Robinson, S. L. Johnson, M. C. Evans, V. H. Barocas, R. T. Tranquillo, *Tissue Engineering Part A* **14**, 83 (2008).
115. M. E. Davis *et al.*, *Circulation* **111**, 442 (February 1, 2005, 2005).
116. J. S. Choi, S. J. Lee, G. J. Christ, A. Atala, J. J. Yoo, *Biomaterials* **29**, 2899 (2008).
117. S. A. Riboldi *et al.*, *Journal of Biomedical Materials Research Part A* **84**, 1094 (2008).
118. A. J. Engler *et al.*, *Journal of Cell Biology* **166**, 877 (Sep, 2004).
119. L. Boldrin *et al.*, *Tissue Engineering* **13**, 253 (2007).
120. W. Bian, N. Bursac, *Biomaterials* **30**, 1401 (2009).
121. W. Yan *et al.*, *Tissue Engineering* **13**, 2781 (2007).
122. T. Neumann, S. D. Hauschka, J. E. Sanders, *Tissue Engineering* **9**, 995 (2003).
123. P. E. Kosnik, J. A. Faulkner, R. G. Dennis, *Tissue Engineering* **7**, 573 (2001).
124. V. Herman H, *Annals of the New York Academy of Sciences* **961**, 201 (2002).
125. H. I. Kroehne V, Schügner F, Lasrich D, Bartsch JW, Jockusch H., *J Cell Mol Med* **12** 1640 (2008 Sep-Oct).

126. E. Hill, T. Boontheekul, D. J. Mooney, *Tissue Engineering* **12**, 1295 (2006).
127. K. Y. Lee, D. J. Mooney, *Chemical Reviews* **101**, 1869 (2001).
128. M. J. Mahoney, K. S. Anseth, *Biomaterials* **27**, 2265 (2006).
129. D. G. Anderson, J. A. Burdick, R. Langer, *Science* **305**, 1923 (September 24, 2004, 2004).
130. J. Y. Kang *et al.*, *International Journal of Pharmaceutics* **In Press, Corrected Proof**.
131. B. N. Bian W, *IEEE Eng Med Biol Mag.* **27**, 109 (2008 Sep-Oct).
132. S. Zhang, F. Gelain, X. Zhao, *Seminars in Cancer Biology* **15**, 413 (2005).
133. M. P. Lutolf, J. A. Hubbell, *Nat Biotech* **23**, 47 (2005).
134. A. A. Mouly V, Périé S, Mamchaoui K, Barani A, Bigot A, Bouazza B, François V, Furling D, Jacquemin V, Negroni E, Riederer I, Vignaud A, St Guily JL, Butler-Browne GS., *Acta Myol* **24**, 128 (2005 Oct).

CHAPTER 2

THREE DIMENSIONAL COLLAGEN SCAFFOLD FOR CELL DELIVERY IN DYSTROPHIC MUSCLE

2.1 INTRODUCTION

As described in details in Chapter 1, the way cells are delivered *in vivo* is of crucial importance in order to accomplish an efficient cell-based therapy.

Our group has been working for some time on the use of different biomaterials to perform cell delivery *in vivo,* in order to overcome problems such as cell death following transplantation. Our first approach was to deliver large number of cells in recipient muscles, something that hence required *in vitro* expansion before transplantation. In order to ensure the myogenicity of our cells we did not use conventional primary myoblasts but myogenic precursors cells (MPCs). The difference was that these latter were isolated from cultured, isolated single muscle fibers (see Figure 2.1.1 for an example), thereby minimizing the contamination from non-myogenic cells that are inevitably present in a conventional primary culture preparation (i.e., obtained by enzymatic digestion of the whole muscle).
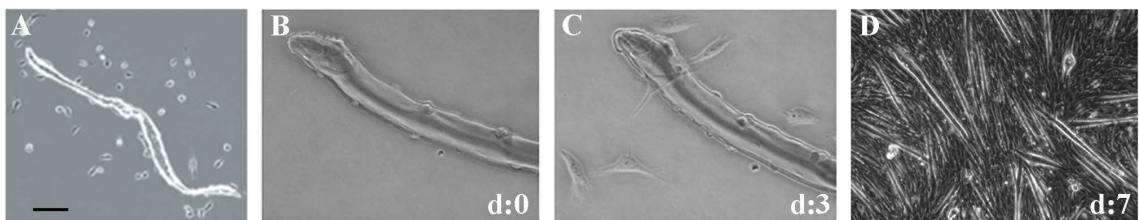
Figure 2.1   **Proliferation of MPCs around a single, isolated muscle fiber. If allowed to reach confluence cells differentiated into myotubes. Numbers in B-D indicate the days elapsed from fiber plating. Scale bar in A is 100 μm.**

GFP-positive MPCs were then seeded onto bi-dimensional PLGA (poly lactic-co-glycolic acid) scaffolds and implanted into the *tibialis anterior* muscles of *wild type* syngeneic animals (*1*). These experiments showed that scaffold-mediated delivery was

superior to direct intramuscular injection in terms of survival, migration and grafting of the implanted cells. Despite the promising results, though, these polymeric scaffolds presented some limitation; PLGA intrinsic rigidity did not mimic muscle tissue consistency and the release of lactic and glycolic acids during PLGA degradation adversely affects the host environment.

For this reason we moved to a different type of biocompatible matrix, porous collagen sponge. Our group had already shown a pro angiogenic effect of this type of matrix in intact and cryoinjured rat heart *in vivo* (*2*), and a similar scaffold, although with an ordered structure, has recently been used as a leading matrix to guide myotubes formation inside host *wt* recipient mice (*3*). Here we investigated the use of three-dimensional collagen scaffold as a potential vehicle for myogenic cell delivery *in vivo* to restore dystrophin expression in *mdx* mice. To the best of our knowledge, this is the first time a biomaterial is coupled with cells in order to perform cell delivery in dystrophic muscles.

From a biomimetic perspective, functionally engineered muscle constructs should exhibit native-like structural properties (*4*); to this end, collagen was deemed to be better than PLGA because, besides being a natural and biodegradable material like PLGA, its sponge is three-dimensional and highly elastic and, therefore, compatible with muscle biomechanical properties. In our experimental design, collagen scaffold would have provided a three-dimensional physical support for transplanted cell growth. Its three-dimensional structure, characterized by elevated porosity and large internal surface, would have allowed to seed high numbers of cells, thereby potentially constituting a cell reservoir for long-term delivery. Last but not least, thanks to its elastic nature, collagen sponge could have had the potential to reduce the cellular suffering derived from the manipulations required during *in vivo* implantation.

2.2 MATHERIALS AND METHODS

2.2.1 MPCs Culture

MPCs cultures were obtained following the protocol previously described (*5*). Briefly, flexor digitorum brevis and extensor digitorum longus were removed from 2 to 3 months old C57BL/6-Tg(ACTB-EGFP)1Osb/J GFP transgenic mice or C57BL/10ScSn/J mice (Jackson Laboratories) and digested with 0,2% Collagenase Type I (Sigma-Aldrich, USA) in Dulbecco's Modified Eagle Medium (DMEM; unless otherwise indicated all cell culture reagents were from Invitrogen). Single fibers were individually harvested, plated on Petri dishes previously coated with 10% Matrigel (BD Bioscience) in DMEM and maintained in a humidified tissue culture incubator in plating medium, (DMEM, 10% horse serum; 1% chicken embryo extract (MP-Biomedicals), 1% penicillin-streptomycin). After 72 hours, culture medium was switched to proliferating medium, (DMEM; 20% fetal bovine serum, 10% horse serum; 0.5% chicken embryo extract and 1% penicillin-streptomycin). Cells were kept in culture with proliferating medium and detached from the plate with 0.5% Trypsin-EDTA before reaching confluence.

2.2.2   3D COLLAGEN SCAFFOLD

3-D porous collagen sponges (Avitene® Ultrafoam™ Collagen Hemostat. Davol Inc., Cranston, USA) were used. Prior to cell seeding, collagen scaffolds (2×2×8mm) were covered with DMEM for 12 hours at 37°C. Afterwards, scaffolds were conditioned with 5% Matrigel in DMEM at 4°C for 20 minutes and then kept at 37° C until cell seeding.

2.2.3   CELL CULTURE ON 3D COLLAGEN SCAFFOLD

At passage number 2, MPCs were detached from the plates, spun down, washed twice in phosphate buffer solution (PBS) to remove the serum and the indicated amount of cells was re-suspended in approximately 15 µl of 5% Matrigel in DMEM. Cell suspension was then seeded onto the collagen scaffold. In order to prevent dehydration, 30 µl of proliferating medium were added onto the collagen pieces every hour and after 4 hours the cellularized scaffolds were covered with 5 mL of the same medium. After 24 hours cellularized scaffolds were either implanted *in vivo* or embedded in OCT (Sigma-Aldrich) and snap-frozen in liquid nitrogen.

2.2.4   CELL VIABILITY WITHIN THE SCAFFOLD

Cell survival inside the scaffold was evaluated with LIVE/DEAD® assay (Molecular Probes, Invitrogen). 150 µL of a solution 3.5 µM Calcein and 3.0 µM Ethidium Bromide in DMEM were added to the seeded scaffolds and incubated 45 minutes at room temperature. Following incubation, the scaffolds were washed in phosphate buffer (PBS) and labeled cells were observed at fluorescence microscope (Leica, DMI 6000B).

2.2.5   CELL INJECTION

At passage number 2, MPCs were detached from the plate with citrate buffer solution (KCl 50 gr, $C_6H_5Na_3O_7 \cdot 2H_2O$ 21,4 gr, to 500 ml with ultrapure water), and the indicated amounts were re-suspendend in 40 µl DMEM 5% Matrigel per each dose. Cells were stored on ice at 4°C until injection. Preliminary experiments had shown that

cells treated in this way and then seeded onto standard cell culture dishes were still able to attach and proliferate.

2.2.6 RECIPIENT ANIMALS FOR IN VIVO IMPLANTS

All animals were housed and operated at the Animal Colony of the "Centro Interdipartimentale Vallisneri", University of Padova, following all relevant bylaws issued by the Italian Ministery of Health. Animals were anesthetized with 2% isoflurane; post-op care included three-days analgesic (tramadol 10mg/kg) and antibiotic treatment (enrofloxacin 15 mg/kg). 2 C57BL/6J recipient mice were treated with GFP positive MPCs, delivered through three-dimensional collagen scaffold or directly injected into *tibialis anterioris* muscles and analyzed 48 hours after transplantation *in vivo* to perform analysis on cell distribution and apoptosis.12 C57BL/10J mdx recipient mice were treated with *wild type* MPCs delivered through three-dimensional collagen scaffold or directly injected in *tibialis anterioris* muscles and analyzed at 10, 20, 30 and 180 days post implant, in order to identify the highest dystrophin yield in collagen-implanted muscles in comparison to injected ones. 6 C57BL/10J mdx recipient mice were treated with *wild type* MPCs delivered through three-dimensional collagen scaffold or directly injected in *tibialis anterioris* muscles and analyzed 30 days post implant, to quantify desmin and dystrophin expression in dystrophic muscles. 6 C57BL/10J mdx recipient mice were engrafted with collagen scaffold delivered *wt* MPCs (Coll. Sc. 10 days, Coll. Sc. 30 days) or with non-cellularized collagen scaffold (Empty Scaffold 30 days) transplanted to *tibialis anterioris* muscles, in order to analyze dystrophin positive fibers distribution at 10 (3 mice) and 30 days (3 mice).

2.2.7 SURGICAL PROCEDURE

3D cellularized collagen scaffolds were delivered into the left *tibialis anterior* (TA) muscles of C57BL/6 wild-type mice 24 hours after cell seeding. Approximately 25% of flesh mass was removed from muscle core and collagen scaffolds were inserted inside it; muscles were then closed with non-absorbable 7/0 sutures. Injections were performed on right *tibialis anterior* (TA) muscles. Upon opening the skin and sectioning the

epimysium to expose the muscle surface, satellite cells were delivered through a 30G needle; before injection, mechanical damage was induced by stirring the needle inside the muscle core, in order to try and minimize differences obtained from the damage caused by scaffold insertion. At the indicated times, mice were killed by cervical dislocation and treated muscles were excised and frozen in melting (159°C) isopentane.

2.2.8   TUNEL ASSAY

Tunel assay was performed using ApopTag® *In Situ Cell Detection Kit* (Roche), according to manufacturer instructions.

2.2.9   LIVE/DEAD ASSAY®

The LIVE/DEAD Viability/Cytotoxicity Kit (Invitrogen) is a two-color assay to determine viability of cells in a population. The kit identifies live versus dead cells on the basis of membrane integrity and esterase activity (green colored); cells with damaged membrane will incorporate Ethidium Bromide (red coloured) .

2.2.10   IMMUNOHISTOCHEMISTRY

Cryogenized muscles and cellularized frozen scaffolds were sectioned with a cryostat in 10 µm slices for immuno-staining. Section of 10 µm were fixed with para-formaldehyde (PFA) 2% in PBS for 7 minutes. Primary antibodies against desmin and dystrophin (rabbit polyclonal, AbCam, UK) were diluted 1:100 and 1:200 respectively in PBS containing 3% bovine serum albumin (BSA) and applied for 1 hour at 37 °C. Primary antibodies against MyoD and Myogenin (rabbit polyclonal, Santa Cruz, Germany) were diluted 1:50 in PBS-3% BSA and individually applied overnight at 4°C. Secondary antibody Cy™3-conjugated anti-rabbit IgG (Jackson Research, UK) was diluted 1:250 in PBS-3% BSA and applied for 45 minutes at 37°C.

After treatment with fluorescent secondary antibodies, slides were mounted in fluorescent mounting medium (DakoCytomation), containing the nuclear counterstain 4',6-diamidino-2-phenylindole (DAPI; 2 µg/µl).

2.2.11   COLLAGEN SCAFFOLD DEGRADATION TIME IN VIVO

Degradation time for collagen scaffold implanted *in vivo* was obtained by measuring scaffold section area inside the implanted muscles at different time points (10 and 30 days); time 0 refers to the scaffold section area prior to *in vivo* transplantation.

2.2.12   DYSTROPHIN POSITIVE FIBERS DISTRIBUTION

Distribution of dystrophin positive fibers in grafted *mdx* muscles was obtained by comparing three different sets of samples: muscles transplanted with cellularized collagen scaffolds analyzed at 10 days (Coll. Sc. 10days), at 30 days (Coll. Sc. 30days), and muscles transplanted with non-cellularized collagen scaffolds (SI-30 days), used as internal control. Image analysis was carried out using the Leica DMI6000 software; at least 10 sections were analyzed per each condition.

2.2.13   DYSTROPHIN QUANTIFICATION

The number of dystrophin positive fibers was obtained by scoring muscle sections upon dystrophin immunostaining, using a fluorescence microscope (Leica, DMI 6000B) equipped with a DFC350FX Leica camera and the Leica DMI6000 software; at least 10 sections were analyzed for each condition. The best section per slide was considered per sample; absolute numbers were normalized with the muscle section area.

2.2.14   STATISTICAL ANALYSIS

Statistical analysis were conducted with function anova1, software MATLAB.

2.3   *RESULTS*

2.3.1   *IN VITRO CHARACTERIZATION OF COLLAGEN SCAFFOLD*

Collagen sponge was cut in small parallelepipeds (~2x2x8 mm) with a volume of approximately 0.3 cm^3. Collagen sponge is a soft, highly elastic material, which is characterized by high porosity and surface-to-volume ratio. This in turn translates into high internal specific surface and therefore into high capacity of the scaffold to contain cells. Fig. 2.3.1, B shows the high porosity of collagen, characterized by many interconnected channels with a diameter of ~100 µm.
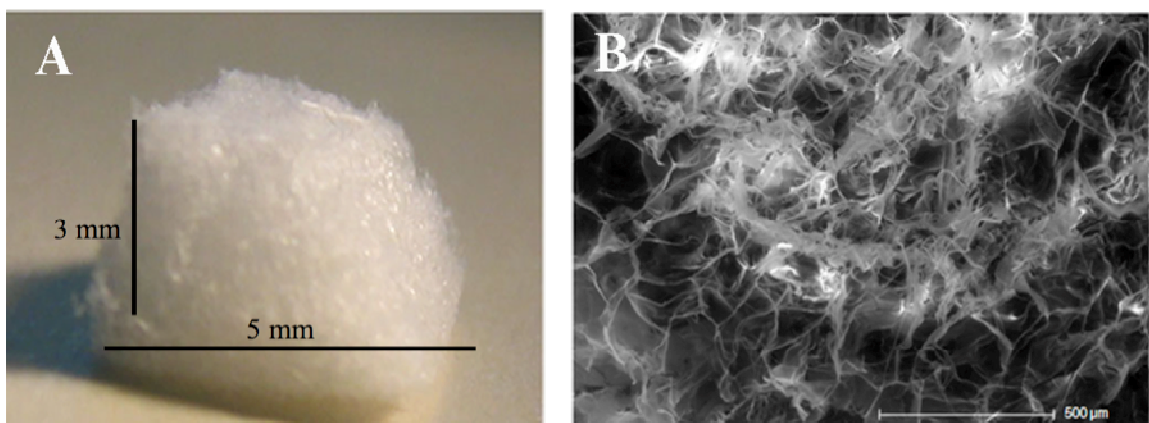

Figure 2.2   **UltrafoamTM collagen sponge. A; dry state. B; ESEM micrograph of dry collagen scaffold at 70X magnification.**

2.3.2   SCAFFOLD BIOCOMPATIBILITY WITH HIGH MYOGENIC CELL DENSITIES

In our experimental rationale collagen scaffold was thought as a cell reservoir for long-term delivery, therefore it was necessary to culture the highest possible number of cells inside the scaffold. Different seeding procedures (involving different volumes of cell suspensions and numbers of applications) were tested in order to obtain both dense and homogeneous cell culture inside the scaffold; the maximum cell number that was reached, while assuring homogeneous cell distribution, was assessed to be around 700000 cells per ~30 mm^3 volume sponge (approximately 23000cells/mm^3).

2.3.3   CELL DISTRIBUTION INSIDE TRANSPLANTED SCAFFOLDS

Cell distribution inside the scaffold was also verified after *in vivo* implant. GFP-positive MPCs isolated from C57BL/6-Tg(ACTB-EGFP)1Osb/J mice were seeded onto collagen scaffold and then transplanted into the tibialis anterior muscles of *wild type*. syngenic animals. Fig. 2.3.2 shows the green cells inside a scaffold as seen 48 hours after implant. It can be noticed how the distribution is quite homogeneous, the GFP-positive MPCs being evenly spread over the entire scaffold section with no differences between its boundaries and its core. Some host-derived (GFP-negative) cells that had migrated inside the scaffold are visible as well. At the same time, some GFP-positive cells had already migrated outside the scaffold into the surrounding muscle (C), occasionally acquiring a satellite-like position (D).
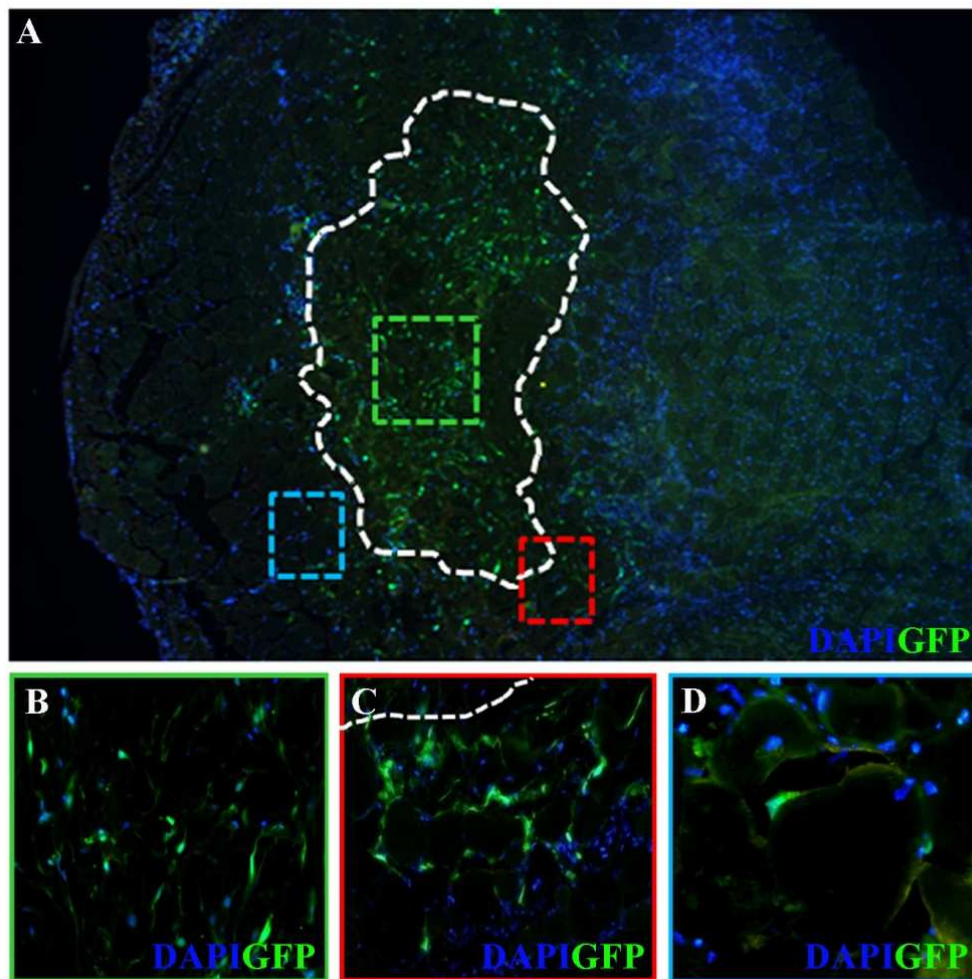
Figure 2.3 **Cell distribution inside the scaffold. A: overview of muscle implanted with collagen scaffold. B: detail of cell distribution inside the scaffold; C: detail of GFP positive MPCs that had migrated outside the scaffold; C: detail of GFP positive MPCs that had acquired a satellite-like cell position. Original magnification was 50x for panel A and 400x for panels B-D.**

2.3.4 CELL DEATH INSIDE IMPANTED SCAFFOLDS IN VIVO

Collagen scaffold functions as a physical support for myoblasts adhesion and growth. In order to investigate whether the scaffold was able to protect MPCs from the host environment, survival of implanted MPCs was evaluated. To this aim, GFP-positive MPCs were transplanted either *via* collagen scaffold or direct injection into *wild type* syngeneic animals and DNA fragmentation was evaluated after 48 hours using a TUNEL (Terminal deoxynucleotidyl transferase mediated dUTP Nick End Labeling) assay. It should be noted that although this procedure is commonly used to identify apoptotic cells, in the context of *in vivo* cell transplantation it also labels necrotic cells (*6*).

41

Muscles implanted with collagen scaffold displayed <5% of GFP-TUNEL-positive cells, whereas injected ones the amount was around 15%. Collagen scaffold-implanted muscles showed TUNEL-positive nuclei mostly at the muscle-scaffold interface, with very little signal present in GFP positive cells (Scaffold, G and merged images in H). On the other hand, injected muscles displayed higher apoptosis level than implanted ones (Injection, C and merged images in D) with most of the apoptotic cells distributed around the injection site. It should be noted that, as expected, in both cases most of the TUNEL-positive cells appeared to be part of the cellular inflammatory infiltrate.
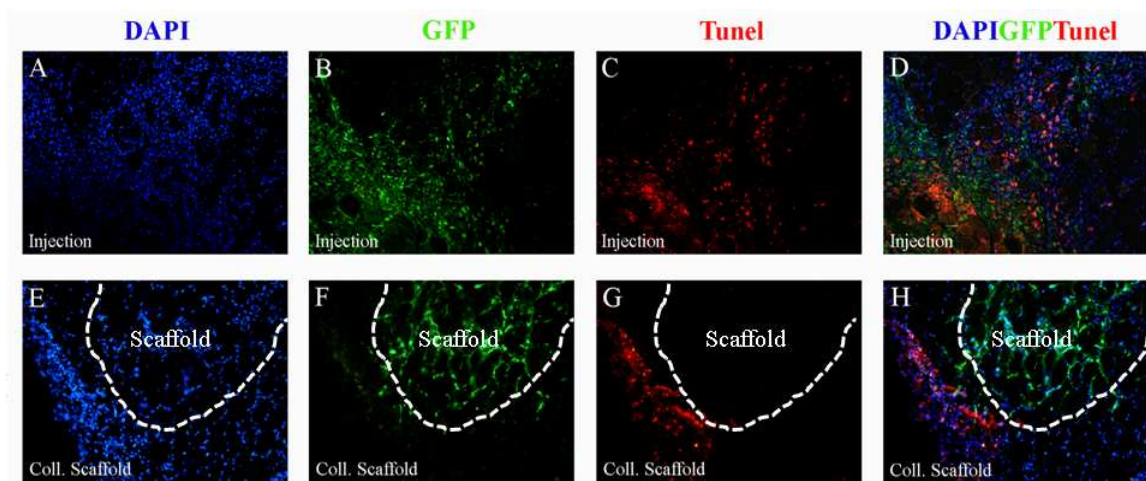

Figure 2.4 **TUNEL quantification in injected muscles (A to D) in comparison to muscles implanted with Collagen Scaffold (E to H), at 48 hours after transplantation. Original magnification 20X.**

2.3.5   CHARACTERIZATION OF COLLAGEN-SEEDED CELLS

In order to investigate whether MPCs in collagen scaffold were viable and myogenic when cultured at high density in a 3D support, cellularized collagen scaffold was characterized prior to transplantation. MPCs were isolated and expanded from *wild type* C57BL/10ScSn/J mice (the background strain of *mdx*) and seeded onto collagen scaffolds. After 24 hours cellularized scaffolds were analyzed for cell viability through LIVE/DEAD® assay and for myogenic markers expression through immunofluorescence analysis. LIVE/DEAD® assay showed that collagen scaffold allowed very good cell viability, as only occasional dead cells could be seen, mostly in the core of the scaffold (fig. 2.3.4, A-B).

MPCs seeded onto collagen scaffold were analyzed for myogenic markers as well (Fig. 2.3.4, D-I), whose expression was quantified (Fig. 2.3.4 C, dark bars). MPCs on the scaffold showed to be positive to desmin (86%), to MyoD (74%) and to myogenin (38%), revealing a similar expression pattern in comparison to what was observed for MPCs cultured on standard culture dishes (Fig. 2.3.4 C, light bars).
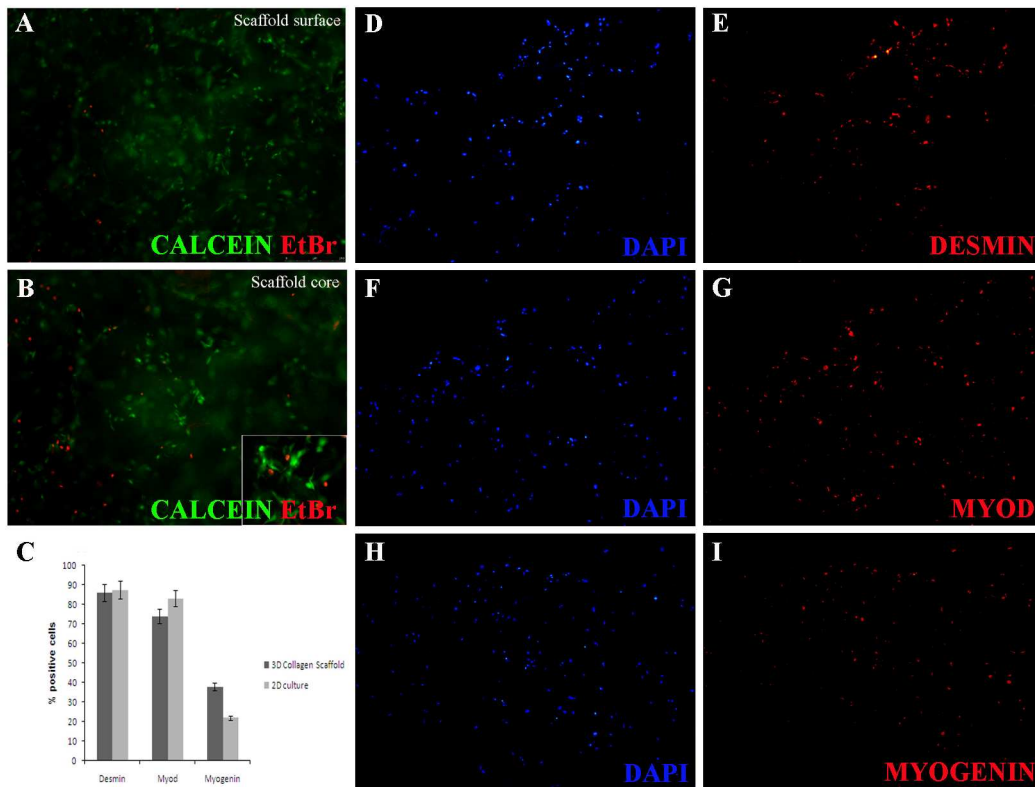

Figure 2.5 **Cellularized collagen scaffold characterization before implant. 24 h after cell seeding, cellularized scaffolds were either analyzed for cell viability (A-B) and for myogenic markers expression (C-I). A-B: Viability cell assay. Cell viability was evaluated in the scaffold surface (A) and the scaffold core (B); green color identifies living cells, red color identifies dead ones. C: Characterization of MPCs seeded onto the scaffold before implant. The graph shows the percentage of cells positive to myogenic markers Desmin, MyoD and Myogenin in MPCs seeded onto 3D CSI (dark bars) and cultured on 2D Petri dish (light bars). D-I: Immunostaining for myogenic markers desmin (D-E), MyoD (F-G) and myogenin (H-I); nuclei were counterstained with DAPI.**

2.3.6 DELIVERY OF DYSTROPHIN EXPRESSING CELLS INTO MDX MICE

Once assessed that collagen scaffold allowed cell viability and myogenic markers expression *in vitro*, collagen scaffold potentialities for cell delivery into dystrophic muscles was investigated with *in vivo* experiments in *mdx* mice. To this aim, MPCs were extracted from EDLs and FDBs muscles of C57BL/10ScSn/J mice, expanded *in vitro* and then either injected or seeded on collagen scaffold and implanted in the tibialis anterior muscles of *mdx* mice using the same procedures described above. Initial

43

experiments were carried out at different time points, sacrificing the animals at 10, 20, 30 and 180 days. These data showed that collagen scaffold implanted muscles yielded the highest number of dystrophin positive fiber in comparison to injected ones at 30 days (Fig. 2.3.5).
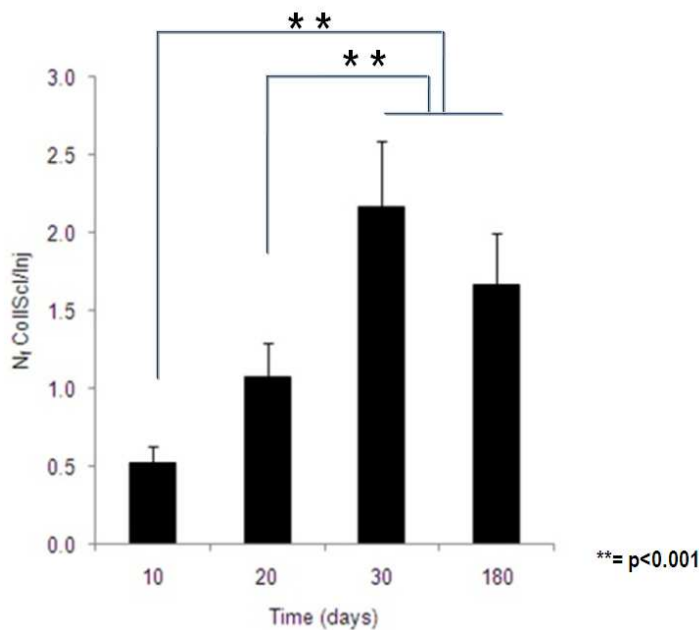

Figure 2.6 **Ratio of the maximum number of dystrophin positive fibers per section (Nf) present in implanted versus injected muscles at 10, 20, 30 and 180 days post delivery. Anova analysis revealed that 30 and 180 days yielded higher numbers of dystrophin positive fibers in comparison to 10 and 20 days (p<0.001); there is no significant difference between yields at 30 and 180 days.**

All following experiments were then carried out at this time point. Muscle sections were analyzed for desmin and dystrophin expression, and the areas of collagen implants were also measured. This latter data was used not only to determine the actual muscle area of the sections to normalize the content of dystrophin fibers, but also to estimate the degradation curve of the implanted scaffolds. As shown in Fig. 2.3.6, panel C, at 30 days collagen scaffold was still visible in treated muscles, constituting about 20% of the entire muscle section area; by using analogous data obtained at the ten days time point and plotting them in a curve, the time needed for scaffold complete degradation *in vivo* was estimated to be around 3 months. As expected, scaffold size reduction was accompanied by the formation of new muscle fibers, as assessed by desmin immunostaining (Fig. 2.3.6, A). Interestingly, desmin positive fibers, as well as some single cells, could also be observed inside the scaffold (Fig. 2.3.6, B). Dystrophin

immunostaining (Fig. 2.3.6, D to F) showed that in injected muscles the number of dys-positive fibers was quite low (up to 50 per section), similar in fact to that of revertant fibers in untreated muscles. On the other hand, collagen scaffold implanted muscles showed higher number (up to 120 per section) of dystrophin positive fibers, mostly organized in clusters localized around the scaffold at the interface with the surrounding muscle (Fig. 2.3.6, E). Occasionally, small dystrophin positive fibers that had grown inside the scaffold were also observed (Fig. 2.3.6, F). The maximum number of dystrophin-positive fibers found in implanted and injected muscles is summarized in Figure 2.3.7.
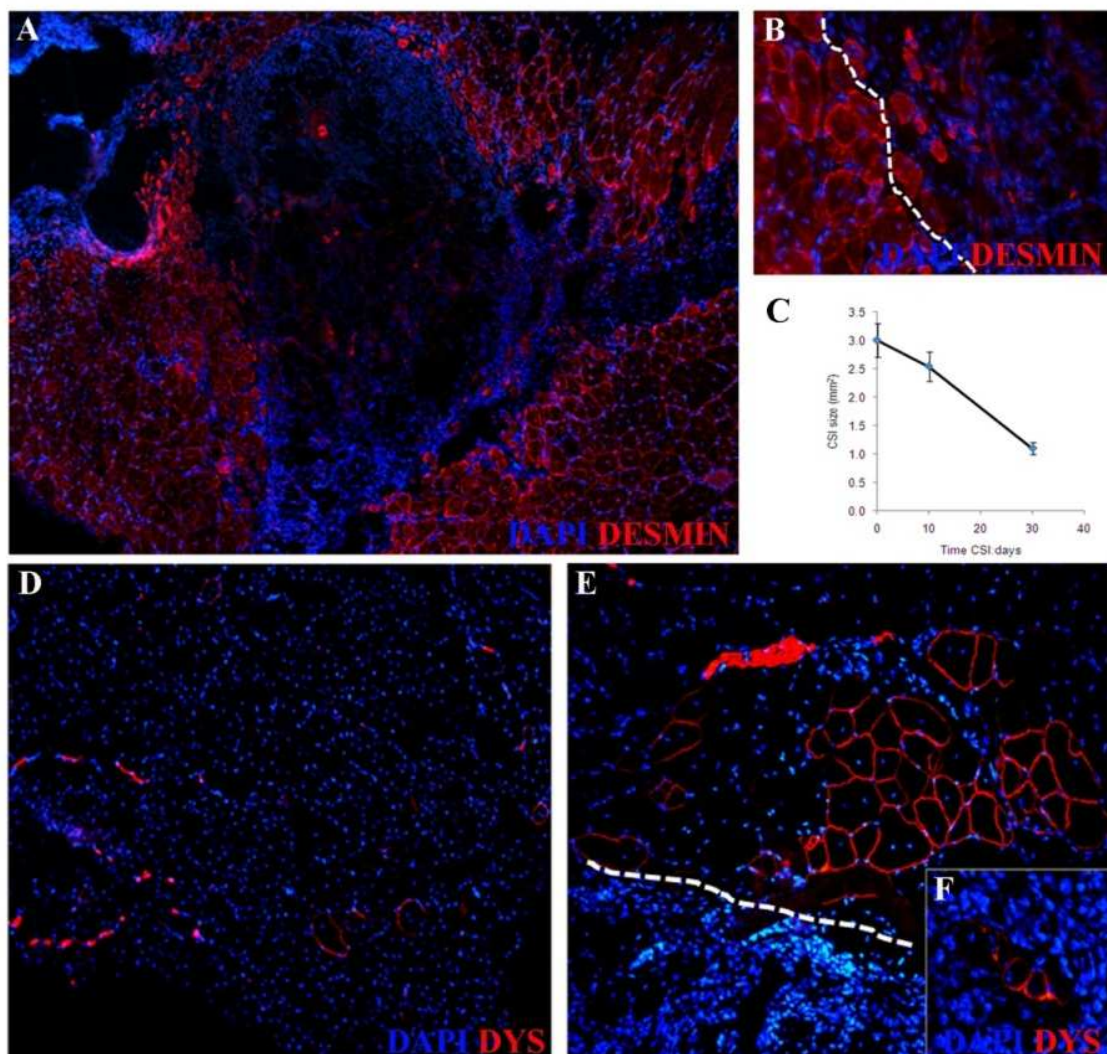
Figure 2.7   **Characterization of implanted and injected muscles *in vivo* at 30 days post implant: immunostaining for desmin (A-B), dystrophin (D-F) positive fibers, and evaluation of *in vivo* collagen scaffold degradation time (C). A: desmin positive fibers in collagen implanted muscles. B: magnification of the interface between scaffold and muscle. C: size quantification of CSI at 10 and 30 days post implant, d:0 corresponds to the size of cellularized collagen scaffolds before implantation. D: dystrophin positive fibers in injected muscles. E: cluster of dystrophin**

positive fibers at the interface between collagen-scaffold and muscle. F: magnification of two fibers found inside the scaffold in collagen implanted muscles. Original magnification was 100x in A and D, 200x in E and 400x in B and F.
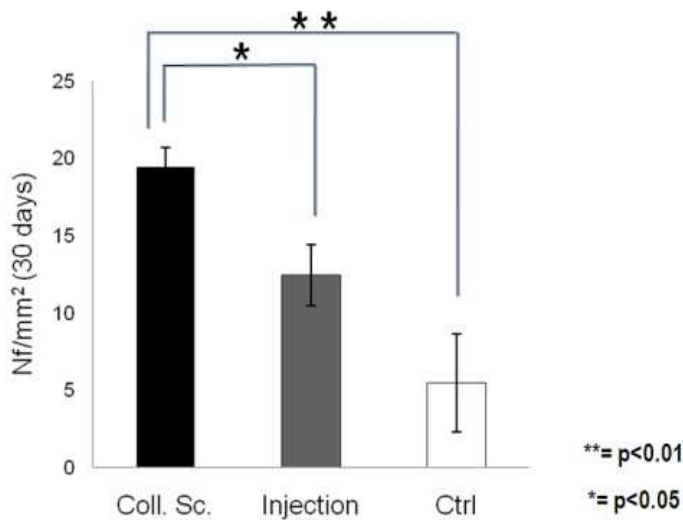

Figure 2.8   Number of dystrophin positive fibers (Nf) quantified in implanted and injected muscles in comparison to untreated muscles (Ctrl) at 30 days. ** corresponds to p≤0,01 ; * corresponds to p≤0,05 (Anova)

2.3.7   *DISTRIBUTION OF DYSTROPHIN POSITIVE FIBERS IN IMPLANTED MUSCLES*

The approach used to assess the distribution of dystrophin positive fibers was as follows: scaffold surface area was traced inside the implanted muscle section area and radial rings around it were traced as well (200 µm spaced; dashed lines in panel A). The distance of every single dystrophin positive fiber from the scaffold, (which was considered as the origin point), was calculated. Each event was classified in groups, based on their increasing distance from the scaffold, whose distribution is depicted in panel B.; Calculations were performed for two time points, 10 and 30 days, and data were compared with those obtained with control muscles that had been implanted with just empty scaffolds. This way we were able to monitor the possible effect of muscle regeneration on the number of revertant fibers. Muscles implanted with cellularized collagen scaffold at 10 days and non-cellularized collagen scaffold at 30 day showed a similar profile, with homogeneous distribution of dystrophin positive fibers within 800 µm from the scaffold. On the contrary, muscles implanted with cellularized scaffolds at

30 days, showed much higher numbers of dystrophin positive fibers, which were distributed close to the scaffold.
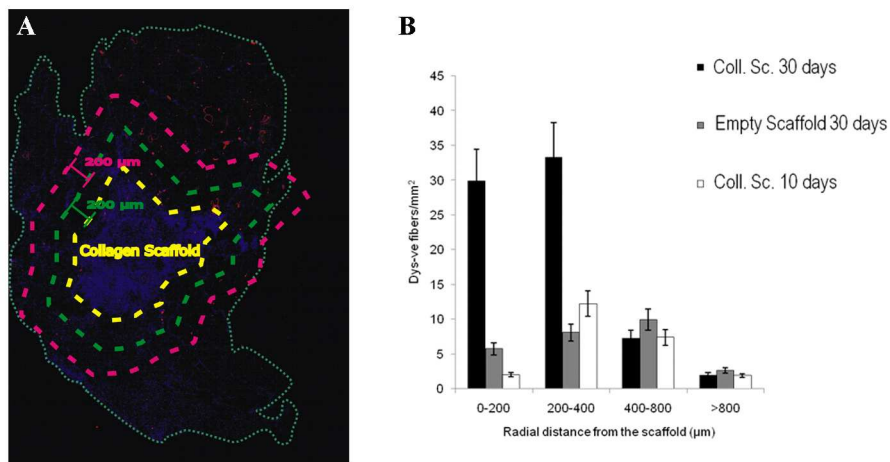
Figure 2.9   Profile of dystrophin positive fibers distribution in collagen scaffold implanted muscles. A: Schematic representation of one of the muscle sections analyzed for this purpose. The area of the scaffold was traced inside a muscle's section (yellow dashed line) and radial areas 200 μm spaced were then traced around the scaffold's area (green and pink dashed lines) in the whole section area. Dystrophin positive fiber density was then measured for each area. B: quantification of dystrophin positive fibers in each area around the scaffold at increasing distance from the scaffold.

2.4 DISCUSSION

In this work a three-dimensional collagen sponge was investigated as a potential vehicle to perform myogenic cell delivery *in vivo*, in order to restore dystrophin expression in *mdx* mice. To date, to the best of our knowledge, this is the first attempt to couple a biomaterial with cells to perform cell delivery in dystrophic muscles.

A three-dimensional collagen scaffold was chosen for its intrinsic natural and biomimetic properties; collagen sponges have already shown their usefulness in tissue engineering studies by others (*3, 7, 8*), and our group had already obtained *in vivo* data on a rat model of rat ischemia (*2*). In this case, we sought to use its three-dimensional elastic and highly porous structure so that implanted scaffolds could act as a cell reservoir for cell delivery. To this aim, we designed the seeding technique for the scaffold so that it could host the highest possible cell density, while at the same time preserving their viability and their myogenic nature.

These points were the subject of both *in vitro* and *in vivo* experiments. In the former case, we analyzed viability and myogenic markers expression of MPCs 24 hours after seeding inside the collagen sponge. Using a cell-membrane permeability test we determined that very little cell death could be found, even in the core part of the scaffolds. Besides being viable, MPCs also showed an expression pattern of myogenic markers that was comparable to what was observed when the same cell preps were instead grown in standard conditions (i.e., 2D Petri dishes). These findings therefore confirmed that collagen scaffolds could satisfactorily host high numbers of myogenic for subsequent *in vivo* delivery.

Given that many previous studies had shown how transplanted cell death occurs shortly after injection in recipient muscles (*6*), cell viability was assessed in experiments

in which muscles had received collagen-delivered cells or injected cells. These experiments were carried out in *wild type* animals, using cells prepared from GFP-positive transgenic mice. Cell death in both implanted and injected muscles was analyzed 48 hours post transplantation with TUNEL assay, which detects genomic DNA fragmentation. Although commonly regarded as a label for apoptotic cells, it has been found to be a more general marker for cell death when used in the context of cell transplantation (*6*). Our findings showed that collagen-delivered cells displayed very low levels of TUNEL-positive nuclei. Interestingly, injected cells did not display dramatic levels of cell death either, even though they were still about three times higher than those seen in collagen. This finding was in agreement with what had been noticed by Skuk and colleagues, who had reported that when using primary myoblasts post-transplantation cell death was not as high as that seen when implanted stabilized myoblasts (*6*).

Short term experiments also indicated that, once implanted *in vivo*, after 48 hours cellularized scaffold also contained host cells, which were obviously able to migrate from the surrounding muscle. That suggested that the scaffold was indeed compatible with cell migration across it, but that, on the other hand, it did not prevent host cells access to transplanted cells. Given that these host cells were most likely macrophages or other players of the early acute inflammatory reaction recruited in the site of injury (as indicated by the results of preliminary experiments with anti-macrophage immunostaining (data not shown) such occurrence could have been potentially harmful for the success of the implant.

In order to evaluate collagen scaffold efficiency as a vehicle for cell-based dystrophin delivery in *mdx* mice, the *in vivo* experiments were carried out comparing the performance of scaffold-delivered cells to that of cells that were injected intramuscularly. This approach was chosen because direct injection was until then the standard way to deliver myoblasts in the muscles of *mdx* mice. Importantly, in each experiment seeded and injected cells belonged to the same prep, thereby excluding that the intrinsic variability of primary cultures could affect the results. It should be noted that when the collagen-*mdx* project was started we did not deem we had satisfactory evidences that the use of GFP positive cells derived from a C57BL/6J strain in a C57BL/10ScSn/J background would not cause any immunological problem. For this

reason the experiments with *mdx* mice were carried out using syngeneic, non GFP positive, donors.

Initial experiments were carried out at different time points, in order to determine when the best yield, in terms of dystrophin positive fibers per muscle section area, was obtained. This analysis showed that this value peaked at 30 days after transplant and remained fairly constant also at three months. This time course analysis also indicated that at ten days after implant, injected muscles contained almost twice as many dystrophin positive fibers compared to scaffold-implanted muscles, a ratio that was reversed at 30 days. This finding suggested that injected cells participated immediately to the formation of dystrophin-positive fibers, while the scaffold did appear to act as a reservoir, from which cells were released more slowly (see also below). On the other hand, the fact that at three months the number of dystrophin positive fibers was similar (or lower) than that found at 30 days suggested that the contribution of delivered cells to the satellite niche of the recipient muscle was likely not significant. In fact, even considering that in adult *mdx* animals the continuous regenerative processes are present but at a low level, we would have expected some indication of an increase in the number of dystrophin positive fibers in time.

Implanted muscles analyzed 30 days post implant revealed several small (i.e., newly formed) desmin positive fibers inside the collagen scaffold, thus indicating that the matrix was able to support muscle regeneration. However, the cells that had formed the majority of these fibers came from the host; in fact, most dystrophin positive fibers were found at the interface between scaffold and host muscle and could be observed only occasionally inside the scaffold.

The quantification of dystrophin positive fibers in muscle implanted with cellularized scaffolds yielded higher numbers that what was found in injected contralateral or control muscles. Such an increase, though, was far too low to be clinically relevant, as it reached just about 5% of the total number of fibers in one tibialis anterior (it is now generally accepted that in order to achieve some physiological improvement it is necessary to express dystrophin in at least 20% of the fibers).

As mentioned in Chapter one, distribution of transplanted cells is a very important parameter to consider in cell therapy studies. For this reason we analyzed the outward migration of collagen-delivered cells into the surrounding muscle. To do so we used an indirect approach and considered the distribution of dystrophin positive fibers. In these

experiment we also implanted non-cellularized scaffold as controls, to be able to tell apart the contribution of implanted cells from the possible increase of revertant fibers due to muscle regeneration. Our data suggested that implanted MPCs were able to migrate out of the matrix but not very far from it, as the majority of dystrophin positive fibers was found within 400 µm from the scaffold. These fibers were likely formed by donor cells that were released while the scaffold was being degraded. In fact the highest number of dystrophin positive fibers was obtained at 30 days, without changing statistically in the longer term (180 days). At 30 days transversal sections across implanted muscles, revealed that the scaffold area was reduced to 2/3 out of its total volume *in vivo* and therefore it likely released most of the transplanted cells that later gave the maximum yield at that time point.

2.5 BIBLIOGRAPHY

1.   L. Boldrin *et al.*, *Tissue Engineering* **13**, 253 (2007).
2.   S. B. Andrea Callegari, Laura Iopa, Angela Chiavegato, Gianluca Torregrossa, Michela Pozzobon, Gino Gerosa, Paolo De Coppi, Nicola Elvassore, Saverio Sartore, *Biomaterials* **28**, 5449 (2007 Dec).
3.   V. Kroehne *et al.*, *Journal of Cellular and Molecular Medicine* **12**, 1640 (Sep-Oct, 2008).
4.   B. N. Bian W, *IEEE Eng Med Biol Mag.* **27**, 109 (2008 Sep-Oct).
5.   P. D. Coppi *et al.*, *Tissue Engineering* **12**, 1929 (2006).
6.   D. Skuk, N. J. Caron, M. Goulet, B. Roy, J. P. Tremblay, *Journal of Neuropathology and Experimental Neurology* **62**, 951 (Sep, 2003).
7.   C. D. Chin, K. Khanna, S. K. Sia, *Biomedical Microdevices* **10**, 459 (Jun, 2008).
8.   G. P. Ciardelli G., Chiono V., Mattioli-Belmonte M., Vozzi G., Barbani N., Giusti P., *Journal of Biomedical Materials Research Part A* **9999**, NA (2009).

CHAPTER 3

HYALURONIC-BASED HYDROGEL FOR CELL DELIVERY IN NORMAL AND DYSTROPHIC MUSCLE

3.1 INTRODUCTION

3.2.1 IMPROVING CELL DELIVERY EFFICIENCY

In chapter 2 we explored the potentialities of a three dimensional collagen scaffold to mediate cell delivery in dystrophic muscle. Collagen scaffold has shown to be a suitable scaffold to mediate muscle tissue formation inside it, but it revealed several points that could be ameliorated in order to improve the efficiency of cell delivery. In designing a suitable biomaterial for this purpose, the biological part (the cells) are combined with the technological one (the biomaterial), hence, we analyzed possible limitations of both in order to optimize cell delivery efficiency.

When we used collagen scaffold, the underlying idea was to create a reservoir for long-term cell release in the dystrophic muscle and the use of high quantities of cells was specifically thought towards his aim. However, our results showed that the grafting efficiency was quite low and little or no satellite cell replenishment was observed. These findings could have been due, at least in part, to *in vitro* expansion and culture conditions, factors that have been shown to impair cell myogenic potential (*1, 2*). Besides, high numbers of cells might limit availability of O_2 and nutrient supply inside the scaffold, while delaying the clearance of metabolites (*3*). More profound myogenic stem cells have been proposed as a preferable therapeutic approach, because they are characterized by extensive proliferative and engrafting capacity inside the host tissue as well as self-renewal properties even when engrafted in small numbers (*1, 4, 5*). Hence, we tried to improve the efficiency of the cellular part of our approach by using satellite cells that were transplanted i*n vivo* as soon as they were separated from freshly isolated myofibers(*6*). Besides changing the cell type, we also worked on the development of a

more suitable biomaterial for cell delivery purpose. As previously mentioned, our previous results suggested some possible limitations of the collagen sponge:

- ✓ impaired molecules diffusion;
- ✓ early penetration of (inflammatory) host cells inside the scaffold;
- ✓ long scaffold degradation time.

Inside the scaffold, diffusion of metabolites could be impaired by the micro-porous structure, that forces molecules to cover long distances before they have access to the transplanted cells; therefore metabolites and signal molecules (fundamental for cell viability) might not arrive at transplanted cells in sufficient amounts and or with the tight timing. On the other hand, we observed cells from the host inside the scaffold within the first 48 hours after implantation, likely attracted by the inflammatory response elicited by the insertion of a foreign body. That suggests that micro porous structure did not prevent cells to interact with transplanted ones, therefore leading potentially to cell loss or minor efficiency (as discussed in chapter 1). Finally, scaffold degradation time could be too long for a cell delivery purpose, in the sense that MPCs might need to be released faster in order to get in contact with the host tissue and contribute more significantly to its repair.

Chapter 1 described different types of biomaterials that are currently under investigation as delivery devices. Among them, the one that best incorporates the requirements necessary for our purposes is hydrogel.

3.2.2 *HYDROGEL PROPERTIES:*

Hydrogels are water-swollen, crosslinked polymeric systems capable of absorbing large volumes of aqueous solution. They are formed by crosslinking water-soluble polymers to form an insoluble polymer network at different conditions (temperature, pH, etc).

Hydrogels are defined as three-dimensional polymer networks that swell, but do not dissolve in water (*7*). They are biocompatible and soft; their high water content can be modified to modulate hydrogel mechanical properties. Moreover, they display high structural similarity to the natural extra cellular matrix (ECM), therefore it's not surprising that hydrogels that have been designed with physical and elastic properties

resembling those of native tissues have found important roles in medicine (e.g., in tissue engineering, artificial organs, and other implantable devices) (*8-10*).

Hydrogels form a permeable but non-porous membrane whose physical characteristics can be engineered with appropriate dimensions. Thus cells can be entrapped in a structure that allows them to interact with soluble molecules of the surrounding environment that can diffuse freely towards and from them, but, on the other hand their contact with host cellular part is prevented, because cells are too big to overcome the molecular barrier provided by hydrogel structure (*11*). The selectivity provided by the gel matrix can be modulated by altering the crosslink density, which affects the structure in two ways: it regulates the size of molecules that have access through the polymer and modifies hydrogel mechanical properties (because it affects the volume of aqueous solution adsorbed by the polymer).

Hydrogel transparency is another advantageous feature for cell culture because it allows the visualization of living cells, optical image analyses and studies on the dynamics of interfacial processes, such as protein-surface interactions, using inverted microscopes (frequently used in cell biology) (*12*).

3.2.3   ENGINEERED HYDROGEL FOR CELL DELIVERY PURPOSE

Hydrogel can be injected into the body with minimal invasive techniques, which do not require open surgery.

Once injected, the biomaterial needs to polymerized *in situ* in order to acquire more solid-like properties that would resemble the ones of the host muscle tissue (in order to accomplish biomimetic property, as already stated in chapter 1). An injectable material presents several advantages, but there are several parameters that need to be controlled in order to ensure efficiency. To this end, our preliminary experiments were aimed at accomplishing:

- ✓ an efficient and homogeneous polymerization *in vivo;*
- ✓ homogeneous physico-chemical properties after the polymerization occurs.

Hydrogels can be prepared with several polymers, either natural or synthetic, including alginate, pluronics, chitosan, fibrin glue and poly-acrylamide (*13*). In recent years, many kinds of hydrogels, especially poly(ethylene glycol) (PEG) and derivatives (*14*), have been widely used for encapsulating living cells or as substrates for cell

culture. Amongst the various hydrogels, those based on hyaluronic acid (HA) have grabbed the attention of scientists and clinicians because they are chemically, structurally and mechanically designed to mimic some of the features of native ECM (*15-17*).

Hyaluronan (HA), also known as hyaluronic acid or hyaluronate, is a major constituent of the ECM (*18*), accounting for >2.5g/L in the human body.

It is a linear, unbranched negatively charged polymer, first discovered by Meyer and Palmer in 1934 in the vitreous humor of cattle eyes (*19*). It is composed of repeating units of two monosaccharides, glucuronic acid and N-acetyl-glucosamine (-4GlcUAβ1-3GlcNAcβ1-)$_n$ (*20*).

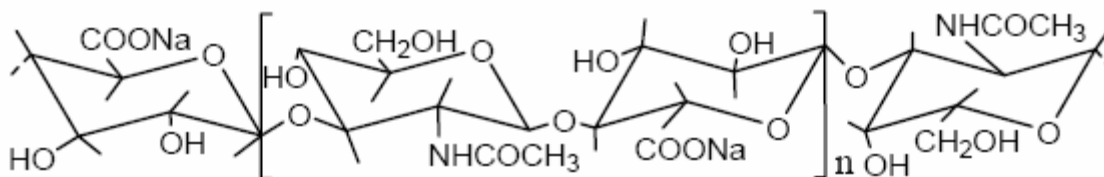**Figure 3.1**   **The repeating disaccharide unit of hyaluronan (-4GlcUAβ1-3GlcNAcβ1-)n**

It has visco-elastic properties and high ability to retain water, thus modulating matrices malleability and porosity (*21*), and therefore cell motility. HA *in vivo* is known to co-regulate gene expression, signaling, proliferation, motility, adhesion, metastasis, and morphogenesis (*22, 23*), as well as to promote wound-healing processes while reducing long term inflammation (*24*).

Moreover, HA can be produced through fermentation. This is an appealing feature for the making of a biomaterial applicable in clinical grade, because the microbial fermentative process does not present risks of animal-derived pathogens.

3.2.4   *HYALURONIC ACID-BASED HYDROGEL (HYAFF120®)*

In collaboration with Fidia Advanced Photopolymers (*f.a.b.*) and the group of Dr Nicola Elvassore of Engineering Dept, University of Padua, a new injectable hyaluronic acid-based hydrogel (HYAFF120®), endowed with novel features designed to bring improvement in cell delivery efficiency for cell-based therapies has been developed.

Beside natural useful hydrogel characteristics described above, HYAFF120® was engineered in order to improve its use in our protocol. Properties of HYAFF120® are summarized below:

- ✓ HYAFF120®, is an injectable hydrogel.

  Therefore it can be introduced into the body with minimal invasive technique. Once injected into the body, the biomaterial can be *in situ* polymerized and therefore acquire more solid-like properties.

- ✓ HYAFF120® is photo-polymerizable *in vivo*.

  In order to obtain an homogeneous polymerization we opted for a photo-polymerization, instead of a chemical one, that would require the mixing of the chemical initiator in the polymer solution; we used a photo-initiator excitable by UV light at 366 nm, a wavelength already used for clinical applications. However, photo-polymerization is not sufficient on its own to obtain a homogeneous and reproducible polymerization. In fact, when photo-initiator is activated by specific light wavelength to link together molecules in the solution, it produces radical initiating species that can be toxic if not quickly removed. In order to avoid the creation of dangerous intermediates, the photo-initiator was covalently and stoichiometrically linked to HA based hydrogel molecules, thus ensuring a completely homogenous dispersion of the photo-initiator within the HA blend (Figure 3.2A). The characteristics described above ensure the homogeneity of the polymeric solution prior and after polymerization. Figure 3.2A shows the reaction of production of HYAFF120® form HA and photo-initiator and then the hydrogel formation after UV light exposure.

- ✓ HYAFF120® can be sterilized by conventional autoclave.

  Therefore, once it is prepared, it is ready to be used with biological samples. It can be mixed with the cells, injected and photo-polymerized *in vivo* without any additional mixing or reagents.

- ✓ HYAFF120® forms a permeable non-porous membrane that is selective for cells and/or soluble molecules.

  As we already described above, the photo-initiator is chemically linked to HA molecules in order to ensure an efficient and homogeneous photo-polymerization that does not require any reagents mixing. The photo-

initiator is stoichiometrically linked to HA molecules and therefore it is present at regular length between two adjacent HA molecules. This distance was thought to provide for free access of soluble molecules to carried cells but on the contrary to protect them from the cellular part of the host. In order to accomplish that, the synthesis process was studied to have a molecular net of approximately 70 nm (as shown in Fig 3.2 B).

✓ Finally, as already mentioned, HYAFF120® is a hyaluronic-acid derived polymer, that can be easily and controllably produced in large quantities through microbial fermentation. Besides eliminating any risk connected to animal-derived products, this also enables the scale-up of HA-derived products (*25*).
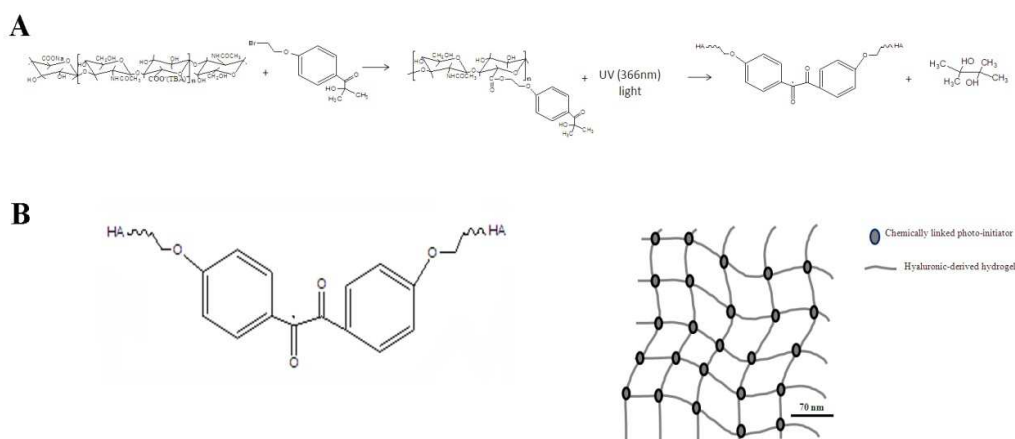

Figure 3.2 **A. Schematic representation of the main reaction for the synthesis of HYAFF120® and photo-polymerized hydrogel. B. Chemical structure of photo-polymerized HYAFF120® (left picture) and schematic representation of the molecular net formed upon exposure to UV light (right picture).**

In this work we characterized HYAFF120® as a cell delivery carrier, suitable for clinical grade.

We first of all set up conditions to obtain suitable visco-elastic properties of the hydrogel for cell injection *in vivo*, thus establishing polymer concentration and all the parameters to obtain an optimal photo-polymerization *in vivo*. We therefore established the best conditions to encapsulated cells inside the polymer, while maintaining them alive and functional during photo-polymerization.

Hydrogel was then tested *in vivo*. First data were obtained on *wt* animals in order to set up experimental conditions for *in vivo* application and test efficiency of hydrogel as a cell carrier. Afterwards hydrogel was used in the diseased *mdx* model.

3.2   MATERIALS AND METHODS

3.2.5   SINGLE MYOFIBER ISOLATION

Single fibers were isolated by adjusting a protocol previously described from De Coppi et al., 2006 (*26*). Briefly, extensor digitorum longus (EDL) and soleus (SOL) muscles were removed from 2 to 6 months old C57BL/6-Tg (ACTB-EGFP)1Osb/J gfp transgenic mice and C57BL/10ScSn mice muscles (Jackson Laboratories) and digested with 0,2% Collagenase Type I (Sigma-Aldrich) in DMEM for 1 hour and 15 minutes at 37°C. Myofibers were gently isolated and serially transferred through three dishes of warmed plating medium (PL), (Dulbecco Modified Eagle's Medium, DMEM; 10% horse serum; 1% chicken embryo, MP-Biomedicals; 1% penicillin-streptomycin). Unless otherwise indicated, all cell culture reagents were from Invitrogen.

3.2.6   SATELLITE CELLS ISOLATION

Satellite cells were separated from myofibers using a method adapted from (*27*). For each graft, twenty intact fibers were isolated from EDL and SOL muscles of 2 to 6 months old C57BL/6-Tg (ACTB-EGFP)1Osb/J GFP transgenic mice and C57BL/10ScSn/J. Groups of 20 fibers were isolated in PL medium and passed 20 times through a 19G needle mounted on a 1 ml syringe. The suspensions were then centrifuged for 5 min at 450 xg, and the resultant pellets were resuspended into

[HYAFF®] 40mg/ml. Hydrogel- encapsulated cells were kept in ice until grafting within few hours from isolation. Aliquots of 250 cells were seeded onto DMEM 10% Matrigel (BD Biosciences) and cultured overnight in PL medium to allow them to adhere to the plate to perform immunocytochemical characterization.

3.2.7 MEASUREMENT OF HYDROGEL VISCOSITY AND ELASTIC-MODULUS

A rheometer (Rheostress RS150 Haake) was used to evaluate visco-elastic and rheological properties of starting solution (fluid-viscous) and the cross-linked hydrogel (solid-elastic). It was equipped with a temperature control ($20.0\pm0.5°$ C) and a plate-cone sensor (1°) of 60 mm diameter. During measurements the distance between cone and plate was 0.051 mm. Experiments were carried out on different concentrations of Hyaluronic acid solutions from 10 up to 75 mg/ml. Higher concentrations gave solutions too viscous and so unlikely workable. Reliable experimental data were obtained in the range from 10 to 30 mg/ml. The solution's rheological behaviour (before irradiation) was evaluated by analyzing the shear stress as function of rising deformation rates (0-5 s^{-1}). Stress sweep measurements on cross-linked hydrogels were performed in order to find its linear viscoelastic region where the complex modulus was independent from the shear stress. Finally, elastic (G') and viscous (G") moduli of cross-linked hydrogels were calculated as function of rising oscillation frequencies (0.1-10 Hz) at constant shear stress ($\tau = 1$ Pa).For all concentrations hydrogel disks (1.5 ml) were prepared by UV curing using UV lamp Blewave-50 Dymax filtered at 366 nm, intensity: 4mW/cm2, probe: samples of different concentrations (10, 20 and 30 mg/ml) and exposition times (from 3 s up to 5 min) were prepared at a distance equal to 2 cm from the probe (427 ± 2.5 mW/cm^2).

3.2.8 CELL ENCAPSULATION INTO HYDROGEL FOR IN VITRO ANALYSIS

In vitro analysis on the coupling of hydrogel and cells was performed with C2C12 cell lines characterized by passage number ranging from 10 to 20. C2C12 cells were cultured in Proliferative medium, PR (PR: DMEM, Sigma-Aldrich; 20% Fetal bovine serum; 1% penicillin-streptomycin), and detached from the dish before confluence.

C2C12 were counted, divided into aliquots of $6 \cdot 10^3$ each. Cells were centrifuged for 5 min at 450 RCF, the supernatant was removed and the resultant pellet was resuspended into different concentrations of HYAFF®: 20, 40 and 60 mg/ml in PBS.

The suspension was then placed into 96-multi well plates, where it underwent photo-polymerization with UV lamp Blewave-50 Dymax filtered at 366 nm, intensity: 4mW/cm2, for 55 sec; the light source was placed at 4 cm from the cells.

After photo-polymerization, Proliferative medium (PR) was added to hydrogel-encapsulated cells and kept in culture; medium was changed every 2 days.

3.2.9   HYDROGEL DEGRADATION IN VITRO

Powder based [HYAFF®] was dissolved at a concentration of 40 mg/ml in physiological solution. A volume of 90 µl of the mixture was photo-polymerized with UV lamp Blewave-50 Dymax filtered at 366 nm, intensity: 4mW/cm2, for 55 sec. Hydrogels were weighed after photo-polymerization and immerged at room temperature in different media (PBS, DMEM, DMEM 10%FBS, DMEM 10%HEPES); then the polymer was weighed at different time points.

The same procedure was used to test hydrogel stability at different pH; photo-polymerized hydrogels were weighed after photo-polymerization and immerged at room temperature in four buffers at different pH (3.8, 5.8, 7.3, and 8.6) obtained using Citric, Phosphate and Borate buffer. The hydrogels were weighed at different time points, and the pH was measured.

3.2.10   EFFECT OF RADIANT ENERGY ON THE VIABILITY OF HYDROGEL-ENCAPSULATED CELLS

$6 \cdot 10^3$ C2C12 cells were encapsulated in HYAFF® [40mg/ml] in physiological solution and photo-polymerized with UV lamp Blewave-50 Dymax filtered at 366 nm, intensity: 4mW/cm^2, for increasing exposition time. Cell viability was tested using LIVE/DEAD® assay (Molecular Probes, Invitrogen); briefly 150 µL of DMEM 3.5 µM Calcein/3.0 µM Ethidium Bromide were added to hydrogel-encapsulated cells and incubated 45 minutes at room temperature. Following incubation, hydrogel-encapsulated cells were washed in phosphate buffer (PBS) and labeled cells were observed at fluorescence microscope (Leica, DMI 6000B).

3.2.11   EFFECT OF HYDROGEL ENCAPSULATION ON CELL DIFFERENTIATION

$6 \cdot 10^3$ C2C12 cells (a standard murine myoblast cell line capable of in vitro differentiation) were encapsulated in 35 µl of HYAFF120® at different concentrations (20, 40 and 60 mg/ml in physiological solution) as described in ¶ 3.2.4; the suspensions were photo-polymerized inside 96-multi well plates that had been previously coated with Laminin [50 µg/ml in PBS] (Sigma Aldrich) for 2 hours at room temperature (RT). As control the same cell number was seeded without previous hydrogel encapsulation, and analyzed with or without exposition to UV radiation energy. Both control and Hydrogel encapsulated cells were cultured in 1:1 PR and Conditioned Medium (CM). This latter was simply PR harvested from a 48 hours culture of C2C12 medium and filtered through a .22 µm filter. Once cells reached sub-confluence, medium was switched to Differentiative Medium (DM: DMEM; 2% horse serum; 1% penicillin-streptomycin) for 4 more days.

3.2.12   RECIPIENT ANIMALS

We used mice from two different strains: C57BL/6J and C57BL/10ScSn-*mdx*/J. All animals (Jackson Laboratories) were housed and operated onto at the Animal Colony of the "Centro Interdipartimentale Vallisneri", University of Padova, following all relevant bylaws issued by the Italian Ministery of Health. Animals were anesthetized with 2% isoflurane; post-op care included three-days analgesic (tramadol 10mg/kg) and antibiotic treatment (enrofloxacin 15 mg/kg).

3.2.13   IN VIVO IMPLANTS

Hydrogel and cells were delivered to left *tibialis anterior* (TA) muscles; contra-lateral TAs were used as control and received either hydrogel alone (no encapsulated cells) or sham surgical procedure. Implants contained approximately 250 GFP positive hydrogel-encapsulated satellite cells from C57BL/6-Tg (ACTB-EGFP)1Osb/J gfp transgenic mice [final hydrogel concentration: 40 mg/ml]. Approximately 15% of flesh mass was removed from the core of TAs in order to create a pocket for hydrogel insertion. When TAs were treated with hydrogel alone, or hydrogel-encapsulated cells,

they were inserted inside the pocket, and photo-polymerized *in situ* with UV lamp Blewave-50 Dymax filtered at 366 nm, intensity: 4mW/cm2, for 55 sec (see ¶3.3.7). After polymerization, or once the surgical sham was performed, muscles were closed with non-absorbable sutures. Mice were sacrificed 2 and 6 weeks post implant. Implanted and sham-injured muscles were excised and fixed in 2% para-formaldehyde (PFA) in PBS at 4 °C for 1-2 hours and then placed in a 30% sucrose solution overnight at 4 °C. The following day samples were then quickly rinsed in PBS and then snap-frozen frozen in liquid nitrogen-cooled isopentane. Muscles were stored at -80 °C until analyses were performed. Two days before sacrifice, mice analyzed 2 weeks post implant were injected intra-peritoneally with EdU (Invitrogen), 0.9 mg in 500 µl normal saline for a 30 gr mouse, for cell proliferation assay.

3.2.14 MUSCLE CRYOSECTIONS

Frozen muscles were sectioned end-to-end with a cryotome (Leica CM 1850), preparing 10 µm-thick sections for antibody staining and 20 µm-thick sections for eosin and hematoxylin staining. Tissue sections were placed onto gelatin-coated microscope slides. Sectioning levels were separated by about 300 µm along the muscle length; ten serial, 20 µm sections were kept aside from each level (for possible further analyses by western blot).

3.2.15 IMMUNOSTAINING

10 µm thick cryosections were used for immuno-histochemical staining of implanted muscles. Freshly isolated satellite cells were seeded onto glass slides previously coated with 10% Matrigel in DMEM.

All the samples were fixed with PFA 2% for 7 minutes. Primary antibodies against Desmin (rabbit polyclonal, AbCam, United Kingdom 1:200), Dystrophin (rabbit polyclonal, AbCam, United Kingdom 1:200), GFP (rabbit polyclonal IgG fraction, Invitrogen, 1:150) and Myosin Heavy Chain (mouse monoclonal, Sigma, 1:100) were diluted in PBS-3% BSA (Sigma-Aldrich, Italy) and applied for 1 hour at 37 °C. Primary antibodies against MyoD (rabbit polyclonal, Santa Cruz, Germany, 1:50 and Mouse monoclonal, Dako, 1:100), Myogenin (rabbit polyclonal, Santa Cruz, Germany, 1:50 and Mouse monoclonal antibody, BD Pharmingen, 1:100) and Pax7 (supernatant of a

hybridoma, Hybridoma Bank, 1:50) were diluted in PBS-3% bovine serum albumin (BSA) and individually applied overnight at 4°C. niente MOM, non riporti monoclonali usati su fetta, solo su cellule

Secondary antibody Alexa Fluors 594-conjugated anti-rabbit IgG, 594-conjugated anti-mouse IgG and 488-conjugated anti-mouse IgG (Invitrogen, USA) , were diluted 1:250 in PBS-3% BSA and applied for 45 minutes at 37°C.

After treatment with fluorescent secondary antibodies, cells were counterstained with DAPI and mounted in fluorescent mounting medium (DakoCytomation, Italy).

3.2.16   HEMATOXYLIN AND EOSIN STAINING

20 μm-thick cryosections of implanted muscles were analyzed by hematoxylin/eosin staining, using standard protocols. The presence of 30% sucrose interfered with the H&E protocol, leading to the formation of noticeable gaps in the sections. In order to minimize this problem, before staining muscles were treated with a decreasing scale of sucrose solutions.

3.2.17   DYSTROPHIN AND GFP QUANTIFICATION

The number of dystrophin and GFP positive fibers was obtained by scoring muscle sections upon dystrophin and GFP immunostaining, using a fluorescence microscope (Leica, DMI 6000B) equipped with a DFC350FX Leica camera and the Leica DMI6000 software; at least 10 sections were analyzed for each condition. The best section per slide was considered per sample.

3.3   RESULTS

3.3.1   VISCOSITY OF INJECTABLE SOLUTION

Hydrogel is an injectable polymer before photo polymerization. The common needle used for *in vivo* cell injection is a 27 Gauge needle. When cells suspended in the polymeric solution (pre-photopolymerization) are injected, they are mechanically stressed by the viscous forces; this forces are proportional to the viscosity of the solution, to the velocity of injection and inversely proportional to the diameter of the needle.

The apparent viscosity measured for non photo-polymerized hydrogel at different concentration, is reported in Table 3.1; the trend of measured values is represented in Figure 3.3

Table 3.1   Viscosity values performed by different hydrogel concentration

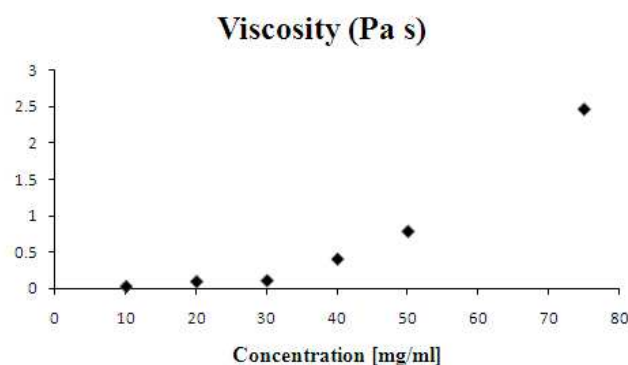| Concentration (mg/ml)	Viscosity (Pa·s)
10	0.025
20	0.094
30	0.107
40	0.403
50	0.783

Figure 3.3   **Viscosity increasing trend for different hydrogel concentration.**

As expected, apparent viscosity increases as the polymer concentration increases, with a variation of viscosity that goes from 0.025Pa•s (for 10mg/ml) up to 2.5Pa•s for (75mg/ml). 40mg/ml was measured to be the maximum hydrogel concentration to have a final viscosity lower than of 0.4Pa•s. This value has been evaluated to be the threshold above which the effect of viscous force can damage the cells (*28*). From this perspective all concentration values between 10 and 40 mg/ml can be used for clinical applications.

3.3.2   *ELASTICITY OF HYDROGEL AFTER POLYMERIZATION*

Polymerized hydrogel displays mechanical properties that are dependent on two main parameters: i) the polymer concentration and ii) the time of polymerization (i.e. time of exposition to UV radiant-energy). Given that HYAFF120® was meant to be utilized in muscle, it should have displayed properties similar to the muscle tissue. We therefore investigated the elastic behavior of polymerized HYAFF120®, as a function of the polymer concentration and the UV exposure time.

In comparison to the HYAFF120® solution, the polymerized one displays a semisolid 3D structure with enhanced elasticity due to chemical bonds among HA molecules. Elasticity (represented by the elastic modulus) of photo-polymerized HYAFF120®, was measured for different HYAFF120® concentration (10, 20 and 30 mg/ml) and different exposure times: 3s, 10s, 30s, 60s. We observed that:

    i.   the elastic modulus increases as hydrogel concentration increases, at any exposure time; in fact, as HYAFF120® concentration increases, there are more HA derived molecules that will be linked together during UV-

polymerization by the chemically linked photo-initiators, thus conferring a more solid-like aspect to the gel;

ii. the elastic modulus increases as exposure time increases for every hydrogel concentration. The longer is the polymer exposed to the UV radiation, the higher is the number of photo-initiators that are activated; that means that more HA molecules are linked together, and therefore the polymer acquires an elastic behavior that is more similar to a solid-like one. Within the first 30 seconds the elastic modulus increases quite rapidly; then the trend becomes asymptotic and elastic modulus stabilizes to a plateau, thus meaning that all HA molecules have been linked together;

iii. considering the trend of elastic modulus we concluded that a suitable time for polymerization could be approximately 55 sec (later confirmed to ensure an homogeneous polymerization *in vivo*, see ¶3.3.7); 55 sec is a polymerization time largely beyond the time where elastic modulus acquires an asymptotic trend; this choice was done in order to ensure conserved properties of the polymerized hydrogel among experimental variability, so that little variations in the polymerization time during the *in vivo* application did not lead to significant differences in the polymer properties.

Table 3.1 shows average values of elastic modulus (Pa), measured for different polymer concentration at different radiant-energy exposure times. Due to instrument sensitivity limitation, elastic modulus could not be measured for hydrogel concentration of 40 mg/ml. We therefore extrapolated it mathematically from the data above; the elastic modulus was shown to be $4 \cdot 10^3$ and so lower, but still within the range of the in vivo muscle stiffness (*29*).

Table 3.2   Average elastic modulus value (Pa) as a function of different polymer concentration and radiant-energy exposure times. * mathematical extrapolation

HA –PI conc. (mg/ml)	3 sec	10 sec	30 sec	60s
10	43 ± 7	162 ± 7	261 ± 24	250 ± 13
20	155 ± 42	646 ± 79	1035 ± 73	1118 ± 137
30	267 ± 13	1113 ± 39	2112 ± 118	2264 ± 92
40*	-	-	-	4000*

3.3.3 HYDROGEL DEGRADATION IN VITRO

Hydrogel stability is one of the fundamental parameters for an efficient cell delivery system. The scaffold degradation should be slow enough to reduce the formation of connective tissue and to protect the stem cells from the acute inflammatory response. On the other hand, implanted matrix should not constitute a steric impairment for tissue regeneration.

Studying the stability *in vitro* is important for two main reasons:

1. to predict the degradation rate in each specific injection site *in vivo*;

2. to understand the reasons/the mechanism of instability and eventually being able to modify the hydrogel structure to tune the degradation rate.

In particular we investigated the effect of different media and of different pH on the hydrogel degradation rate.

We observed that, while in PBS, hydrogel displays long stability, when DMEM is added (conditioned or not, with serum or buffers) the stability is strongly reduced, as shown in Table 3.3

Table 3.3   **In vitro stability of HYAFF® 40mg/ml in physiological solution, and immerged at room temperature in different media. The stability is evaluated as the time necessary to see a reduction of weight if compared with the initial weight.**

Media	*In vitro* stability
PBS	~ 500h
DMEM	< 15h
DMEM 10%FBS	< 15h
DMEM 10%HEPES	< 20h

We then measured whether differences in hydrogel stability were correlated to different pH, and observed that stability strongly decreases at basic pH, as shown in Table 3.4.

Table 3.4   *In vitro* stability of HYAFF 40mg/ml in physiological solution, and immerged at room temperature in buffers with different pH. The stability is evaluated as the time necessary to see a reduction of weight if compared with the initial weight.

Buffer pH	*In vitro* stability
3.8	> 1200h
5.8	~ 1000h
7.3 (PBS)	~ 500h
8.6	< 15h

Given the stability of hydrogel in PBS, powder-based HYAFF120® was dissolved in PBS for encapsulation of cells for both *in vitro* and *in vivo* analysis.

3.3.4   EFFECT OF RADIANT ENERGY ON VIABILITY OF HYDROGEL-ENCAPSULATED CELLS

HYAFF120® is photo-polymerized *in situ* through UV light; therefore, when cells are encapsulated into the polymer, they receive the UV radiation as well. The radiation used (366 nm) is currently used in clinical applications where it did not show to be harmful for cells. Nevertheless, when energy is irradiated by the source there is heat emission, which is potentially dangerous for encapsulated cells. We therefore tested effect of radiant-energy emitted by UV source on the viability of hydrogel-encapsulated cells.

Cells were encapsulated in HYAFF120® [40mg/ml], photo-polymerized with UV lamp Blewave-50 Dymax filtered at 366 nm, intensity: 4mW/cm2, for increasing exposition time and cell viability was evaluated. Fig. 3.4 shows cells analyzed with LIVE/DEAD® assay, where green-colored cells are alive and red-colored are dead. We did not observe differences in cell viability up to approximately 100 sec of radiant energy exposure in these conditions. For times longer than 100 sec, cells death was observed. However, it is important to note that temperature of the wells where cells were cultured, increased with prolonged exposure time. Cell death can be avoided by lowering the power of the radiant-energy source (thus working at greater distances) or if heat produced by the UV-lamp is efficiently dispersed; for instance Petri dishes are heat insulator whereas muscle tissue allows good heat dispersion, thus preventing overheating.
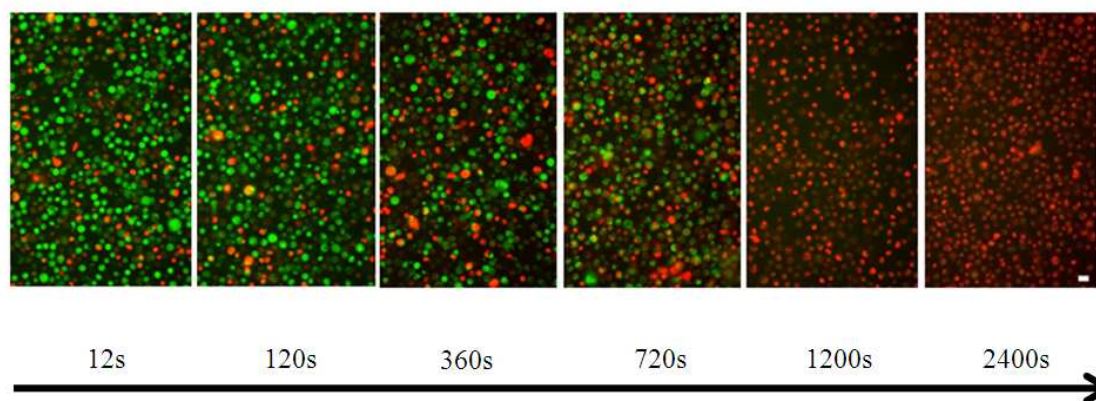
Figure 3.4 **Effect of radiant energy on viability of hydrogel-encapsulated cells. Cells exposed to radiant-energy for approximately 100 sec did not show any difference with non irradiated cells, in these conditions; for times longer than 100 sec cell death was observed. White bar on the bottom right corresponds to 20 μm.**

3.3.5 EFFECT OF HYDROGEL ENCAPSULATION ON CELL DIFFERENTIATION

Beside viability, we verified that hydrogel-encapsulated cells did conserve their ability to attach to the plate, differentiate and fuse into myotubes *in vitro*, once they were released from the hydrogel. Cells were encapsulated into HYAFF120® at 20, 40 and 60 mg/ml in physiological solution, and the mix was photo-polymerized and then kept in culture. When cells released from hydrogel reached sub-confluence growing onto the plate, they were induced to differentiate with the appropriate medium for 4 more days. As control, cells were seeded without hydrogel encapsulation, with or without exposition to radiant-energy. Control cells, exposed or not to radiant-energy, did not show much difference, beside a slight delay in attachment to the plate (approximately 30 min). After 24 hours from seeding, they were induced to differentiate.

Hydrogel-encapsulated cells showed different behavior depending on the hydrogel concentration they were encapsulated into. Immediately after encapsulation and photo-polymerization, cells lie in the three-dimensional environment created by hydrogel (Fig. 3.5 A); then, as the hydrogel starts to be degraded, cells are released in culture and adhere to the plate (Fig. 3.5 B), proliferate and eventually differentiate (Fig. 3.5 C and D). Cells encapsulated into HYAFF120® [40mg/ml] showed an overall delay of two days for cells to attach to the plate, and proliferate to sub-confluence before the media could be changed to DM, in comparison to control cells. However cells did attach,

proliferate and fuse into myotubes *in vitro* quite homogeneously (Fig. 3.5, C-D). Cells cultured in DM for 4 days showed MHC (Fig. 3.5, C) and myogenin expression (Fig. 3.5, D).

Cells encapsulated into HYAFF120® [20mg/ml] were released within few hours from hydrogel encapsulation, because of low polymer concentration and therefore faster *in vitro* degradation; however, released cells did attach and fused into myotubes *in vitro* with one day delay in comparison to control cells.

In HYAFF120® [60mg/ml], cells were released at much slower rate and therefore fewer cells were attached to the plate compared to the other concentrations. However, in this case wells contained also numerous dead cells (floating, non-translucent). Cells that were released did proliferate but their distribution was not homogeneous inside the plate and did not differentiate, thus suggesting that at this concentration hydrogel interfered with cells viability.
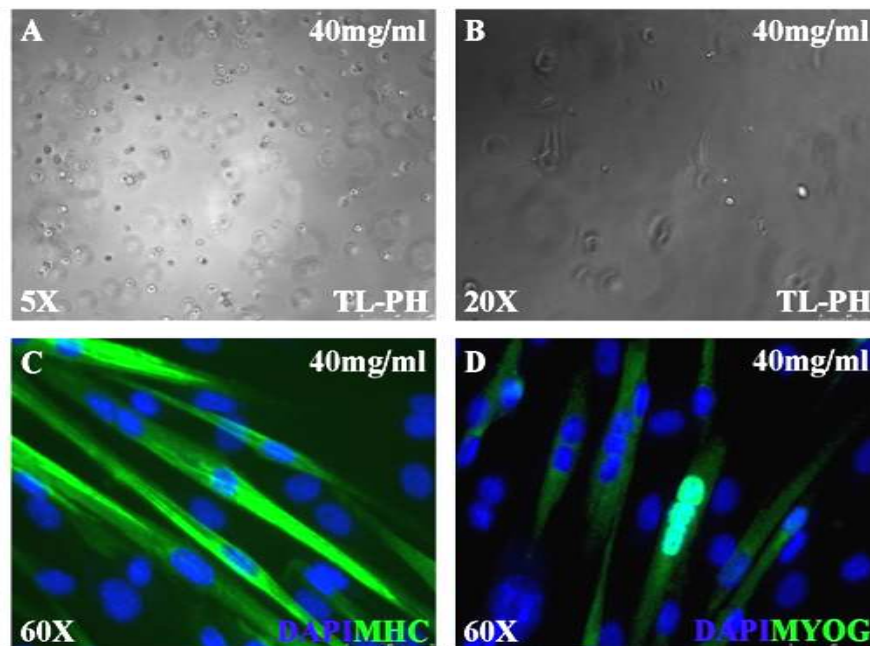

Figure 3.5 **Hydrogel-encapsulated cells in HYAFF120® [40 mg/ml]. A: HYAFF120® [40mg/ml] hydrogel encapsulated cells just after seeding and after 24 hours (B). C and D; HYAFF120® [40mg/ml] encapsulated cells have fused after 4 days in DM, MHC (C) and Myogenin (D) immunostaining, nuclei were counterstained with Dapi.**

These data indicated that *in vitro* cells that are released from hydrogel, preserve their ability to proliferate and fuse into myotubes when encapsulated in 20 and 40 mg/ml

hydrogel; on the other hand, when encapsulated in 60 mg/ml their ability to proliferate and fuse is impaired.

3.3.6   SATELLITE CELLS CHARACTERIZATION

Freshly isolated satellite cells were dissociated from muscle fibers for *in vivo* transplantation. Part of these cells was seeded onto DMEM 10% Matrigel and characterized by immunofluorescence analysis, as soon as they attached to the plate (about 24 hours).

Pax7, Myf5, MyoD and Desmin expression was analyzed, whose quantification is depicted in Fig. 3.6, E. Fig. 3.6 shows an example of cells positive to Pax7 (A-B) and MyoD (C-D).
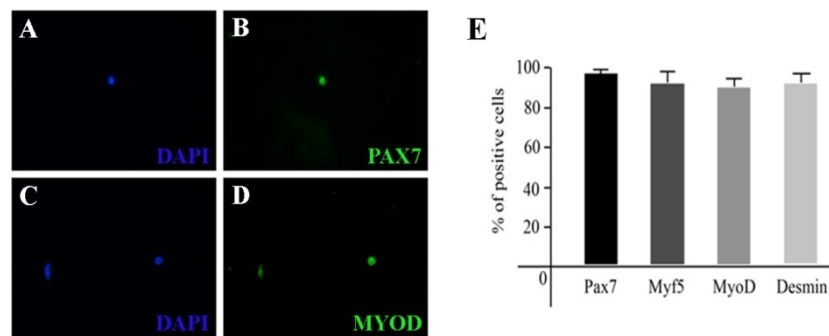

Figure 3.6   **Freshly isolated satellite cells characterized 24 hours post dissociation from muscle fibers. A-B. Example of satellite cells positive to Pax7. B. Example of satellite cells positive to MyoD. E. Quantification of myogenic markers determined by immunofluorescence analysis.**

3.3.7   HYDROGEL IMPLANTS IN VIVO: EXPERIMENTAL DESIGN AND SURGICAL PROCEDURE

Hydrogel-encapsulated cells were delivered to left TAs of recipient animals, while contralateral muscles received either hydrogel without cells or sham surgical procedure.

Fig 3.7 describes the implant protocol. Mice were anesthetized and the skin was cut in order to expose the TA (A-B); then approximately 15% of flesh mass was removed from the core of TAs (C) and a pocket inside muscle was created (D). That pocket was necessary to allow hydrogel insertion inside the muscle (E). In the case of surgical sham, the pocket was not filled with hydrogel or cells, but immediately closed with sutures. Once hydrogel and cells had been applied in place (E), the suspension was photo-polymerized *in situ* (F-H) with UV lamp Blewave-50 Dymax filtered at 366 nm,

intensity: 4mW/cm2, for 55 sec (G). After photo-polymerization muscles were closed (J) with non-absorbable sutures (H).

The polymerization parameters were chosen on the basis of the *in vitro* experiments. A polymerization time of 55 sec with the light source placed at about 4 cm ensured homogeneous polymerization.
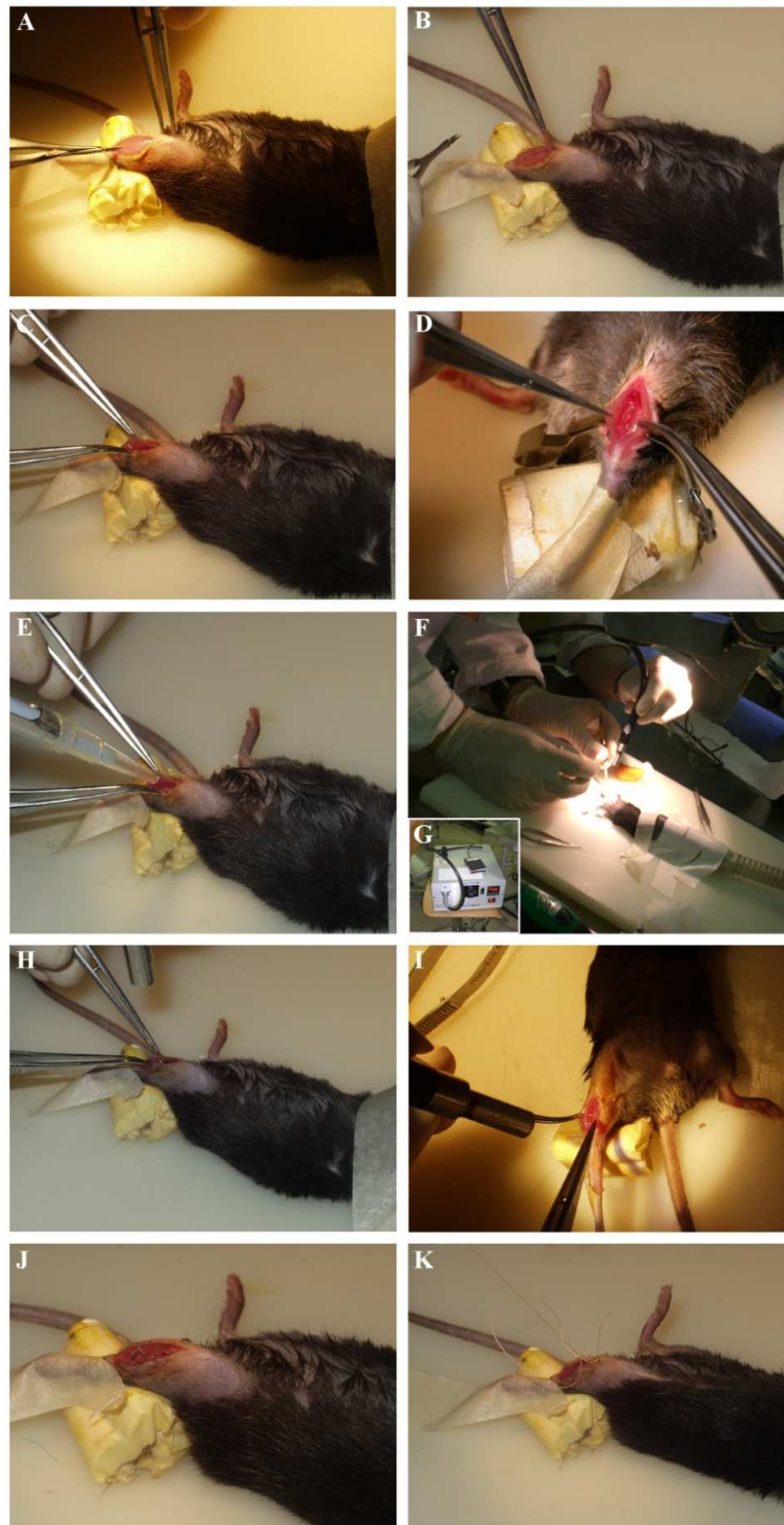
Figure 3.7 Surgery procedure of hydrogel implantation in vivo. Mouse skin is opened (A) and TA is exposed (B). Approximately 15% of flesh mass is removed from the core of TAs (C) to create a pocket (D) for hydrogel insertion (E). Hydrogel and encapsulated cells are photo-polymerized in situ (F and H), using UV lamp Blewave-50 Dymax filtered at 366 nm, (G). After photo-polymerization, implant margins are sutured together (I-J). Finally, skin is also sutured (K).

3.3.8   HYDROGEL IMPLANTS IN WT MICE

Once the surgical procedure for *in vivo* implantation and the *in situ* photo-polymerization of hydrogel-encapsulated cells was set up, hydrogel-encapsulated GFP positive cells were transplanted into *wt* animals; 4 animals were analyzed 2 weeks post-implant, 6 mice were analyzed 6 weeks post-implant.

Mice sacrificed 2 weeks post-implant showed up to 100 GFP positive muscle fibers per section inside the host muscle (Fig. 3.8, A), that was not completely regenerated yet. Moreover, among GFP positive fibers, GFP positive mononucleated transplanted cells were still present inside the recipient muscle, as it is shown in Fig. 3.8, B. GFP positive fibers from donor cells were mostly localized around the insertion site, clearly identifiable thanks to the ongoing regeneration.

When implanted mice were analyzed 6 weeks after transplantation, muscles showed almost complete regeneration and up to 384 ± 34 GFP positive fibers per section were observed. Importantly, GFP positive fibers were well distributed over the transversal sections. Fig 3.4, C shows an overview of GFP positive fibers distributions around treated muscles; panel D shows a magnification of a cluster of newly formed (centrally nucleated) GFP positive fibers.
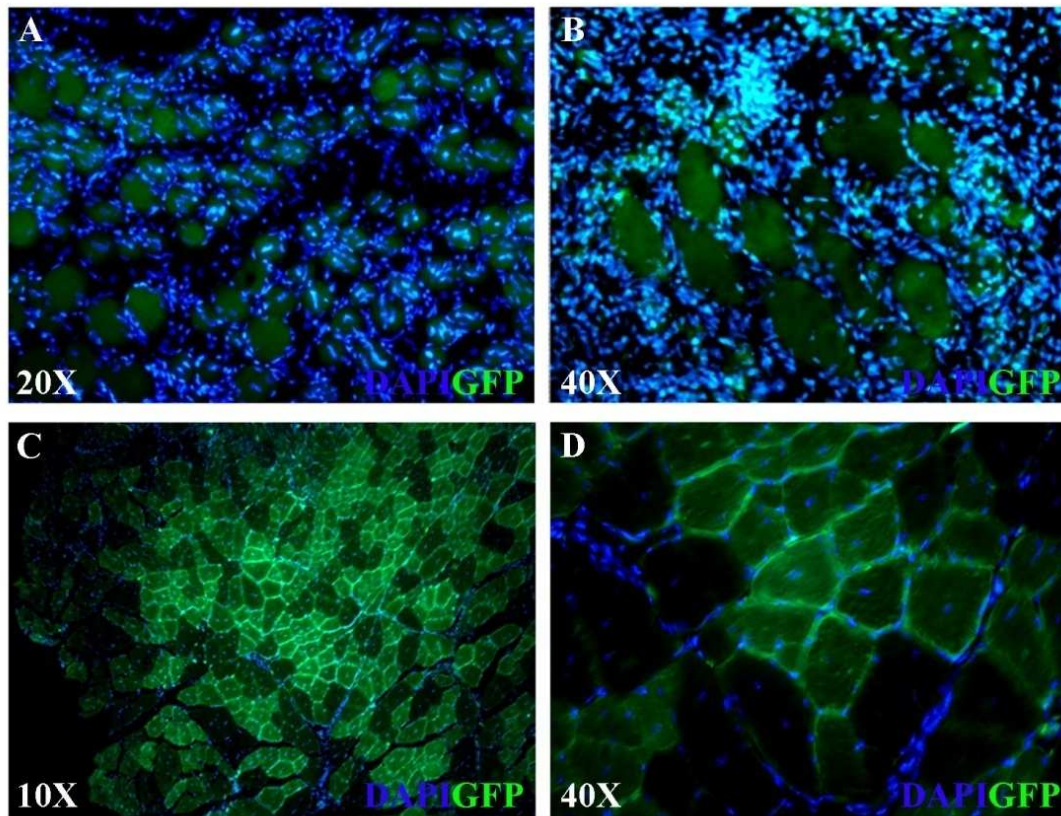
Figure 3.8 **Hydrogel implants in wt mice. Animals engrafted with hydrogel-encapsulated GFP positive satellite cells were analyzed 2 weeks (A-B), and 6 weeks (C-D), after transplantation.**

3.3.9 HYDROGEL IMPLANTS IN MDX MICE

Hydrogel-encapsulated GFP positive cells were then transplanted into *mdx* animals; 4 animals were analyzed 2 weeks post-implant, 5 mice were analyzed 6 weeks post-implant. Engrafted *mdx* mice displayed a very different situation in comparison to *wt* animals. In fact, at the two weeks time point we observed far less GFP positive fibers per muscle section (ranging from 2 to 40 in different muscles, Fig. 3.9 A-B) and many more GFP positive mononucleated cells. Similarly to what was observed in *wt* mice, had not completely regenerated yet and still lots of infiltrate was very evident at 15 days. Muscles at 6 weeks also yielded unexpected results, in that despite the amount of tissue recovery was comparable to that seen in the *wt* animals, very few GFP positive fibers were observed per section (27±4). Once again, only occasional co-expression of GFP and dystrophin could be seen (fig. 3.9, D).

Two of the animals sacrificed at two weeks were also used to analyze the proliferative state of the implanted cells. To this aim both had received an intra-

peritoneal injection of the nucleotide analog EdU before sacrifice. This novel type of label was chosen over the conventional BrdU in that its protocol does not require harsh pre-treatments of the sections (which in our previous experience resulted to be deleterious in muscles that had received a partial ablation). Our findings showed that the vast majority of GFP positive cells did not show EdU labeling (Fig. 3.9, E). However, at the same time we realized we had an unanticipated technical problem, in that EdU reagents caused a dramatic reduction in the intensity of GFP fluorescence (Fig. 3.9, F is the magnification of GFP positive cells cluster in Fig. 3.9, E). For this reason before drawing a firm conclusion about the proliferative state of implanted cells we will have to solve this problem.

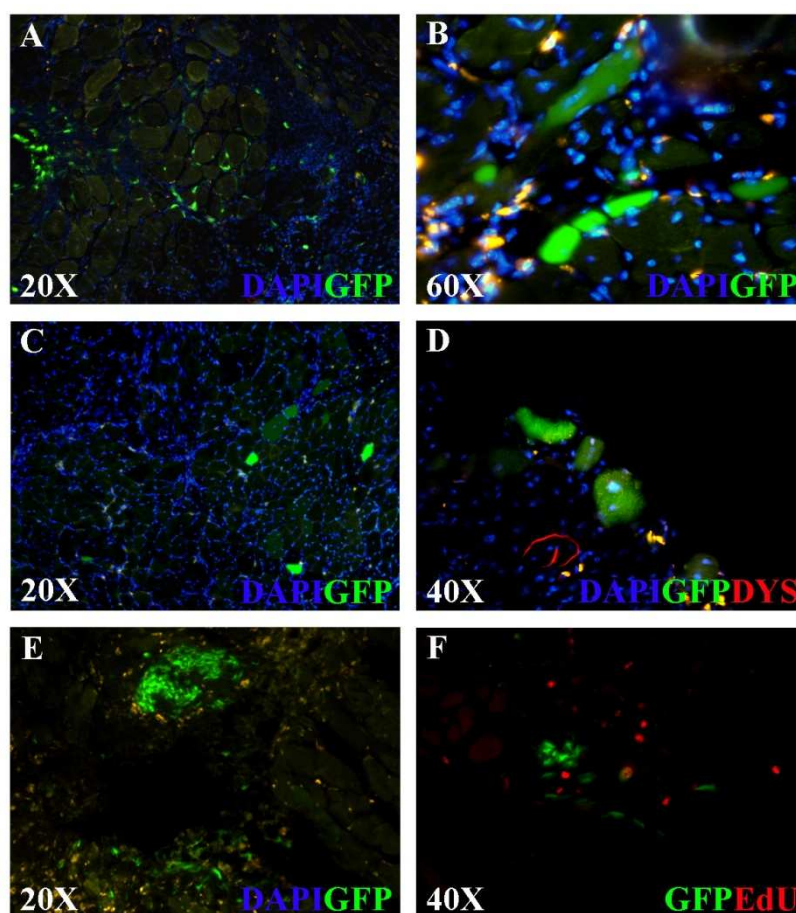**Figure 3.9** **Hydrogel implants in mdx mice. Animals engrafted with hydrogel-encapsulated GFP positive satellite cells were analyzed 2 weeks (A-B), and 6 weeks (C-D), after transplantation. E: cluster of GFP positive cells that was also stained for EdU (F), that seems to interfere with GFP signal. The area shown in panel F corresponds to the GFP positive cluster visible in the upper part of panel E.**

3.3.10   ANTI-FIBROTIC PROPERTIES OF HYDROGEL

Implanted *mdx* muscles were also stained for hematoxylin-eosin, in order to observe whether the effect of hydrogel implants had any effect on the quality of muscle repair. In particular, we wanted to see if its presence could reduce the amount of fibrosis that would normally characterize the repair of an ablation damage.

Fig. 3.10 shows representative images of two *mdx* TAs, that received sham surgical procedure (A) or only Hydrogel (B). TAs that underwent sham surgical procedure (n=3) displayed a still ongoing regeneration with large fibrotic areas; on the contrary, hydrogel-treated muscles showed very little fibrosis and smaller areas of regeneration. In terms of general histological appearance, no obvious difference was found between muscles treated with Hydrogel-encapsulated cells (n=6) and those treated with Hydrogel alone (n=3).
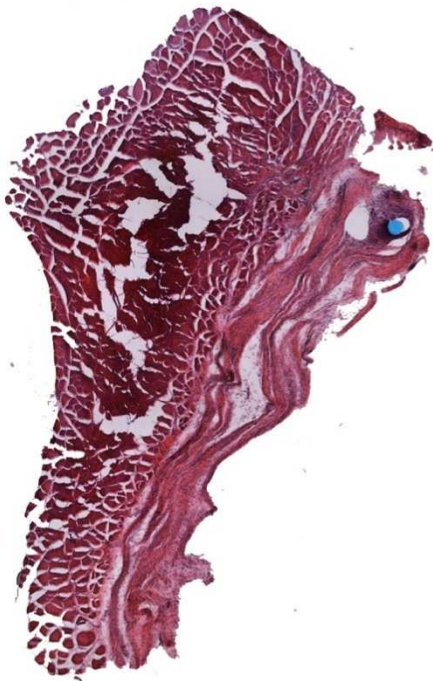
Figure 3.10   **Eosin and Hematoxylin staining of *mdx* TAs analyzed at 6 weeks. A. *mdx* TA which underwent surgical sham B. *mdx* TA that received hydrogel insertion. The light blue round areas are sections of the suture thread.**

3.4   DISCUSSION

In this part of the work, the combination of freshly isolated satellite cells with a novel hyaluronic acid based hydrogel was investigated. Coupling of hydrogel with satellite cells represented a novel combination in comparison to the one used in chapter 2, both in regard to the biomaterial and cell source.

Hydrogel intrinsic characteristics make it a suitable biomaterial for clinical applications, but its mechanical and elastic properties first needed to be optimized for our specific purpose; to this end, hydrogel working concentration was decided in order to be handled by a 27 gauge needle (that is, the size that would likely be used for in vivo cell injection in a human patient), and polymerization conditions were set up in order to guarantee biomaterial homogeneous polymerization and encapsulated cell viability.

The combination of hydrogel and cells was then tested *in vivo*, in both *wt* and *mdx* animals. Of course, given the small size of our recipient animals, delivery of the gel through a needle was not feasible. For this reason we had to opt for a open-surgery approach. Initial experiments carried out in *wt* animals showed very promising results, with approximately 100 GFP positive fibers present at two weeks post implant, and up to 400 GFP positive at 6 weeks post implantation. These numbers compared very favorably with what we had seen in the past with expanded MPCs (*30*), despite the fact that this time the number of injected cells was very low (approximately 250 cells per graft).

Muscle that received hydrogel-encapsulated cells and that were analyzed 6 weeks post implantation showed almost complete regeneration with up to 300 GFP positive fibers per section; these results showed that hydrogel worked as a very efficient cell

carrier for muscle regeneration and on the other side, confirmed previous findings obtained from other groups, in that good regeneration was obtained by engrafting small numbers of satellite cells (*1, 4*), instead of large quantities of expanded myoblasts.

Data obtained in *mdx* mice, however, turned out to be very different from what was observed in *wt*. In fact, 2 weeks post implantation muscles that received hydrogel encapsulated cells contained many more mononucleated GFP positive cells than what was seen in *wt* animals, but very few GFP positive fibers, thus suggesting that those cells likely had not fused yet. Nevertheless, when muscles at 6 weeks post implant were analyzed, only very few GFP positive fibers were observed, and moreover most of them did not display co-expression with dystrophin. Such finding, that had already been reported in the literature (*31*) was most likely due to the fact that very few donor-derived nuclei had entered the GFP positive fibers. In these cases, the small and cytoplasmic GFP protein likely had diffused all along the fiber, away from the location of the producing nucleus, whereas the little dystrophin produced was confined in its near proximity and was therefore easily missed by single sections.

Given that at 2 weeks from implant the number of GFP positive cells found in the muscles clearly exceeded that of the initial implant, it was evident that proliferation had occurred. On the other hand, due to the technical problems we encountered with EdU we could not determine if at two weeks proliferation had already ceased or was still ongoing. The small number of dystrophin positive fibers found at six weeks might suggest that the former hypothesis is more likely, although specific experiments (with intermediate time points and analyses of myogenic markers) will be needed to determine the fate of the implanted cells.

Although implants in *mdx* did not yield satisfying numbers of GFP nor dystrophin positive fibers, muscles that received hydrogel (or hydrogel-.encapsulated cells) showed in general good muscle regeneration with poor fibrotic areas 6 weeks after transplantation; on the contrary muscles that received sham surgical procedure displayed delayed regeneration with large areas of fibrosis. This finding confirmed the anti-fibrotic properties of hyaluronic-based hydrogels (indeed, some types of HA-hydrogels are already used in clinical application to reduce scars formation after open surgery). On the other hand, the low number of GFP positive fibers clearly indicated that the vast majority of muscle repair was carried out by resident satellite cells (which in the *mdx* mice are not depleted, as opposed to what happens in human patients).

The reasons why hydrogel encapsulated cells failed in restoring dystrophin expression in mdx mice, could be linked to physiological differences between *wt* and *mdx* muscle environments and/or to an incomplete immunological compatibility between donor cells (obtained from C57BL/6J animals) and recipient muscles (C57BL/10ScSn-*mdx*/J). However, this latter explanation is not very likely, given that the reason we had decided to use GFP positive cells in the mdx animals was that not only such combination had already been reported in the literature (*32*) but we had also received further positive indications from Dr. Cavazzana's group in Paris.

Other possible causes could reside in the peculiarity of the dystrophic muscle environment, which could affect biomaterial degradation kinetics and therefore cell release. Indeed, the dystrophic muscle is characterized by chronic inflammation with, among other factors, enhanced cytosolic and sub-sarcolemmal calcium concentration (*33, 34*) and protein degradation (*35-37*). Moreover, dystrophic muscles are characterized by enhanced reactive oxygen species (ROS) (*38, 39*) that are a possible cause of native hyaluronan degradation *in vivo* (*40*) and that therefore could be involved in [HYAFF120®] premature degradation as well. However, to what extent these and other factors, would affect hydrogel (and hydrogel-encapsulated cells) performance in dystrophin delivery has not been addressed yet and more experiments will be needed.

Hydrogel represents a promising innovation that needs to be studied and investigated in order to exploit its potentialities. At present, most limiting problems regarding the use of hydrogels in general as cell delivery devices, are the control of the artificial microenvironment provided by the biomaterial. In our case, HYAFF120® has shown to disappear in approximately 10 days once implanted *in vivo*, due to hydrolysis, the action of enzymes, and/or dissolution in the host animal, and in just 10 days hydrogel itself was able to promote wound healing with reduced fibrosis, which could be also observed 6 weeks after transplantation. However in general, the degradation rate of a scaffold, should be coordinated to host tissue development (*41*); therefore, a degradation time of 10 days could be a short time, given that in our system complete regeneration should require 4 to 6 weeks.

Another important line of investigation will be the coupling of the biomaterial with adhesion proteins or biological factors capable of promoting cell adhesion, thus better

mimicking a three-dimensional ECM that could enhance cell survival while inducing their proliferation or differentiation inside host tissue (*10, 42*).

3.5   BIBLIOGRAPHY

1.   D. Montarras *et al.*, *Science* **309**, 2064 (September 23, 2005, 2005).
2.   E. E. S. F. W. B. S. Machida, *Cell Proliferation* **37**, 267 (2004).
3.   G. Cossu, S. Biressi, *Seminars in Cell & Developmental Biology* **16**, 623 (2005).
4.   M. Cerletti *et al.*, **134**, 37 (2008).
5.   A. Sacco, R. Doyonnas, P. Kraft, S. Vitorovic, H. M. Blau, *Nature* **456**, 502 (2008).
6.   C. A. Collins *et al.*, **122**, 289 (2005).
7.   M. R. Burnham, J. N. Turner, D. Szarowski, D. L. Martin, *Biomaterials* **27**, (2006).
8.   G. Chan, D. J. Mooney, *Trends in Biotechnology* **26**, 382 (2008).
9.   A. Khademhosseini, R. Langer, *Biomaterials* **28**, 5087 (2007).
10. M. P. Lutolf, J. A. Hubbell, *Nature Biotechnology* **23**, 47 (2005).
11. A. R. Beck Jonathan, Madsen Ben, Britt David, Vernon Brent, Nguyen Kytai T., *Tissue Engineering* **13**, 589 (2007).
12. D. Falconnet, G. Csucsb, H. M. Grandina, M. Textora, *Biomaterials* **27**, 3044 (2006).
13. J. Elisseeff, C. Puleo, F. Yang, S. B., *Orthod Craniofacial Res* **8**, 150 (2005).
14. J. A. Burdick, A. Khademhosseini, R. Langer, *Langmuir* **20**, 5153 (Jun, 2004).
15. J. A. Burdick, C. Chung, X. Jia, M. A. Randolph, R. Langer, *Biomacromolecules* **6**, 386 (January 10, 2005, 2005).
16. D. G. Anderson, J. A. Burdick, R. Langer, *Science* **305**, 1923 (September 24, 2004, 2004).
17. G. E. J. Y. J. F. J. B. I. I. I. R. L. J. A. B. Ali Khademhosseini, *Journal of Biomedical Materials Research Part A* **9999**, NA (2006).
18. B. P. Toole, *J. Clin. Invest.* **106**, 335 (2001 Aug).
19. K. Meyer, *The Journal of biological chemistry* **107:629**, (1934).
20. W. B. RAPPORT MM, LINKER A, MEYER K., *Nature* **168**, 996 (1951 Dec).
21. B. P. Toole, *Seminars in Cell & Developmental Biology* **12**, 79 (2001).

22. B. P. Toole, M. G. Slomiany, *Seminars in Cancer Biology* **18**, 244 (2008).
23. B. P. Toole, *Nat Rev Cancer* **4**, 528 (2004).
24. G. A. W. Y. John Chen, *Wound Repair and Regeneration* **7**, 79 (1999).
25. L. Lapcik, S. De Smedt, J. Demeester, P. Chabrecek, *Chemical Reviews* **98**, 2663 (Dec, 1998).
26. P. D. Coppi *et al.*, *Tissue Engineering* **12**, 1929 (2006).
27. G. Shefer, M. Wleklinski-Lee, Z. Yablonka-Reuveni, *J Cell Sci* **117**, 5393 (October 15, 2004, 2004).
28. E. Figallo, Padova (2008).
29. A. J. Engler *et al.*, *Journal of Cell Biology* **166**, 877 (Sep, 2004).
30. L. Boldrin *et al.*, *Tissue Engineering* **13**, 253 (2007).
31. F. Chretien *et al.*, *American Journal of Pathology* **166**, 1741 (Jun, 2005).
32. R. T. Auda-Boucher G., Lafoux A., Levitsky D., Huchet-Cadiou C., Feron M., Guevel L., Talon S., Fontaine-Perus J., Gardahaut M. F., *Experimental Cell Research* **313**, 997 (Mar, 2007).
33. V. Robert *et al.*, *J. Biol. Chem.* **276**, 4647 (February 9, 2001, 2001).
34. N. Mallouk, V. Jacquemond, B. Allard, *Proceedings of the National Academy of Sciences of the United States of America* **97**, 4950 (April 25, 2000, 2000).
35. S. S. Assereto Stefania, Sotgia Federica, Bonuccell, Gloria, Broccolini Aldobrando, Pedemonte Marina, Traverso Monica, Biancheri Roberta, Zara Federico, Bruno Claudio, Lisanti Michael P., Minetti Carlo, *Am J Physiol Cell Physiol* **290**, C577 (February 1, 2006, 2006).
36. G. Bonuccelli *et al.*, *Am J Pathol* **163**, 1663 (October 1, 2003, 2003).
37. P. R. Turner, T. Westwood, C. M. Regen, R. A. Steinhardt, *Nature* **335**, 735 (1988).
38. D. Marie-Helene *et al.*, *Journal of the neurological sciences* **161**, 77 (1998).
39. A. R. Thomas, D. Marie-Helene, Y. Yip, F. Alexa, *Neuromuscular disorders : NMD* **8**, 14 (1998).
40. K. Yamazaki *et al.*, *Pathophysiology* **9**, 215 (2003).
41. E. A. D. J. M. Kuen Yong Lee, *Journal of Biomedical Materials Research* **56**, 228 (2001).
42. D. J. Mooney, H. Vandenburgh, **2**, 205 (2008).

CONCLUSIONS

This work focused on the coupling of cells and biomaterial as a possible tool to perform efficient cell delivery *in vivo,* ultimately aimed at an efficient cell-based therapy for dystrophic muscles. The work was carried out in *mdx* mice, the murine model for Duchenne Muscular Dystrophy; however, once established, an efficient protocol for cell therapy could be used for every type of monogenic dystrophy.

Initially, a three-dimensional collagen sponge was investigated as a myogenic cell reservoir for long-term delivery *in vivo* of *in vitro* expanded myoblasts; later, the delivery protocol was changed, and improved, by using a hyaluronic acid based-hydrogel scaffold as a cell carrier for non-expanded satellite cells.

The use of a collagen scaffold has its origins in previous experience carried out by our group[1-3]. Collagen scaffold was used as a reservoir for high quantity of *in vitro* expanded myoblasts that were meant to engraft the recipient muscle once they were released *in vivo*. This approach yielded better results than conventional intramuscular injection and appeared to have some success in term of cell reservoir. Dystrophin restoration was far too low to be functionally relevant; on the other hand, several new muscle fibers were generated inside the scaffold by host cells that colonized the scaffold *in vivo*. This latter observation suggested that collagen sponge could be used as a tool for muscle replacement/reconstruction upon trauma. In fact, although in our study muscle was partially ablated (flesh mass was removed from the core of TA to allow scaffold insertion), regeneration was observed inside the transplanted collagen sponge, that likely behaved as a leading scaffold to promote/guide myofibers formation

(instead of fibrotic tissue deposit), carried out by endogenous myogenic precursors. This aspect is very important, considering that a muscle that undergoes ablation is not capable of *de novo* regeneration and forms, instead, scars and fibrotic tissue. In the case of a human application though, angiogenic aspect needs necessarily to be taken into account. Collagen scaffold has already shown some angiogenic properties *in vivo* [1], but when dealing with large masses of tissues one should envisage the coupling of cellularized scaffolds with specific growth factors, such as the vascular endothelial growth factor VEGF.

The use of collagen scaffold revealed several points that could be ameliorated in order to accomplish a more efficient cell delivery in dystrophic muscle, beside promoting muscle regeneration. Collagen sponge, although endowed with intrinsic natural and elastic properties, was principally thought as a scaffold for cells. Scaffold's structure enhanced myoblast adhesion but on the other side it likely impaired the diffusion of soluble molecules (i.e. growth factors), while not preventing host cell access. Moreover, collagen scaffold is a type of biomaterial that, in the case of any clinical application, would necessarily require open surgery to be inserted, thus constituting a limitation, especially when pathological states, where muscles are compromised at some degree, are treated.

To address these problems we turned our attention to a novel type of biomaterial, hydrogels. These are an appealing tool for cell delivery because of their intrinsic ECM like-structure, that allows the entrapment of cells, as well as biological molecules [4]. Different types of hydrogel exist but the idea of our group was to design a new type of hydrogel with specific characteristics specifically conceived for cell delivery purpose; to this end, a novel hyaluronic-based hydrogel was produced and therefore characterized to accomplish this goal. Beside the biomaterial, the cell source was also improved, as we switched from expanded myoblasts to freshly isolated satellite cells [5].

Despite very good results obtained in the initial experiment with non-dystrophic muscles, though, this combination still did not yield the needed levels of dystrophin restoration in *mdx* muscles. The large differences found using the same protocol in the two model systems are likely due to intrinsic physiological differences between normal and dystrophic muscle. There are several levels that can be modulated in order to work

out this aspect, such as degradation time of hydrogel *in vivo* and hydrogel functionalization with growth factors that could enhance cell performance. In fact, controlling the presentation of soluble and adhesive cues available to transplanted cells, can affect their survival and ability to both form new tissue structures and participate in regeneration of damaged tissues [4, 6]. The proper combination of biological molecules and physico-chemical biomaterial features could direct cell proliferation, differentiation and orchestrate cell response [7, 8], overall enhancing *in vivo* delivery efficiency.

Even when optimized, hydrogel combined with freshly isolated satellite cells to perform cell delivery *in vivo* would not completely solve the problem of cell source availability described in Chapter 1. However, it would represent an improvement because sufficient amounts of freshly isolated satellite cells would be relatively easy to obtain from living patients (for example during orthopedic surgery), and this protocol does not rely on isolation through FACS (that would involve antibodies approval for clinical use).

To the best of our knowledge, this is the first time a biomaterial is coupled with cells in order to perform cell delivery in dystrophic muscles. The ultimate goal, i.e., a functional dystrophin restoration, was not accomplished in these studies. Nevertheless, the information gained provided and the instruments, to improve efficiency.

1.   Andrea Callegari, S.B., Laura Iopa, Angela Chiavegato, Gianluca Torregrossa, Michela Pozzobon, Gino Gerosa, Paolo De Coppi, Nicola Elvassore, Saverio Sartore, *Neovascularization induced by porous collagen scaffold implanted on intact and cryoinjured rat hearts* Biomaterials, 2007 Dec. **28**(36): p. 5449-5461
2.   Boldrin, L., et al., *Satellite Cells Delivered by Micro-Patterned Scaffolds: A New Strategy for Cell Transplantation in Muscle Diseases.* Tissue Engineering, 2007. **13**(2): p. 253-262.
3.   Serena, E., et al., *Electrophysiologic stimulation improves myogenic potential of muscle precursor cells grown in a 3D collagen scaffold.* Neurological Research, 2008. **30**: p. 207-214.
4.   Hill, E., T. Boontheekul, and D.J. Mooney, *Designing Scaffolds to Enhance Transplanted Myoblast Survival and Migration.* Tissue Engineering, 2006. **12**(5): p. 1295-1304.
5.   Collins, C.A., et al., *Stem Cell Function, Self-Renewal, and Behavioral Heterogeneity of Cells from the Adult Muscle Satellite Cell Niche.* 2005. **122**(2): p. 289-301.

6.   Davis, M.E., et al., *Injectable Self-Assembling Peptide Nanofibers Create Intramyocardial Microenvironments for Endothelial Cells.* Circulation, 2005. **111**(4): p. 442-450.

7.   Lutolf, M.P. and J.A. Hubbell, *Synthetic biomaterials as instructive extracellular microenvironments for morphogenesis in tissue engineering* Nature Biotechnology, 2005. **23**(1): p. 47-55.

8.   Mooney, D.J. and H. Vandenburgh, *Cell Delivery Mechanisms for Tissue Repair.* 2008. **2**(3): p. 205-213.

APPENDIX A

ELECTROPHYSIOLOGICAL STIMULATION IMPROVES MYOGENIC POTENTIAL OF MUSCLE PRECURSOR CELLS GROWN IN A 3D COLLAGEN SCAFFOLD

Elena Serena[1], Marina Flaibani[1], Silvia Carnio[2], Luisa Boldrin[3], Libero Vitiello[2], Paolo De Coppi[3], Nicola Elvassore[1]∗

[1] Department of Chemical Engineering, University of Padua, Via Marzolo, 9 Padua, Italy

[2] Department of Biology, University of Padova, Via Bassi, 58 I-35131 Padova, Italy

[3] Department of Pediatrics, University of Padua, Via Giustiniani, 3, Padua, Italy

∗Corresponding author

Abstract

The production of engineered three-dimensional (3D) skeletal-muscle grafts holds promise for treatment of several diseases. An important factor in the development of such approach involves the capability of preserving myogenicity and regenerative potential during ex vivo culturing. We have previously shown that electrical stimulation of myogenic cells grown in monolayer could improve the differentiation process. Here we investigated the effect of exogenous electric field, specifically designed to mimic part of the neuronal activity, on muscle precursor cells (mpcs) cultured within 3D collagen scaffolds. Our data showed that electrical stimulation did not affect cell viability and increased by 65.6% the release rate of NOx, an early molecular activator of satellite cells in vivo. NOx release rate was decreased by an inhibitor of NO-synthase, both in stimulated and non-stimulated cultures, confirming the endocrine origin of the measured NOx. Importantly, electrical stimulation also increased the expression of two myogenic markers, MyoD and Desmin. We also carried out some preliminary experiments aimed at determining the biocompatibility of our seeded collagen scaffolds, implanting them in the tibialis anterior muscles of syngeneic mice.

Ten days after transplant, we could observe the formation of new myofibers both inside the scaffold and at the scaffold-muscle interface. Altogether, our findings indicate that electrical stimulation could be a new strategy for the effective 3D expansion of muscle precursor cells in vitro without loosing myogenic potential and that 3D collagen matrices could be a promising tool for delivering myogenic cells in recipient muscles.

A.1. Introduction

The reconstruction of skeletal muscle tissue, either lost because of traumatic injury or surgical ablation or functionally damaged due to congenital myopathies, is limited by the lack of availability of functional substitutes of this native tissue[1]. In the past few years, different approaches to recreating skeletal muscle tissue in vitro and in vivo have been proposed[1, 2]: from myoblast injection for cell therapy[3] or gene therapy[4],to muscle tissue engineering[5]. All these therapeutic strategies for skeletal muscle reconstruction would require an efficient and robust procedure for the expansion of muscle precursor cells in vitro in order to obtain an adequate cell number for subsequent autologous transplantation[6]. Moreover, it would be of fundamental importance that the ex vivo expansion of myogenic (stem) cells could preserve their differentiative and regenerative potential upon *in vitro* expansion. At present there are evidences that traditional techniques for *in vitro* expansion of muscle precursor cells cause loss of myogenicity. Montarras and colleagues demonstrated that the in vitro 2D culture of mouse satellite cells strongly reduces their regenerative efficiency in vivo[7]. The loss of myogenic potential in rat satellite cells has been correlated by Machida and colleagues with the number of cell passages: from isolation through third passage, there was a decline in the percentage of cells with myogenic/satellite cells markers (from 90% to 55%), in proliferation rates and in differentiation potential (from 46.7% to 12.5%)[6]. In general, the design of a culture system capable of recreating in vitro the spatio-temporal evolution of the main environmental cues that regulate the stem cell fate *in vivo*[8, 9] would be highly desirable. In the case of muscle, 3D cultures and exogenous electrical stimulation have been proposed as tools for successfully expand skeletal muscle[10] and cardiac tissues culture[11]. The architecture of the in situ environment of a cell in a living organism is three-dimensional, and muscle satellite cells are no exception[12]. In traditional 2D cell culture cells alter their gene expression patterns and their production

of extracellular matrix proteins; cells in 3D environment follow chemical and molecular gradient that are impossible to establish in 2D culture[13]. So far, only few studies on differentiation of myoblasts within 3D scaffold have been reported[14, 15] and most of the studies that used primary cultures of mouse myoblasts focused on in vivo implantation and not on in vitro culture[16, 17]. In addition, we also recently showed how 3D culture of satellite cells on collagen scaffolds could benefit in terms of cell viability using a perfusion bioreactor[15, 4] Electrical stimulation is fundamental in controlling several aspects of tissue formation[18]. Few articles report the effects of electrical stimulation on skeletal muscle precursor cells in vitro and most of them employed 2D cell culture methods[19]. To our knowledge, only two previous studies investigated the effects of electrical stimuli on 3D myoblasts culture[10, 14]. Niklason and colleagues showed an increase on cell proliferation of adult rabbit myoblasts due to electrical stimulation[14], but they reproduced the environment of an infarcted heart, which does not correspond to the physiological stimulus of skeletal muscle tissue. On the other hand, Stern-Straeter and colleagues observed a negative impact of electrical stimulation on the myogenic differentiation process[10]. However, the choice of the wave form of electrical stimuli could strongly affect cell behavior; in fact, in a previous study we showed that for 2D cultures exogenous electrical stimulation increased the differentiative potential of rat mpcs[16]. In this work we wanted to take a step forward, coupling 3D culture with electrical stimulation. Our data indicated that collagen scaffold is a good substrate to culture satellite cells and that electrical stimulation increases the secretion of a mediator involved in myogenesis, NO_x as well as the expression of myogenic markers MyoD and Desmin. We propose the coupling of 3D cell culture with electrical stimulation as new strategy for the maintenance of myogenic potential of muscle precursor cells during their in vitro expansion. Our biomimetic approach provides an environment more similar to the in vivo tissue, by using electrical stimulation to mimic part of the neuronal activity, and it allows the development of implantable grafts.

A.2. Material and Methods

A.1.1 Isolation and culture of muscle precursor cells

Mpcs were obtained following the protocol previously described 20. Briefly, flexor digitorum brevis (FDB) and extensor digitorum longus (EDL) from C57BL/6J mouse muscles were removed and enzymatically digested with 0.2% Collagenase Type I (Sigma-Aldrich, USA). Fibers were individually harvested, plated on Petri dishes previously coated with 10% Matrigel (BD Bioscience, USA) and maintained in a humidified tissue culture incubator in plating medium, consisting of Dulbecco Modified Eagle's Medium (DMEM) (Sigma-Aldrich, USA), 10% horse serum (Gibco-Invitrogen, Italy), 1% chicken embryo (MP-Biomedicals, Italy), 1% penicillin-streptomycin (Gibco-Invitrogen, Italy). After 72 hours, culture medium was switched to proliferating, consisting of DMEM, 20% foetal bovine serum, 10% horse serum, 0.5% chicken embryo and 1% penicillin-streptomycin. Cells were kept in culture with proliferating medium and detached from plate with 0.5% Trypsin-EDTA (Gibco- Invitrogen, Italy) before fusion in myotubes occurred. Cells were then re-plated and expanded. For in vivo experiments, cells were derived from C57BL/6-TgnEGFP transgenic mice.

A.1.2 Cell seeding on collagen scaffolds

3D scaffold of porous bovine collagen sponges (Avitene® UltrafoamTM Collagen Hemostat. Davol Inc., USA) was used. Before seeding, scaffolds (sized 5×10×3mm) were conditioned for 12h at 37°C in proliferating medium. At passage 2 or 3, satellite cells were detached from the plates using 0.5% trypsin-EDTA and seeded onto the scaffolds at the concentration of $3.3×10^6$cells/cm^3. 50µl of medium were then added every hour. After 4 hours, seeded scaffolds were covered with 5mL of medium. Scaffolds were maintained in culture in a Petri dish for 7days, at 37°C and 5% CO_2. Medium was changed every day.

A.1.3 Electrical stimulation of cell culture

The apparatus for electric stimulation (Figure 1) was composed of two stainless steel electrodes, 0.8 cm in height and 1 cm in length, which were placed at 14 mm distance (Figure 1A). A poly(dimethylsiloxane) (PDMS, Sylgard 184, Dow Corning, MI, USA) holder was specifically designed to fit a 35 mm Petri dish and to keep the electrodes in a position perpendicular to the collagen scaffold immersed in the culture medium during the culture (Figure 1A–C). The holder had a central hole of 26×6×6 mm, which allowed to keep the scaffold in a position parallel to the electrical field (Figure 1A,C). The

electrodes were connected to a NI 6035E I/O terminal interfaced with NI LabView software (National Instruments Corporation, Austin, TX, USA). LabView was programmed to produce a square wave with a 0 V baseline and impulses of 70 mV/cm for 3 ms with frequency of 33.3 mHz (Figure 1D). The amount of current flowing between the electrodes was measured by monitoring the potential drop across a 50 V resistor placed in series with the culture chamber. Electrical stimuli were applied starting 3 days after cell seeding on collagen scaffold.

A.1.4 Cell viability

The Cell viability was measured by the MTT test (Sigma-Aldrich, USA). Briefly, a 0.5mg/mL solution of the tetrazolium salt MTT in phosphate buffer solution (PBS) was added to the cell samples, which were then incubated for 3h at 37°C. After the removal of the dye solution, cells were lysed in a 10% DMSO, 90% isopropanol solution, which also dissolved the formazan crystals. Samples were placed again at 37°C allowing complete dissolution and then centrifuged at 1200rpm for 5min to precipitate cell debris. Clear solutions were then processed for absorbance readings at 580nm with a spectrophotometer, the recorded optical density (OD) being directly proportional to the number of viable cells. Cell survival after seeding was evaluated with the LIVE/DEAD® assay (Invitrogen, Italy). Briefly, 150μL of Calcein 3.5μM and Ethidium Bromide 3.0μM in D-PBS (Gibco-Invitrogen, Italy) were added to the seeded scaffold and incubated for 45min at room temperature. Following incubation, the scaffold was washed with PBS and labeled cells were observed under fluorescence microscope.
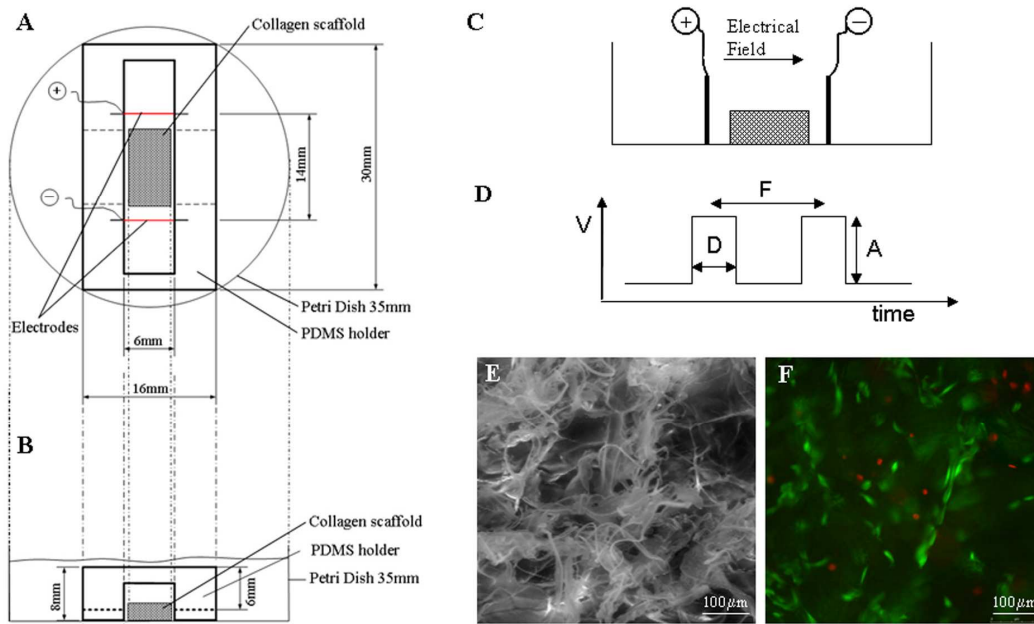
Figure A.1   **Figure 1. Schematic of experimental set-up used for electrophysiologic stimulation. (A and B) Top and front view of electrical stimulation apparatus: 35 mm Petri dish, PDMS holder, stainless steel parallel plate electrodes placed at 14 mm separation distance and collagen scaffold. Symbols 'z' and '–' show connections to the electric field function generator. (C) Schematic view of lateral prospective of 3D scaffold between two electrodes. (D) Square pulsed electric potential (V) applied to the cells within 3D scaffold: A: amplitude (70 mV/cm); D: duration (3 ms); F: 1/frequency (33.3 mHz). (E) SEM image of collagen scaffold. (F) Live and dead assay performed on scaffold 24 hours after cell seeding (cytoplasm of living cells are stained in green and nuclei of dead cells are stained in red).**

A.1.5 NO$_x$ concentration

NOx released by satellite cells in the medium culture were measured, as nitrite (NO$_2^-$), using Griess reagent (Fluka-Aldrich, Italy). The medium was collected every 24h. Briefly, the culture medium was mixed with Griess reagent 3:1 v/v. After 10 to 15min the absorbance at 524nm was measured at UV spectrophotometer, using non-conditioned medium as the baseline. A standard calibration curve, obtained from known concentration of sodium nitrite in non-conditioned culture medium, was used to determine 2 $\tilde{NO}$ concentration. The total amount of nitrite released in the medium during the culture and the release rate were calculated.

To study the inhibition of Nitric Oxide Synthase (NOS), 100µl of 0.1mM L-Nitroarginine methil ester (L-NAME) (Sigma-Aldrich, USA), an analogous of its substrate, were added to the culture medium every day.

A.1.6 Immunostaining

3D scaffolds were harvested at 7 days, embedded in OCT (Sigma-Aldrich, USA) and snap-frozen in liquid nitrogen. Section of 10μm were fixed with PFA 2% for 7min. Desmin primary antibody, rabbit polyclonal, (AbCam, United Kingdom) was diluted 1:200 in PBS-3% BSA (Sigma-Aldrich, USA); GFP primary antibody, rabbit polyclonal, (Molecular Probes, Invitrogen, Italy) was diluted 1:100 in PBS-3% BSA. Each antibody was individually applied for 1h at 37°C. MyoD primary antibody, rabbit polyclonal, (Santa Cruz, Germany), was diluted 1:10 in PBS-3% BSA and applied over night at 4°C. Secondary antibody, Cy™3-conjugated anti-rabbit IgG (Jackson, UK) was diluted 1:250 in PBS-3% BSA and applied for 45min at 37°C. Secondary antibody Alexa Fluor 488-conjugated anti-rabbit IgG (Chemicon, UK) was diluted 1:100 in PBS-3% BSA and applied for 45min at 37°C. After treatment with fluorescent secondary antibodies, cells were counterstained with DAPI and mounted in fluorescent mounting medium (DakoCytomation, Italy).

A.1.7 Protein isolation

Satellite cells on collagen scaffold were placed in sample buffer (12.5 % upper-tris (Tris 0.5M, SDS 0.4%), 10% glycerol, 30% SDS10%, 0.025% bromophenol blue, 5% □-mercaptoethanol) for 20min. Cell lysates were then collected into microfuge tubes and centrifuged at 5000rpm for 1min to eliminate cell debris.

A.1.8 Western blot analysis

A volume of 20 μl was loaded per lane for all protein samples and gels were run at 100V in running buffer (Tris-HCl 25mM, glycine 192mM and 0.1% SDS). Proteins in the gels were transferred to PROTRAN nitrocellulose membranes (Schleicher & Schuell GmbH, Germany) in blotting buffer (Tris-HCl 25mM and glycine 192mM) 300mM for 2 hours at +4°C. Membranes were rinsed three times in TBS (Tris-HCl and NaCl 0.02M) for 5 min each at room temperature, blocked for 1h with 6% non-fat dry milk in TBS-T (TBS, 01.% Triton X100), and rinsed with TBS-T two times. Membranes were then incubated with primary antibody ON at 4°C, rinsed with TBS-T three times, incubated with a secondary antibody for 1h, and rinsed with TBS-T three times. Protein expression signals were visualized by incubating each membrane with 5mL SuperSignal West Pico Chemiluminescent Substrate (Pierce, USA) for 4min, and

then exposing membranes to HyperFilm ECL (Amersham) for up to 5min. The primary antibodies used for Western blot analysis were mouse anti-myosin (1:1000; Sigma-Aldrich, USA), mouse anti-desmin (1:2000; Sigma-Aldrich, USA), rabbit anti-MyoD (1:2000; Sigma-Aldrich, USA), mouse anti-actin (1:800; Sigma-Aldrich, USA). The secondary antibodies used were goat anti-mouse horseradish peroxidase (1:2000; Pierce, USA) and goat anti-rabbit horseradish peroxidase (1:400; Pierce, USA). Quantitative analysis of the western blot lane were performed with image program "ImageJ".

A.1.9 *In vivo* experiments

We used 4 to 6 months-old C57BL/6 wild-type mice and C57BL/6-Tg(ACTBEGFP) 1Osb/J transgenic mice from Jackson Laboratories. In transgenic animals, the GFP transgene was under the control of the cytoplasmic beta actin promoter. The animals were housed and operated onto at the Animal Colony of the "Centro Interdipartimentale Vallisneri", University of Padova, following all relevant bylaws issued by the Italian Ministery of Health. Animals were anesthetized with isoflurane; post-op care included three-days analgesic treatment (tramadol 10mg/kg). Scaffolds seeded with GPF positive satellite cells were implanted into the tibialis anterior (TA) muscles of C57BL/6 wild-type mice. Approximately 25% of muscle mass was removed from the central core of the muscle and scaffolds were inserted inside the pocket, which was then closed with non-absorbable sutures. At the indicated time, muscles were harvested and snap frozen in isopentane pre-cooled in liquid nitrogen. 10μm cryosections were then used for immunohistochemical analyses, using the same protocols described above.

A.1.10 Statistical analysis

One-way ANOVA test was used. $p < 0.01$ and $p < 0.05$ were considered statically significant.

A.3 Results

Cell characterization

Single muscle fibers were successfully isolated from skeletal muscle of adult mice. Once seeded on matrigel-coated dishes, fibers originated a rather homogeneous population of satellite cells. In each experiment, part of the cells was used for the characterization analyses. Flow cytometric analysis (data not shown) were consistent with our previously reported data[21].

Live&Dead assay showed that 24 hours after seeding almost all satellite cells attached to the collagen scaffold were alive (Fig. 1F). We also assessed the efficiency of our seeding procedure, by counting the number of cells that had not attached to the matrix (i.e., that were still in suspension or had adhered to the plate). These measurements showed that after 24 hours approximately 85% of the seeded cells were indeed attached to the scaffold. To monitor how cell viability evolved with time, MTT test was performed at 1, 4 and 7 days of culture. MTT test confirmed a good viability 24 hours after seeding (Abs580nm=0.77); an increased absorbance value at day four (Abs580nm=0.95) indicated that seeded cells had undergone some divisions. After 7 days of culture the viability remains similar to initial values (Abs580nm=0.62). Electrophysiological coupling Stainless steel electrodes have been chosen for their combination of good electrical conductibility and resistance to galvanic corrosion. Stainless steel is an inert material commonly used for clinical tools, i.e. syringe needles, and suitable for fabrication of electrodes for bio-medical application 22. The application of an electric potential difference at the electrodes induces the migration of small and large electrolytes (medium conductance was estimated to be 22mS/cm), causing charge redistribution within the media and related phenomena such as changes in trans-membrane potential and charges flow through the membrane. The current flowing through the culture chamber during electrode charging and discharging periods was monitored and showed a 10-5s duration of this transient regime. The total current flowing during the charging period was equal to the discharging current, confirming the absence of non-reversible faradaic reaction on the electrode surface. This behavior ensured the absence of toxic electrolytic reactions, electrode oxidation and, in general, of harmful temporal changes of culture conditions due to the imposed electrical potential 16. Moreover, the flat shape of the electrodes ensured the generation of an

uniform electric field, capable to homogeneously influence the whole 3D cells environment.

Effect of electrical stimulation on NO_x release

Being that it has been demonstrated on satellite cells that NO_x mediates injury-induced activation in vivo[23] and stimulation-induced in vitro 16, in this study we investigated NO_x release in mouse satellite cells and the effect of electrical stimulation on NO_x release rate. The application of electrical stimulation enhanced the total amount of NO_x released in the medium in comparison to non-stimulated culture (Fig. 2A, full symbol). Specifically, the release rate was increased by 65.6%, from 0.12 d-1 to 0.19 d-1. We performed the electrical stimulation of scaffolds not seeded with cells to verify the negligible presence of NO_x produced by electrochemical oxidation of medium components. In this case, the values of NO_x were extremely low and almost constant, thereby indicating that the increase in NO_x release rate we observed in electrically stimulated satellite cells was cell specific and not due to electrochemical oxidation of components of the medium (Fig. 2A, open symbol).

Furthermore we verified that the measured NO_x were a cell endogenous product and did not derive from oxidation of other released molecules. With this aim, we inhibited the nitric oxide synthase (NOS), which is responsible for NO_x production, using an analogous of its substrate: L-Nitroarginine methyl ester (L-NAME)[24]. In the presence of 0.1mM L-NAME, the NO_x release rate was drastically reduced, both in stimulated and non-stimulated cultures (Fig. 2B). Lastly, we assessed cell viability of the cultures treated with L-NAME (using MTT assay); no toxicity was caused by the inhibitor and the consequent lack of NOS (data not shown).
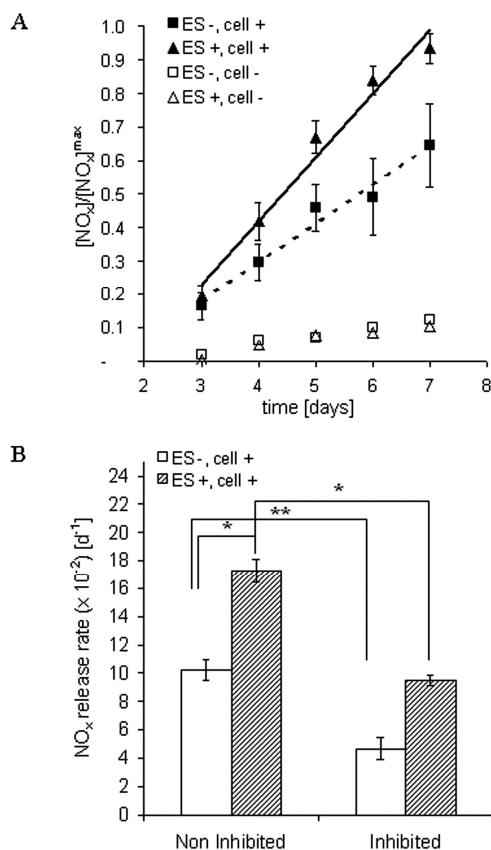
A

B

Figure A.2   Figure 2. NOx release in the culture medium at different time points for electrically stimulated 3D culture (ES +, cell +) and non-electrically stimulated 3D culture (ES -, cell +). Negative controls are represented by not-seeded 3D scaffold (ES ±, cell -). (A) NOx release in the culture medium normalized by the maximum value measured: full symbols refer to 3D cell culture, open symbols are negative control. Electrical stimulation (ES) starts at day 3 (arrow). (B) The release rate of NOx obtained by linear correlation of data in (A), and analogue ones, for stimulated and non stimulated cells, with and without 0.1 mM of L-NAME, the inhibitor of NO-synthase. *p,0.01; **p,0.

Effect of electrical stimulation on muscle marker expression

Considering the enhanced release of NO_x, we investigated the effect of electrical stimulation on the expression of three specific muscle markers, Desmin, MyoD and Myosin, trough immunohystochemistry and western blot. Immunostaining on seeded scaffolds showed that our mpcs expressed Desmin and MyoD after 7 days of in vitro culture (Fig. 3A and 3B), both in stimulated and non-stimulated condition. In order to better evaluate the difference in marker expression we performed semi-quantitative western blot analysis of MyoD, Desmin and Myosin (Fig. 3D and 3E). We observed that satellite cells cultured in electrically stimulated scaffold had a higher expression of MyoD ($p<0.01$) and Desmin ($p<0.05$), while Myosin expression was not significantly affected by electrical stimulation (Fig. 3E).
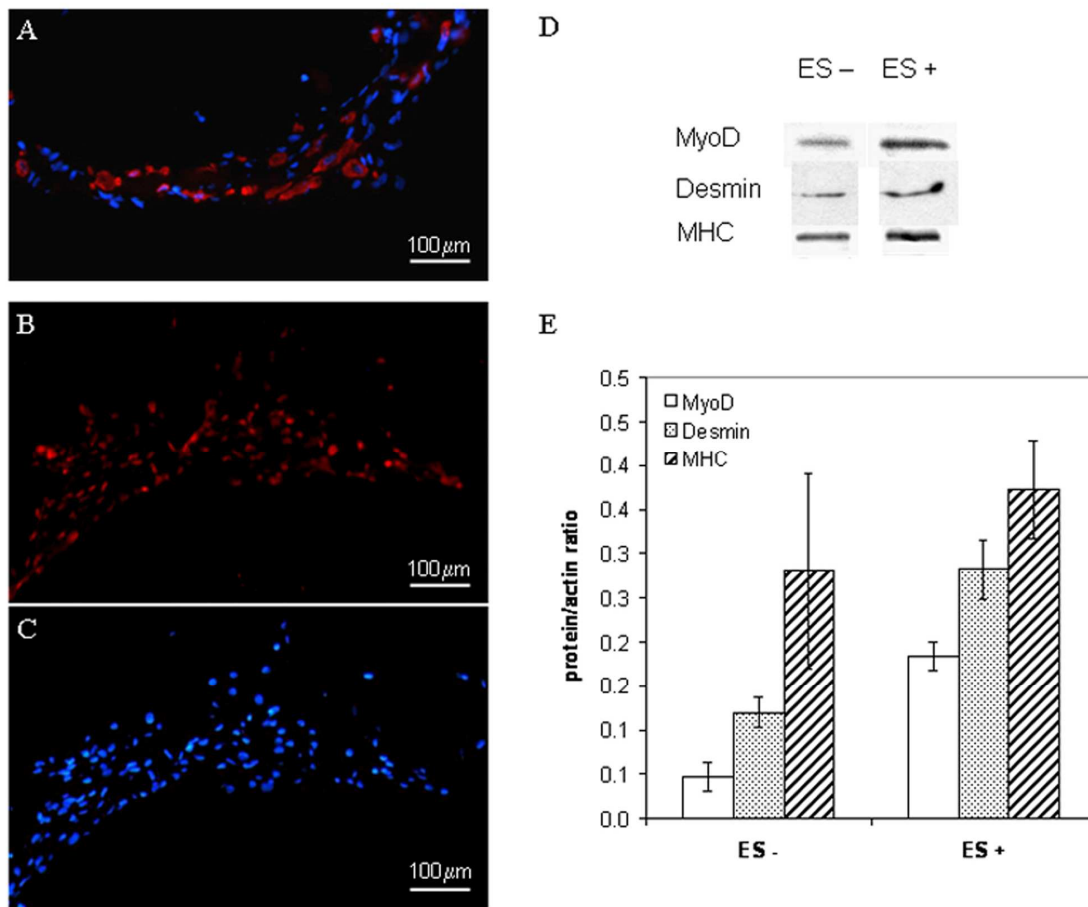
Figure A.3   **Figure 3. Analysis of muscle skeletal marker expression after 7 days of in vitro culture. (A–C) Immunofluorescence analyses: scaffold sections were stained for desmin (A) and MyoD (B), and nuclei were counterstained with DAPI (A and C). (D) Images of Western blot analysis on MyoD, desmin and myosin heavy chain (MHC) of non-electrically stimulated scaffold (ES -) and electrically stimulated scaffold (ES +). (E) Quantification of protein expression based on intensity of lanes in D normalized for intensity of the respective actin lane. *p,0.01; **p,0.05. Bar=100 mm**

In vivo implantation

We performed *in vivo* preliminary analyses in order to verify collagen scaffold biocompatibility and cell response upon in vivo implant. Figure 4 shows sections of tibialis anterior muscles 10 days after implantation. GFP satellite cells were clearly visible within both stimulated (Fig 4A) and nonstimulated (Fig 4B) scaffolds; no evident differences in cell number and/or distribution could be seen between the two conditions. Importantly, at this early time point mpcs inside the implanted scaffold were still desmin positive (Fig. 4C) and there were some newly formed myotubes inside the implanted scaffold (Fig. 4C, magnification).
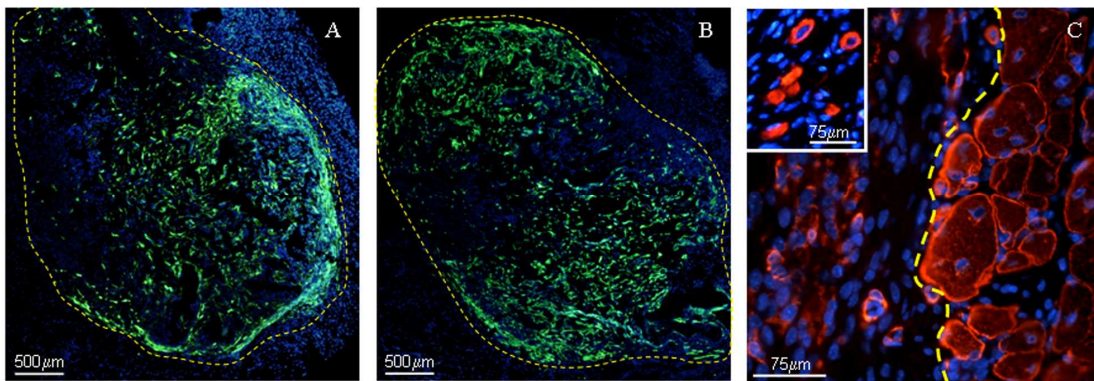
Figure A.4   **Figure 4. Immunofluorescence analysis of *in vivo* implant of cellularized 3D scaffold in syngeneic mice 10 days after the surgery. A and B show muscle section stained for GFP, while C shows staining for desmin. Nuclei were counterstained with DAPI. Dashed lines represent the interface muscle/scaffold. (A) Section of tibialis left muscle implanted with non-electrically stimulated scaffold; (B) section of tibialis right muscle implanted with electrically stimulated scaffold; (C) particular of the interface between muscle (right) and implanted scaffold (left); magnification: newly formed myotubes inside the implanted scaffold. Bar=500 μm in A and B; bar=75 μm in C**

A.4 Discussion

Tissue engineering aims to reconstitute functional tissues starting from two major components: cells and scaffolds. With regards to skeletal muscle, several types of scaffold have already been tested, from synthetic polymers[15, 21] to natural scaffolds[25]; besides, several biomimetic approaches have been developed in order to increase scaffold biocompatibility. In this work we used a 3D porous collagen scaffold, characterized by biochemical and mechanical properties similar to those of *in vivo* tissues. We had already tested this kind of substrate for *in vitro* cell cultures, finding it particularly well suited for cultures of muscle precursor cells[15]. The choice of an appropriate cellular source is also fundamental for the generation of a functional homogeneous tissue *in vitro*. Satellite-derived muscle precursor cells can be an appealing solution, as they are relatively easy to isolate and represent the direct precursor of myoblasts. We previously used these cells for in vivo implants and proved that they display a high regenerative potential[21]. When it comes to clinical application of mpcs, the first issue to overcame is their *in vitro* expansion. This is one of the most critical steps, since cell proliferation and differentiation capacity can be greatly influenced by external stimuli derived by the culture environment. In particular, it has already been demonstrated that the 2D expansion of primary myoblasts in Petri dishes

leads to a loss of their potential to differentiate in myotubes[6]. The aim of this work was the development of a biomimetic culture environment capable of preserving the myogenic potential of mpcs during in vitro expansion, in sight of their in vivo implantation. For this purpose, we coupled 3D culture and electrical stimulation. Electrical stimulation plays an important role in muscle; we thus re-created in vitro an electrical field capable of influencing the distribution of ions, small peptides and proteins without being cytotoxic or affecting the cell viability. It has been shown that the application of an exogenous electrical stimulus enhances the expression of specific skeletal muscle, such as MyoD and Desmin. The not relevant effect of electric filed on Myosin suggests the hypothesis of a stronger influence of electrical stimuli in the early stages of satellite cell differentiation, in agreement with our previous work[16]. This suggests that our system could be used for preventing loss of cell myogenicity during *in vitro* expansion. Interesting results were obtained studying NO_x. Anderson and colleagues demonstrated that NO_x are one of the first activation markers of satellite cells *in vivo*[23]. In this work we observed that electrical stimulation enhances the total amount and the release rate of NO_x in culture medium. We verified that the observed increase in NO_x release rate was effectively due to cell release and not to galvanic oxidation of some medium components: not only stimulated scaffolds without cells showed negligible NO_x release but also inhibition of NOS by an analogous of his substrate causes a drastic decrease in the release rate. Recent findings on NO and HGF effects on satellite cells activation showed that NO concentration regulates a balance between quiescence and activation on fibers[23] but NO pathway has still many dark connections to by clarified. A step further could be the study of electrical stimulation on HGF signaling and coupling with stretching. The in vivo study was performed in order to obtain preliminary data on the feasibility of the surgery and on the scaffold biocompatibility. During the operation, collagen scaffolds were easily manipulated

and fitted in the injury site. Our preliminary results showed that the scaffold did not hinder the muscle regeneration, since a lot of neo-formed myofibers were observed in the muscle-scaffold interface. The collagen scaffold can act as myogenic cells reservoir, since 10 days after the implantation we observed GFP positive cells and the formation of small myotubes inside it. Further investigation at longer time points is required to confirm these promising results. With our preliminary study we explored the effect of an alternative in vitro culture system based on coupling of culture systems already

verified and tested (3D collagen scaffold and electrical stimulation); such system can be upgraded and upscaled with dynamic cell culture system, such as a perfusion bioreactor coupled with electrical stimulation. This could lead to a great improvement regarding cell proliferation, survival and cell distribution along the scaffold that could result in a more uniform and functional implantable graft. In our work, muscle precursor cells are seeded into the scaffold and then cultured in that environment (more similar to the physiological tissue), instead of being expanded in vitro using traditional Petri dishes and then seeded into the scaffold just before implantation, resulting in a reduced manual intervention by the operators. Further and exhaustive studies are needed to elucidate the effect of electrical stimulation on muscle precursor cells, however, we believe that this could be a promising approach for in vitro muscle precursor cell expansion offering new therapeutic tools. Moreover, our methodology represents a very flexible and versatile culture system: knowing cell excitability properties and scaffold dielectric properties, our culture system could be easily adapted to several cell type and different culture substrate or scaffold.

A.5 Conclusions

Here we describe for the first time a novel biomimetic tissue-engineering approach that can improve the efficacy of muscle precursor cell expansion in vitro and consequently the efficiency of cell delivery after in vivo implantation. In particular, we developed a culture methodology to reproduce in vitro the best conditions for satellite cell expansion and maintenance of their myogenicity. Our biomimetic approach is based on the coupling of 3D cell culture on a collagen scaffold, which provides an environment more similar to the in vivo tissue, to electrical stimulation, which mimics part of the neuronal activity.

A.6 Acknowledgments

A.7 References

1. Bach AD, Beier JP, Stern-Staeter J, et al. Skeletal muscle tissue engineering. Journal of Cell. Mol. Med 2004; 8: 413-422.
2. Deasy B, Li Y and Huard J. Tissue engineering with muscle-derived stem cells. Current Opinion in Biotechnology 2004; 15: 419–423.
3. Menaschè P. Skeletal myoblast for cell therapy. Cor Art Dis 2005; 16: 106-110.
4. Urish K KY, Huard J. Initial failure in myoblast transplantation therapy has led the way toward the isolation of muscle stem cells: potential for tissue regeneration. Current Topics in Developmental Biology 2005; 68: 263-280.
5. Levenberg S, Rouwkema J, Macdonald M, et al. Engineering vascularized skeletal muscle tissue. Nature Biotechnology 2005; 23: 821-823.
6. Machida S, Spangenburg E and Booth F. Primary rat muscle progenitor cells have decreased proliferation and myotube formation during passages. Cell Prolif 2004; 37:
7. Montarras D, Morgan J, Collins C, et al. Direct isolation of satellite cells for skeletal muscle regeneration. Science 2005; 309: 2064-2067.
8. Freed LE and Vunjak-Novakovic G. Culture of organized cell communities. Advanced Drug Delivery Reviews 1998; 33: 15-30.
9. Powell K. Stem-cell niches: it's the ecology, stupid! Nature 2005; 435: 268-270.
10. Stern-Straeter J, Bach A, Stangenberg L, et al. Impact of electrical stimulation on three dimensional myoblast cultures – a real-time RT-PCR study. J. Cell. Mol. Med 2005; 9: 883-892.
11. Radisic M, Park H, Shing H, et al. Functional assembly of engineered myocardium by electrical stimulation of cardiac myocytes cultured on scaffolds. Proc Natl Acad Sci U S A 2004; 101: 18129-18134.
12. Partridge TA. Cells that participate in regeneration of skeletal muscle. Gene Therapy 2002; 9: 752-753.
13. Zhang S, Gelain F and Zhao X. Designer self-assembling peptide nanofiber scaffolds for 3D tissue cultures. Seminars in Cancer biology 2005; 15: 413-420.
14. Pedrotty D, Koh J, Davis B, et al. Engineering skeletal myoblasts: role of 3D culture and electrical stimulation. Am J Physiol Heart Circ Physiol 2005; 288: H1620-H1626.
15. Cimetta E, Flaibani M, Mella M, et al. 3D culture of muscle precursors stem cells in a perfusion bioreactor. International Journal of Artificial Organs 2007; 30: 415-428.
16. Flaibani M, Boldrin L, Cimetta E, et al. Muscle precursor cells differentiation and myotubes alignment by micro-patterned surfaces and exogenous electrical stimulation. submitted;

17. Hill E, Boontheekul T and Mooney D. Regulating activation of transplanted cells controls tissue regeneration. Proc Natl Acad Sci U S A 2006; 103: 2494-2499.

18. McCaig C, Rajnicek A, Song B, et al. Controlling cell behaviour electrically: current views and future potential. Physiol Rev 2005; 85: 943-978.

19. Naumann K and Pette D. Effects of cronic stimulation with different impulse patterns on the expression of myosin isoforms in rat myotubes cultures. Differentiation 1994; 55: 203-211.

20. P De Coppi, S Bellini, M Conconi, et al. Myoblast-acellular skeletal muscle matrix constructs guarantee a long-term repair of experimental full-thickness abdominal wall defects. Tissue Eng 2006; 12: 1929-1936

21. Boldrin L, Elvassore N, Malerba A, et al. Satellite cells delivered by micro-patterned scaffolds: a new strategy for cell trasplantation in muscle diseases. Tissue Engineering 2007; 13: 253-262.

22. Cannizzaro C, Tandon N, Figallo E, et al. Practical aspects of cardiac tissue engineering with electrical stimulation. Methods in molecular medicine: Tissue engineering, 2007.

23. Wozniak A and Anderson J. Nitric Oxide-Dependence of Satellite Stem Cell Activation and Quiescence on Normal Skeletal Muscle Fibers. Developmental Dynamics 2007; 136: 240-250.

24. Zhang J, Kraus W and Truskey G. Strech induced mitric oxide modulates mechanical properties of skeletal muscle cells. Am J Physiol 2004; 287: 292-299.

25. Borschel GH, Dennis RG and Kuzon WM. Contractile skeletal muscle tissue-engineered on an acellular scaffold. Plast Reconstr Surg 2004; 113: 595-602.